Received: 17 March 2023 | Revised: 15 July 2023 | Accepted: 8 August 2023

DOI: 10.1002/ar.25312

RESEARCH ARTICLE

The Anatomical Record WILEY

The fossil record of appendicular muscle evolution in Synapsida on the line to mammals: Part I—Forelimb

Peter J. Bishop[1,2] | **Stephanie E. Pierce**[1]

[1]Museum of Comparative Zoology and Department of Organismic and Evolutionary Biology, Harvard University, Cambridge, Massachusetts, USA

[2]Geosciences Program, Queensland Museum, Brisbane, Queensland, Australia

Correspondence
Peter J. Bishop, Museum of Comparative Zoology and Department of Organismic and Evolutionary Biology, Harvard University, Cambridge, MA, USA.
Email: pbishop@fas.harvard.edu

Funding information
William F. Milton Fund, Harvard University; National Science Foundation, Grant/Award Numbers: DEB-1754459, EAR-2122115

Abstract

This paper is the first in a two-part series that charts the evolution of appendicular musculature along the mammalian stem lineage, drawing upon the exceptional fossil record of extinct synapsids. Here, attention is focused on muscles of the forelimb. Understanding forelimb muscular anatomy in extinct synapsids, and how this changed on the line to mammals, can provide important perspective for interpreting skeletal and functional evolution in this lineage, and how the diversity of forelimb functions in extant mammals arose. This study surveyed the osteological evidence for muscular attachments in extinct mammalian and nonmammalian synapsids, two extinct amniote outgroups, and a large selection of extant mammals, saurians, and salamanders. Observations were integrated into an explicit phylogenetic framework, comprising 73 character–state complexes covering all muscles crossing the shoulder, elbow, and wrist joints. These were coded for 33 operational taxonomic units spanning >330 Ma of tetrapod evolution, and ancestral state reconstruction was used to evaluate the sequence of muscular evolution along the stem lineage from Amniota to Theria. In addition to producing a comprehensive documentation of osteological evidence for muscle attachments in extinct synapsids, this work has clarified homology hypotheses across disparate taxa and helped resolve competing hypotheses of muscular anatomy in extinct species. The evolutionary history of mammalian forelimb musculature was a complex and nonlinear narrative, punctuated by multiple instances of convergence and concentrated phases of anatomical transformation. More broadly, this study highlights the great insight that a fossil-based perspective can provide for understanding the assembly of novel body plans.

KEYWORDS

evolution, forelimb, fossils, mammal, musculature, synapsid

1 | INTRODUCTION

Mammals are one of the most diverse and ecologically versatile groups of extant vertebrate, and they owe much of their evolutionary success to a profound reorganization of the ancestral amniote body plan over the course of >320 Ma. The origin and evolution of mammals from nonmammalian synapsid ancestors is documented by an exceptionally rich fossil record (Kemp, 1982, 2005, 2016), permitting detailed investigation into the history of many facets of organismal biology. Key aspects that have received extensive attention include the evolution of

dentition and feeding mechanics (Bhullar et al., 2019; Lautenschlager et al., 2018; Ungar, 2010), hearing and other senses (Allin & Hopson, 1992; Benoit et al., 2022a; Luo, 2011), growth and physiology (Araújo et al., 2022; Benton, 2020; Chinsamy-Turan, 2011), vertebral regionalization and mobility (Jones et al., 2018; Jones et al., 2021), parental care (Hoffman & Rowe, 2018), and breathing (Carrier, 1987; Crompton et al., 2015). Collectively, these studies have painted a rich, complex history of transformation in many anatomical, physiological, and behavioral systems on the line to mammals.

Another key trait underpinning the success of modern mammals is their diverse locomotor strategies. This fundamentally stems from a major shift in stance and gait within Synapsida, from a "sprawled" posture plesiomorphic for amniotes (and tetrapods generally), to an "erect" (or parasagittal) posture in terrestrial therians. Mammals also evolved the capacity for novel high-speed gaits, such as galloping and bounding. Not surprisingly, the evolution of erect limb posture and mammalian locomotion has a long history of study, with attention principally focused on the documentation and analysis of skeletal structure and its transformation along the mammalian stem lineage (e.g., Blob, 2001; Boonstra, 1967; Colbert, 1948; Guignard et al., 2019a; Jenkins & Parrington, 1976; Jenkins, 1970a, 1971, 1973; Jones et al., 2021; Kemp, 1978, 1980a, 1980b; King, 1981a; Lai et al., 2018; Lungmus & Angielczyk, 2019; Lungmus & Angielczyk, 2021; Romer, 1922; Watson, 1917). In addition to the skeleton, understanding transformations in muscular anatomy is crucial to achieving a comprehensive assessment of functional changes, such as biomechanics, behavior, and performance (Bishop, Cuff, & Hutchinson, 2021, and references cited therein). Reconstructing muscular anatomy is hence a key prerequisite for investigating the evolution of locomotor systems, and for providing context for interpreting skeletal evolution itself (e.g., bone–muscle co-evolution). More broadly, deciphering the evolutionary history of synapsid musculature can provide an enriched understanding of evolution of the synapsid lineage as a whole, and how the distinctive body plan of extant mammals arose.

Although nonmammalian synapsids were the focus of some of the earliest detailed attempts at muscle reconstruction in extinct species (Gregory & Camp, 1918; Romer, 1922; Watson, 1917), analyses of synapsid appendicular musculature have historically tended to be scant and superficial, particularly in comparison to other prominent amniote lineages such as nonavian dinosaurs. After the seminal works of Gregory and Camp (1918) and especially Romer (1922), subsequent studies largely followed their lead, often with little novel interpretation or critical evaluation of additional evidence (Angielczyk et al., 2009; Cluver, 1978; Colbert, 1948; Cox, 1959; Cox, 1972; De Oliveira et al., 2010; de Oliveira & Schultz, 2016; DeFauw, 1986; Guignard et al., 2018; Guignard et al., 2019a, 2019b; Jenkins & Parrington, 1976; Jenkins, 1970a, 1971; Kemp, 1978, 1980a, 1980b, 1982, 1986; King, 1981a, 1981b, 1985; Parrington, 1961; Ray, 2006; Ray & Chinsamy, 2003; Romer, 1924; Sulej & Niedźwiedzki, 2018; Walter, 1988b). Such studies almost exclusively considered only those muscles crossing the shoulder or hip, neglecting more distal limb musculature, although Haines (1939) independently reconstructed some muscles in the distal forelimb of the "pelycosaur" *Ophiacodon*. Problematically, many of the aforementioned studies" interpretations provided little (if any) justification, and sometimes were framed without consideration of the anatomy of extant species, relying more on geometric arguments. Most prior studies were also founded upon now-outdated hypotheses of homology (Diogo et al., 2016; Smith-Paredes et al., 2022). Collectively, this has repeatedly resulted in conflicting assessments of muscular anatomy, and, in turn, locomotor function and its evolution.

Only recently has a more rigorous approach to nonmammalian synapsid muscular anatomy been taken, by evaluating fossilized osteology in an explicit phylogenetic framework (Lai et al., 2018). Generally referred to as the "extant phylogenetic bracket" approach (Bryant & Russell, 1993; Carrano & Hutchinson, 2002; Witmer, 1995), the musculoskeletal anatomy of multiple extant outgroup taxa is used to infer the configuration of a muscle (including its presence or absence) in an extinct taxon of interest, and gauge the relative plausibility of a given inference. The success of this approach is predicated on the recognition of homologous and unambiguous osteological correlates of muscle attachment (e.g., muscle scars) common to extant and extinct species. However, overreliance on just extant taxa to inform inferences of a single extinct taxon encounters difficulty the further back in time one goes. The older (more stemward) an extinct focal taxon is, the more that extant outgroups become phylogenetically distant and morphologically disparate from both each other and the extinct taxon, hindering the recognition of homologous osteological correlates and reducing the precision with which inferences can be made (Bishop, 2014). This problem can be addressed by incorporating data from *additional* extinct taxa into the analysis, also framed within an explicit phylogenetic context (Burch, 2014; Hutchinson, 2001a, 2001b, 2002; Molnar et al., 2018, 2020). By harnessing a greater diversity of skeletal morphologies, including transitional forms, this facilitates the recognition (and testing) of homology between anatomically disparate extant or extinct taxa, and enables the incorporation of transformational hypotheses in producing inferences (Bishop, Cuff, & Hutchinson, 2021). Adopting a fossil-rich, explicit phylogenetic approach will

in turn more precisely constrain inferences of musculature in a given extinct species, especially when unambiguous osteological correlates are absent. More broadly, the incorporation of fossil evidence creates a rich dataset through which to explore how and when the body plan of a particular extant group was assembled (Hutchinson, 2001a, 2001b, 2002; Molnar et al., 2018, 2020).

This study conducts a comprehensive assessment of the osteological evidence for appendicular musculature and its evolution on the line to mammals, exploring taxa that span >300 Ma. Drawing upon the exceptional synapsid fossil record, the study seeks to establish the extent to which the distinctive musculoskeletal anatomy of extant mammals is unique to crown Mammalia, as opposed to a suite of traits with greater antiquity, inherited from their distant ancestors. Here, focus is directed toward the forelimb, documenting muscles crossing the shoulder, elbow, and wrist (i.e., muscles that originate proximal to the manus); see the companion study for an investigation of the hindlimb (Bishop & Pierce, 2023). The forelimb of extant mammals exhibits a wide diversity of uses in locomotor and nonlocomotor behaviors, in almost every environment, and consequently exhibits a wide diversity of musculoskeletal adaptations (Polly, 2007). Irrespective of specific ecological adaptations, the musculoskeletal anatomy of the mammalian forelimb is, in general, highly distinctive among extant tetrapods, including the reduction or total loss of most pectoral girdle bones, well-developed processes for muscle attachment (e.g., olecranon of the ulna), dorsal translocation of ventral muscle masses proximally, and extensive muscular differentiation distally (Diogo et al., 2016; Gregory & Camp, 1918; Romer, 1922, 1962). At least therian mammals also exhibit a unique sequence of embryonic development (Cheng, 1955; Smith-Paredes et al., 2022). Understanding the deep evolutionary history of mammalian forelimb musculature can provide important context for exploring how and why these distinctive traits evolved, and how this may have shaped the diversification of forelimb functions. In addition to charting the evolution of musculature on the line to mammals, the present study lays the foundation for the rigorous, phylogenetically informed inference of forelimb anatomy and function in extinct species, paving the way toward a more complete synthesis of locomotor evolution within Synapsida.

2 | MATERIALS AND METHODS

2.1 | Source of data—Extant taxa

Data for the musculoskeletal anatomy of extant tetrapods was principally drawn from previously published descriptions, supplemented by first-hand observation of in situ anatomy in two additional species (Bishop, Wright, & Pierce, 2021; Fahn-Lai et al., 2020), as well as first-hand examination of osteological material. In addition to the ingroups of monotremes and therians, two successive synapsid outgroups were considered: saurian amniotes and lissamphibians. Salamanders (Caudata) were used to represent lissamphibians, since they retain a generalized quadrupedal tetrapod body form and other extant lissamphibians are highly apomorphic; the literature consulted include Mivart (1869), Davison (1895), Wilder (1912), Miner (1925), Francis (1934), Haines (1939), Walthall and Ashley-Ross (2006) and Diogo and Tanaka (2012). The vast majority of prior synapsid studies have neglected the anatomy of salamanders (but see Lai et al., 2018), yet their incorporation as a second outgroup here helps to better estimate character polarity, especially given the large phylogenetic and morphological gulf separating extant mammals from other amniotes. Three principal saurian groups were included to represent Sauropsida: Rhynchocephalia (i.e., *Sphenodon*), Squamata, and Crocodylia, the latter used to exclusively represent Archosauria on account of the highly derived forelimb anatomy of Aves (Burch, 2014). Studies of *Sphenodon* that were consulted include Osawa (1897), Fürbringer (1900), Gregory and Camp (1918), Byerly (1925), Miner (1925), and Haines (1939). Studies of squamates that were consulted include De Vis (1884), Fürbringer (1900), Romer (1922), Haines (1939), Haines (1950), Lécuru (1968), Jenkins and Goslow (1983), Landsmeer (1984), Dilkes (1999), Zaaf et al. (1999), Abdala and Moro (2006), Russell and Bauer (2008), Anzai et al. (2014), Burch (2014) and Fahn-Lai et al. (2020). Studies of crocodylians that were consulted include Haines (1939), Cong et al. (1998), Meers (2003), Brinkman (2000), and Allen et al. (2015). Testudines were not considered, again due to their derived forelimb anatomy.

Within mammals, studies on monotremes that were consulted include Westling (1889), McKay (1894), Gregory and Camp (1918), Howell (1937), Haines (1939), Walter (1988a), Gambaryan et al. (2015), and Regnault et al. (2020). For therians, focus was directed toward basal taxa with a "generalized" quadrupedal anatomy for both marsupials (ameridelphians, peramelemorphians, dasyuromorphians, phalangeriids, and vombatiforms) and placentals (tupaiids, myrmecophagids, dasypodids, procaviids, and rodents), in an attempt to limit the potential for apomorphies to exert spurious influence on the results. The literature consulted include Murie and Mivart (1865), Coues and Wyman (1872), MacCormick (1887), Romer (1922), Le Gros Clark (1924), Le Gros Clark (1926), Greene (1935), Haines (1939), Rinker (1954), Barbour (1963), George (1977), Taylor (1978), Jenkins and Weijs (1979), Stein (1981), Stein (1986),

Carry et al. (1993), Warburton et al. (2013), Olson et al. (2016), Warburton and Marchal (2017), Fahn-Lai et al. (2020), and Richards et al. (2023).

2.2 | Source of data—Extinct taxa

The osteology of extinct taxa was investigated through extensive first-hand observation and photography of fossil material; abbreviations used herein for institutional collections are as follows: AMNH: American Museum of Natural History, New York, USA; BP: Evolutionary Studies Institute, University of the Witwatersrand, Johannesburg, South Africa; BSPG: Bayerische Staatssammlung für Paläontologie und Geologie, Munich, Germany; CGS: Council for Geosciences, Pretoria, South Africa; FMNH: Field Museum of Natural History, Chicago, USA; GPIT: Paläontologische Sammlung, Eberhard Karls Universität, Tübingen, Germany; MACN: Museo Argentino de Ciencias Naturales "Bernardino Rivadavia," Buenos Aires, Argentina; MCZ: Museum of Comparative Zoology, Harvard University, Cambridge, USA; NHMUK: Natural History Museum, London, UK; NMQR: National Museum, Bloemfontein, South Africa; PVL: Instituto Miguel Lillo (Paleovertebrados), Universidad Nacional de Tucumán, Tucumán, Argentina; RC: Rubidge Collection, Wellwood, Graaf-Reinet, South Africa; SAM: Iziko South African Museum, Cape Town, South Africa; TM: Ditsong National Museum of Natural History, Pretoria, South Africa; UCMP: Museum of Paleontology, University of California, Berkeley, USA; UFRGS: Departamento de Paleontologia e Estratigrafia, Instituto de Geociências, Universidade Federal do Rio Grande do Sul, Porto Alegre, Brazil; UMZC: University Museum of Zoology, Cambridge, UK; USNM: National Museum of Natural History, Smithsonian Institution, Washington, DC, USA.

Study of fossil material was supplemented with reference to the published literature including Williston (1911), Pravoslavev (1927), Watson (1931), Boonstra (1934), Romer and Price (1940), Broom (1947), Young (1947), Brink and Kitching (1951), Brink and Kitching (1953), Boonstra (1955), Brink (1955), Attridge (1956), Boonstra (1964), Kühne (1956), Orlov (1958), Cox (1959), Bonaparte (1963), Boonstra (1965), Brink (1965), Fox and Bowman (1966), Cruickshank (1967), Cys (1967), Jenkins (1971), Cox (1972), Sigogneau and Tchudinov (1972), Jenkins and Parrington (1976), Holmes (1977), Cluver (1978), Kielan-Jaworowska and Dashzeveg (1978), Kemp (1980a), Kemp (1980b), Brinkman (1981), King (1981a), King (1981b), Krause and Jenkins (1983), Tchudinov (1983), Sun and Li (1985), DeFauw (1986), Kemp (1986), Sigogneau-Russell (1989), Rougier (1993), Kielan-Jaworowska and Gambaryan (1994), Rubidge et al. (1994), Sereno and McKenna (1995), King (1996), Gambaryan and Kielan-Jaworowska (1997), Gow (2001), Berman et al. (2004), Maisch et al. (2004), Martin (2005), Martinelli et al. (2005), Sereno (2006), Sues and Jenkins (2006), Fourie and Rubidge (2007), Govender (2008), Govender et al. (2008), Hurum and Kielan-Jaworowska (2008), Fourie and Rubidge (2009), Liu and Powell (2009), Campione and Reisz (2010), De Oliveira et al. (2010), Botha-Brink and Modesto (2011), Fröbisch and Reisz (2011), Sumida et al. (2014), Cisneros et al. (2015), Luo (2015), De Oliveira and Schultz (2016), Gaetano et al. (2017), Liu et al. (2017), Sidor and Hopson (2017), Wynd et al. (2017), Butler et al. (2019), Guignard et al. (2018), Guignard et al. (2019a), Guignard et al. (2019b), Berman et al. (2020), Mocke et al. (2020), Benoit et al. (2022b) and Kerber et al. (2022).

In a study such as this that involves the assessment of fine-scale surface features, the taphonomic, diagenetic, or tectonic alteration of fossil material may complicate or confound interpretations. Distinguishing between such instances of alteration and genuine biological structures associated with soft tissue attachment was made possible in three ways. First, distinctive signatures of taphonomy or diagenesis are recognized, such as sharp, broken edges indicative of brittle deformation or recrystallization (e.g., Fernández-Jalvo & Andrews, 2016). Second, comparison of a given specimen to other specimens of the same or related taxon (where available), or between left and right elements of the same specimen, aids in the identification of features that are consistently present, and those which may be anomalous (due to taphonomy, diagenesis, tectonics or other sources, such as pathology). Lastly, the overall quality of specimen preservation, such as completeness, degree of articulation, and retention of bilateral symmetry can provide further evidence of potential damage or alteration of the bones (e.g., extent of post-mortem transport).

2.3 | Homology framework

Inferred homologies of muscles across crown tetrapods, and particularly within amniotes, follow those outlined by previous studies (Table 1; Burch, 2014; Cheng, 1955; Diogo et al., 2016; Romer, 1922, 1944; Russell & Bauer, 2008). These hypotheses are based on topographic similarities of origin, insertion, and spatial relationships with respect to adjacent musculature and other soft tissues; patterns of embryological development; and innervation. Based on an extensive embryological dataset, Smith-Paredes et al. (2022) recently revised some homology correspondences across amniotes, and for the most part, these are accepted here. However, the fossil evidence surveyed during the

TABLE 1 Homology scheme used here for muscle correspondences across extant taxa, with names (and abbreviations) used in this study.

Muscle	Caudata	*Sphenodon*	Squamata	Crocodylia	Monotremata	Theria
Latissimus dorsi	LD	LD	LD	LD "teres major"	LD, two subdivisions	LD
Pectoralis	PECT	PECT, three subdivisions	PECT, two or three subdivisions	PECT, two or three subdivisions	PECT, two subdivisions	PECT, three or four subdivisions
Deltoideus						
scapularis	DSc	DSc	DSc	DSc	DSc	Deltoideus spinalis (DSp)
clavicularis	DCl	DCl	DCl	DCl	Deltoideus acromialis (DAc)	Deltoideus acromialis (DAc)
Scapulohumeralis anterior	SHA	SHA	SHA		Teres minor (TMI)	Teres minor (TMI)
Subscapularis	SSc	SHP	SHP	SHP		
		SSc	SSc	SSc	SSc	SSc
					Teres major (TMA)	TMA
Subcoracoideus		SCo	SCo	[a]	"SCo"	
Supracoracoideus	SPC	SPC	SPC, sometimes subdivided	SPC, three heads	Supraspinatus (SSP)	Supraspinatus (SSP)
					Infraspinatus (ISP)	Infraspinatus (ISP)
					DCl	DCl
					"remnant SPC"	
Coracobrachialis						
longus	CBL	CBL	CBL		CBL	CBL
brevis	CBB	CBB	CBB	CBB, two heads	CBB	CBB
Biceps brachii	"coracoradialis proprius" (in part)	BICB, two heads	BICB, usually two heads	BICB, two heads	BICB, two heads	BICB, two heads (variably divided)
Brachialis	BRA	BRA	BRA	BRA	BRA, two subdivisions	BRA
Humeroradialis		HR				
Triceps						
coracoideus	TRIC	TRIC	TRIC, absent in some species	TRIC	Dorsoepitrochlearis (DEP)	Dorsoepitrochlearis (DEP)
scapularis	TRIS	TRIS	TRIS	TRIS	TRIS, two heads	TRIS
humeralis medialis	TRIM	TRIM	TRIM	Three humeral heads,	TRIM, two heads	TRIM
humeralis lateralis	TRIL	TRIL	TRIL		TRIL	TRIL

TABLE 1 (Continued)

Muscle	Caudata	*Sphenodon*	Squamata	Crocodylia	Monotremata	Theria
				homologies uncertain		
Epitrochleoanconaeus	EPI	EPI	EPI	[a]	EPI	EPI
Pronator						
teres		PRTE	PRTE	PRTE	PRTE	PRTE
accessorius		PRAC	PRAC, usually two heads	[a]		
Flexor digitorum longus						
superficial	FDLs	FDLs	FDLs, 2–4 heads ("humeral heads" of Russell & Bauer, 2008)	FDLs	FDLs ("flexor digitorum profundus caput humerale superficiale" of Gambaryan et al., 2015)	At least two heads: flexor digitiorum superficialis (FDS) and palmaris longus (PALM)
deep	FDLd, two or three heads	FDLd, three heads	FDLd ("ulnar head" of Russell & Bauer, 2008)	FDLd	FDLd, three heads ("flexor digitorum profundus caput humerale profundum," "caput olecrani," and "caput ulnare" of Gambaryan et al., 2015)	Generally four heads: flexores digitorum profundus humeralis (FDPh), radialis (FDPr) and ulnaris (FDPu), and flexor pollicis longus (FPL)
Flexor carpi radialis	FCR	FCR	FCR		FCR	FCR
Flexor carpi ulnaris	FCU	FCU	FCU, rarely two heads	FCU	FCU, two heads	FCU
Anconaeus		ANC			ANC ("epitrochleoanconaeus lateralis" of Gambaryan et al., 2015)	ANC
Brachioradialis	BRR	BRR	BRR ("supinator longus" of Russell & Bauer, 2008)	BRR ("supinator" of Meers, 2003)	BRR	BRR
Extensor digitorum longus	EDL	EDL	EDL	EDL	EDL, three heads ("communis," "lateralis" and "pollicis et indicis" of Gambaryan et al., 2015)	at least three heads: extensores digitorum "communis" (EDC), "lateralis" (EDLa) and "profundus I" (EDP1)
Extensor carpi radialis	ECR, two heads	ECR, three heads	ECR, two heads	ECR, two heads	Supinator (SUP) ECR	Supinator (SUP) ECR, two heads
Extensor carpi ulnaris	ECU	ECU	ECU, two heads	ECU ("flexor ulnaris" of Meers, 2003)		ECU

(Continues)

TABLE 1 (Continued)

Muscle	Caudata	*Sphenodon*	Squamata	Crocodylia	Monotremata	Theria
Abductor pollicis longus	APL	APL	APL ("supinator manus" of Russell & Bauer, 2008)	APL, two heads ("extensor carpi radialis brevis" of Meers, 2003)	APL	APL
Pronator quadratus	PRQU	PRQU	PRQU	PRQU	PRQU	PRQU

Note: This table omits the "contrahentium caput longum" found in the salamander forelimb (see Diogo et al., 2016; Diogo & Tanaka, 2012; Miner, 1925), which has no clear equivalent in amniotes. Further work is needed to clarify this muscle's homology with respect to amniotes; in the present study it will be tentatively treated as a salamander apomorphy and not considered further. The "humeroradialis" of *Sphenodon* is not included here, as it may be apomorphic for that taxon (Smith-Paredes et al., 2022). The "teres major" of crocodylians is not homologous to the (true) teres major of mammals (Smith-Paredes et al., 2022). Gray cells denote the absence of a muscle.

[a]Present in Aves (Burch, 2014).

course of the present study suggests an alternative hypothesis for the homology of the mammalian deltoids and teres minor, different from that of both Smith-Paredes et al. (2022) and previous studies (Table 1). This will be discussed below as appropriate.

2.4 | Character formulation and codification

An explicit phylogenetic approach was used to document and analyze osteological evidence of muscle attachment, through the construction of character–state complexes and codification of a dense sample of operational taxonomic units (OTUs). Fundamentally, characters are discrete, heritable traits that comprise a set of varying states that are hypothesized to be homologous. In the context of investigating soft-tissue evolution, the rationale for how characters and their states are constructed has been outlined by Hutchinson (2001b) and Hutchinson (2002); see also de Pinna (1991) for a broader discussion of the issue. Both taxic and transformational perspectives to homology (Patterson, 1982) were considered in the construction of states, when it was deemed appropriate (see Results). A transformational hypothesis of homology across disparate anatomical features was articulated as a single multistate character; conversely, possession of multiple osteological features in a single species or specimen necessitated the creation of multiple characters (principle of conjunction). Across a disparate sample such as crown Tetrapoda, the undertaking of this process is frequently only made possible through recognition of transitional (intermediary) morphologies, preserved only in the fossil record. In some cases, subsequent analysis of character evolution (see below) revealed the distribution of states to be consistent with the phylogenetic interrelationships of the OTUs considered, retrospectively supporting the inference of homology (i.e., principle of congruence; Patterson, 1982).

The present study sought to trace the evolution of forelimb musculature within the synapsid lineage, leveraging information from a broad suite of taxa spanning 330+ Ma of evolution. Striking a balance between this overarching goal, and what is practical, guided the construction of character–state complexes, the codification of OTUs, and subsequent phylogenetic analysis. Firstly, a broad taxonomic resolution was adopted, by which most OTUs were monophyletic, suprageneric taxa ("groundplan approach"; Prendini, 2001; Figure 1). The comprising genera contributed to a "consensus" codification, and multiple states (polymorphisms) were recognized in cases of significant disparity within the clade; see Supporting Information Appendix S1 for a list of taxa that contributed to the coding of suprageneric OTUs, and Supporting Information

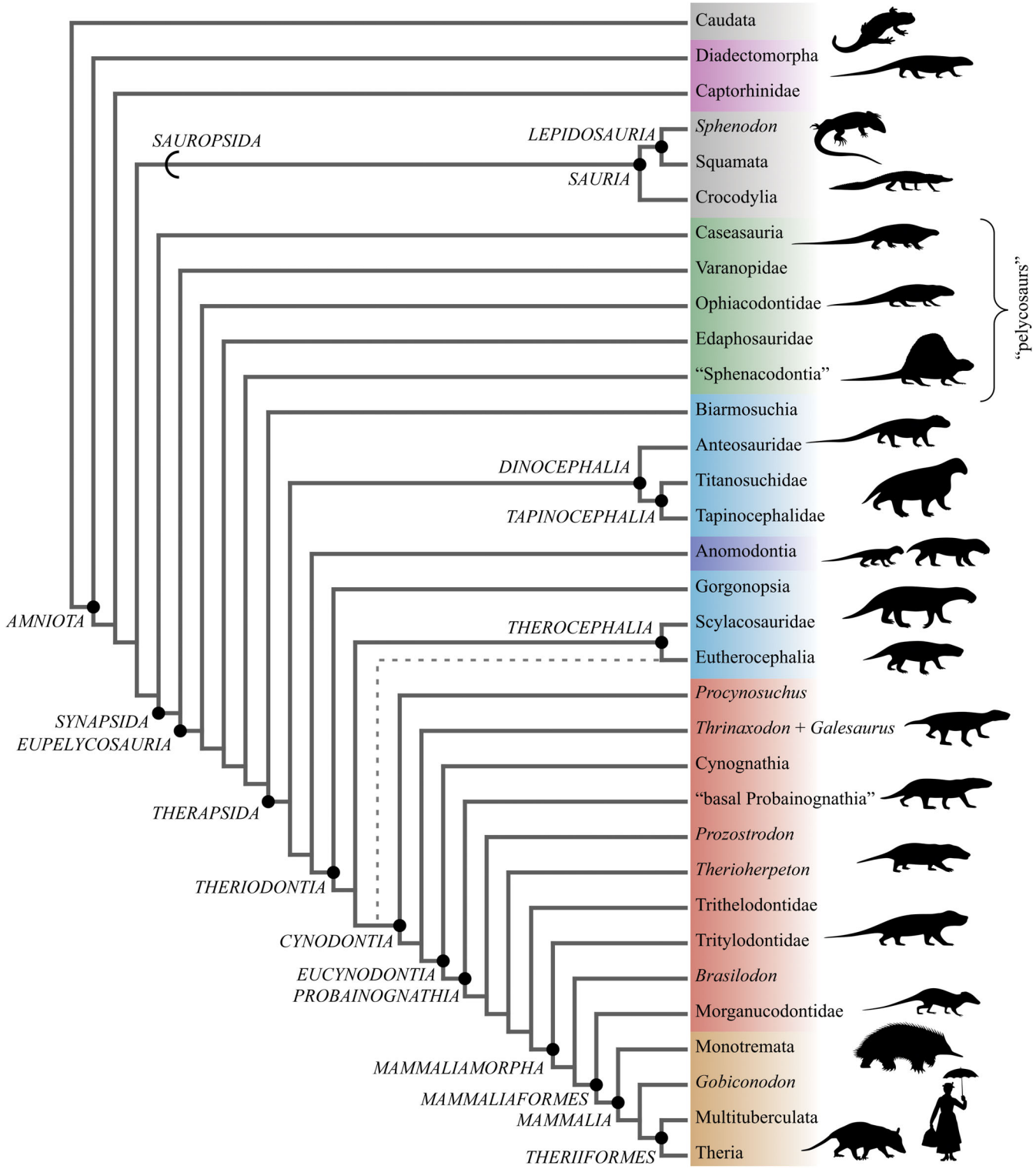

FIGURE 1 Phylogenetic interrelationships of operational taxonomic units used for character state mapping in the study. A single consensus tree is drawn from the results of prior analyses, including those of Kerber et al. (2022), Simões et al. (2022), and Hellert et al. (in press). Key clades are labeled, and major groups referred to in subsequent figures are indicated by different colors. Note that "Sphenacodontia" as coded here is a paraphyletic taxon comprising all nontherapsid sphenacodontians, and that "basal Probainognathia" is a paraphyetic taxon comprising all probainognathian cynodonts more basal than *Prozostrodon*. The term "pelycosaur" refers to any nontherapsid synapsid. For the purposes of this study, "Scylacosauridae" includes both lycosuchid and scylacosaurid therocephalians. Note that Sauropsida is a far more inclusive clade than Sauria, although in the present study both are represented by extant saurian lineages only. The dashed line indicates an alternative topology that was considered here, where eutherocephalians are more closely related to cynodonts than other therocephalians (see text).

Appendix S2 for the taxon–character matrix developed. Only a few genera were coded individually in their own right. Two paraphyletic OTUs were also included: "Sphenacodontia," denoting all nontherapsid sphenacodontians, and "basal Probainognathia," denoting all probainognathian cynodonts more basal than *Prozostrodon*. The entirety of Anomodontia was represented by a single OTU, and multiple states were possible due to character evolution within dicynodonts (Supporting Information Appendix S2); when this occurred, the state observed in more basal members (especially nondicynodonts) was used for the purpose of analyzing character evolution along the mammalian stem lineage. Extant taxa were codified into six OTUs: Caudata, *Sphenodon*, Squamata, Crocodylia, Monotremata, and Theria. Following a consensus approach to OTU coding, this allowed for traits related to ostensibly derived ecologies in individual extinct taxa (e.g., Cluver, 1978; Cox, 1959, 1972; Fröbisch & Reisz, 2011; King, 1985; Sues & Jenkins, 2006) to be more readily recognized and excluded from consideration. Furthermore, inference of ancestral character states is based upon identification of clade-level synplesiomorphies (i.e., commonalities across many taxa), further avoiding potential problems posed by apomorphic individual genera or species.

A relatively broad anatomical resolution was also taken. In a study such as this, the construction of character–state complexes must sometimes gloss over fine-scale nuances to capture broad-scale patterns, if phylogenetic analysis is to be tractable (i.e., limited number of states per character) and provide meaningful results (i.e., the sequence and timing of changes along the stem lineage can be resolved with precision). This was particularly the case for muscles inserting on the manus, due to the numerous carpals and more evolutionary labile nature of manual construction across crown tetrapods as a whole. In addition to the coarse taxonomic treatment of saurians, in some instances less emphasis was placed on the anatomical nuances observed within Sauria, considering that this work was designed to focus on Synapsida. The present set of character–state complexes may therefore not be entirely appropriate for addressing evolution within amniotes as a whole. Nevertheless, they provide a first foundation that can be refined in subsequent studies.

2.5 | Analysis of muscle evolution

To explore the evolution of forelimb musculature along the mammalian stem lineage, the character–state complexes were subjected to a formal phylogenetic analysis and ancestral state reconstruction (ASR; Supporting Information Appendix S3). Phylogenetic relationships of OTUs were expressed with a single "consensus" tree drawn from the results of prior studies (Figure 1; Kerber et al., 2022; Simões et al., 2022; Hellert et al., in press). The relationships within Anomodontia, used to determine the plesiomorphic states entered into the analysis, followed Kammerer et al. (2013). Prior studies of phylogenetic interrelationships among the taxa considered here have been based principally on craniodental characters; when information from the postcrania has been taken into account, such characters are almost invariably distinct from those created in the present study. Indeed, the vast majority of features that are codified here have never been used in cladistic analysis. There is hence no concern of circularity in the inference of forelimb muscle evolution.

Although a single primary tree topology was used, cranial-focused studies have occasionally recovered a paraphyletic Therocephalia, with cynodonts nested within them (Abdala, 2007; Abdala et al., 2019; Botha et al., 2007). This result is consilient with the notable stratigraphic gap (ghost lineage) between the earliest-known members of Therocephalia and Cynodontia; in the Karoo Basin of South Africa, the *Eodicynodon* Assemblage Zone and *Endothiodon* Assemblage Zone (*Tropidostoma–Gorgonops* Subzone), respectively (Abdala et al., 2008; Botha et al., 2007). Therocephalian paraphyly is also consistent with several differences between the postcrania of scylacosaurids and eutherocephalians. Such differences include an anteroposteriorly abbreviated interclavicle, an enlarged obturator fenestra between pubis and ischium, and a markedly reduced body size in eutherocephalians (see also Bishop & Pierce, 2023). Each of these features is also observed in cynodonts, but not scylacosaurids. To evaluate if this affected inferences of muscle evolution, Therocephalia was here treated as two OTUs, Scylacosauridae (including, for the purposes of this study, Lycosuchidae) and Eutherocephalia, and two tree topologies were considered: a monophyletic Therocephalia, and a paraphyletic one with Eutherocephalia as the sister taxon to Cynodontia (Figure 1).

To document character state distributions and obtain branch lengths for ASR, a Bayesian phylogenetic analysis was undertaken in MrBayes 3.2.7 (Ronquist et al., 2012). Calculating branch lengths in terms of accrued character state changes (i.e., a phylogram) has been shown to produce more accurate ASRs, when the characters of interest in an ASR are used to determine branch lengths (Wilson et al., 2022). This approach was indeed necessitated by the anatomically and temporally uneven sample of fossil specimens that contributed information for the coding of extinct OTUs, wherein rigorously estimating branch lengths in terms of time (i.e., a chronogram) is problematic. For each tree topology, phylogenetic analysis was

performed using a single taxon–character matrix combining the forelimb (this study, 73 characters) and the hindlimb (Bishop & Pierce, 2023; 80 characters) datasets together. All characters were left unordered. Analysis used a Markov (Mkv) model for morphological evolution with ascertainment bias corrected for the absence of invariable sites, as described by Lewis (2001). Among-character rate variation followed a gamma distribution, with alpha sampled from an exponential distribution with mean of 1.0. The Markov-chain-Monte-Carlo sampler used was set to 5 million generations, using four independent runs with four chains each (sampling every 1000 generations), with temperature at 0.05 and relative burn-in of 25%. Convergence of independent runs was assessed using the average standard deviation of split frequencies (ASDSF $\sim$ 0.01), potential scale reduction factors (PSRF $\sim$ 1.0 for all parameters), and effective sample size for each parameter greater than 200.

ASRs were undertaken using median branch length values, employing a maximum likelihood and joint estimation procedure with the "ape" (v.5.6-2; Paradis et al., 2004) and "phytools" (v.1.2-0; Revell, 2012) packages in R v.4.1.0 (R Core Team, 2021). This assumed a Brownian motion model of character evolution, with an equal-rates model of state transition; again, all characters were left unordered, to provide a more objective evaluation of anatomical evolution and homology hypotheses. To quantitatively examine character evolution along the mammalian stem lineage, a change in state was recognized when the likelihood of an alternate state equaled or exceeded a predefined threshold, conservatively set to 0.75 (i.e., a high level of confidence is required to infer a transition). Under such a criterion, sequential comparisons of node likelihoods will tend to delay the recognition of a state change in the direction that the comparison is made, whenever the requisite threshold >0.5. Moving up the tree from root to tip, and down the tree from tip to root, is therefore somewhat analogous to the "DELTRAN" and "ACCTRAN" algorithms of maximum parsimony methods (Swofford & Maddison, 1987), respectively. Considering root-up and tip-down approaches together can hence bracket the earliest and latest nodes at which a state transition likely occurred, and both were used to estimate the number of node-specific state changes along the stem lineage, as a way of gauging the "pace" of muscular evolution.

Given the incomplete nature of the fossil record, and the fact that not all muscles have recognizable osteological correlates (which are indicative of a specific character state), the taxon–character matrix produced here lacks data for many characters, for all extinct OTUs concerned. The extent of missing data, and which parts of synapsid phylogeny this issue is more acute, could affect how precisely the timing of a given state change can be detected. Considered across all characters, this may in turn weaken inferences of the pattern or pace of character evolution. To explore this, the number of state changes inferred for each node on the stem lineage was compared against the amount of missing data in the immediate vicinity of that node. Here, node-specific missing data was computed as the proportion of uncoded characters (i.e., scored as "?") collectively across the immediate bracket of a given node. This bracket spanned OTUs branching one node down and one node up from the focal node. For instance, the node Mammalia is bracketed by Morganucodontidae and *Gobiconodon* (Figure 1), and hence there are three OTUs across which the proportion of missing data is computed (Morganucodontidae, Monotremata, and *Gobiconodon*). In contrast, five OTUs are involved in computing the proportion of missing data for the node Therapsida ("Sphenacodontia," Biarmosuchia, Anteosauridae, Titanosuchidae, and Tapinocephalidae; Figure 1). It would be expected that all else being equal, if missing data did negatively impact the detection of when character state changes occurred, fewer state changes would be resolved at nodes with a greater proportion of missing data.

On a final note, it should be recognized that, while maximum likelihood offers a means for quantifying inferences of ancestral character states (i.e., confidence levels), the reliance on an arbitrary threshold for detecting a change in state can limit its utility. Even if the relative likelihoods of two alternate states shift markedly from one node to another (e.g., from 70:30 to 30:70), if neither exceeds the threshold then a state change will not be detected. Moreover, reaching a given threshold may be more difficult for characters with more available states, or when observations for OTUs are scarce (as is often the case for extinct taxa) and/or disparate. In addition, inferences based on likelihoods alone may be incongruent with evidence afforded by the fossil record, when explicit osteological correlates for a muscle's attachment (or even presence) have been recognized (e.g., see characters 4 and 24 below). To that end, the additional use of maximum parsimony, in tandem with observation of character state associations in fossil taxa, can contribute to a more holistic evaluation of ancestral states (Bishop, Cuff, & Hutchinson, 2021). In the present study, calculation of maximum parsimony was undertaken using Mesquite v.3.6.1 (Maddison & Maddison, 2021).

3 | RESULTS

A total of 73 character complexes were devised for all the muscles crossing the shoulder, elbow, and wrist (see also Supporting Information Appendix S2). In a similar fashion

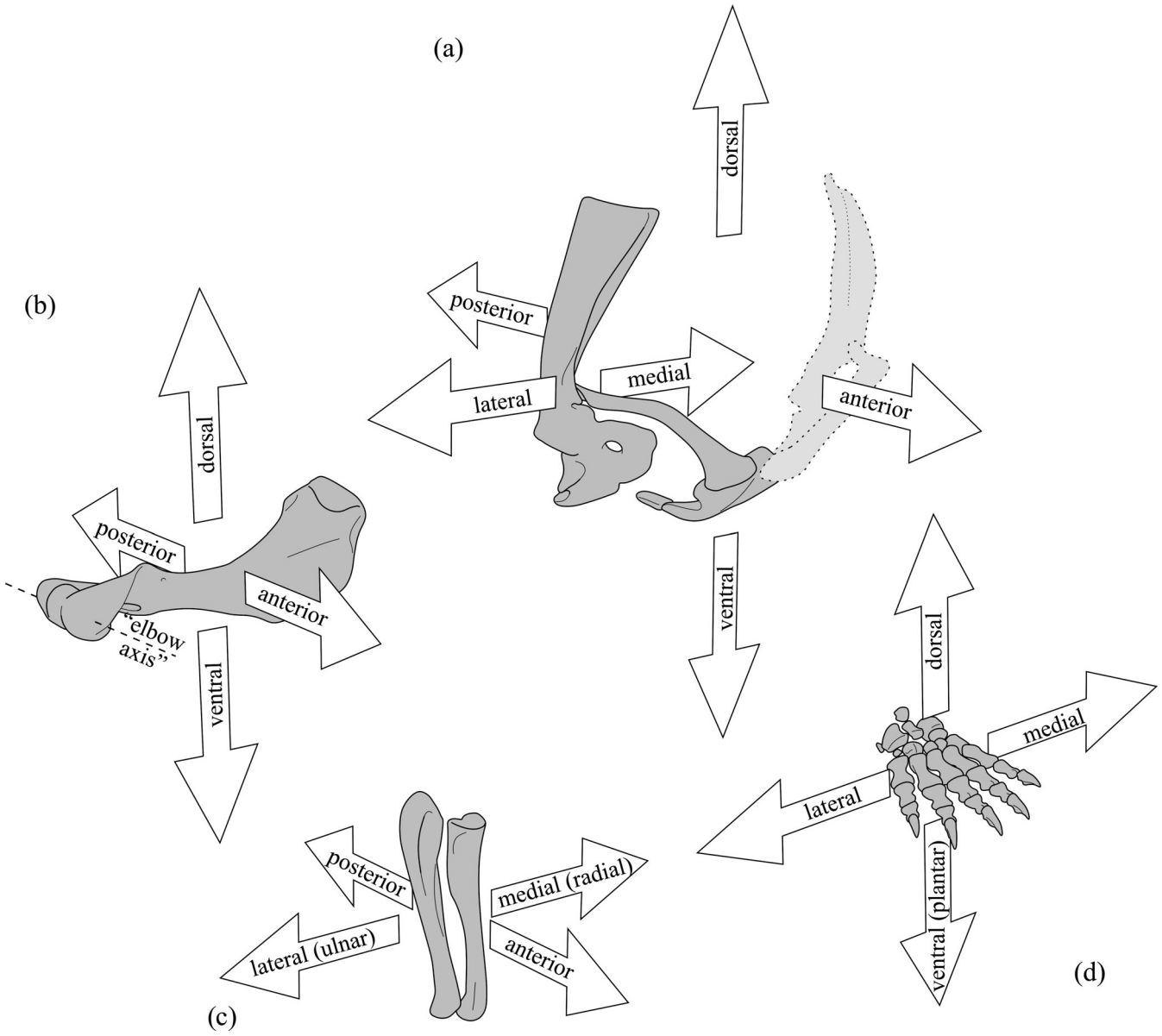

FIGURE 2 Convention of terms used in this study to describe anatomical positioning of each bone, shown with a cynodont pectoral girdle (a), humerus (b), antebrachium (c), and manus (d) as an example. In this and all subsequent figures, bones are illustrated from the right side of the body.

to Hutchinson (2002), the characters and states for each muscle or muscle group are presented below, sequentially addressing the number of muscle heads, the origin(s), and the insertion(s). The states for each character are outlined, and pertinent notes of discussion or justification are presented in a "Remarks" section immediately following. Square brackets are used to denote osteological correlates of muscle attachment. Only if such osteological correlates were observed in fossils was a given extinct OTU coded numerically in the phylogenetic analysis, otherwise, it was coded as unknown ("?").

For clarity, a consistent set of anatomical terms is employed to describe the spatial positioning of attachments on the bones (Figure 2). While the amniote femur has four homologous bone surfaces that can be easily recognized and defined with respect to the femoral condyles (Hutchinson, 2001a), this is less straightforward for the humerus, due to this bone's extreme longitudinal twisting (torsion) in basal amniotes, including "pelycosaurs." Previously, Romer (1922) identified four surfaces of the basal amniote humerus which corresponded to the four faces of a tetrahedron; tracing the "untwisting" of the humerus from "pelycosaurs" through to cynodonts, his "proximal dorsal" and "distal dorsal" surfaces evidently become part of a single "dorsal" surface, and likewise "proximal ventral" and "distal ventral" become part

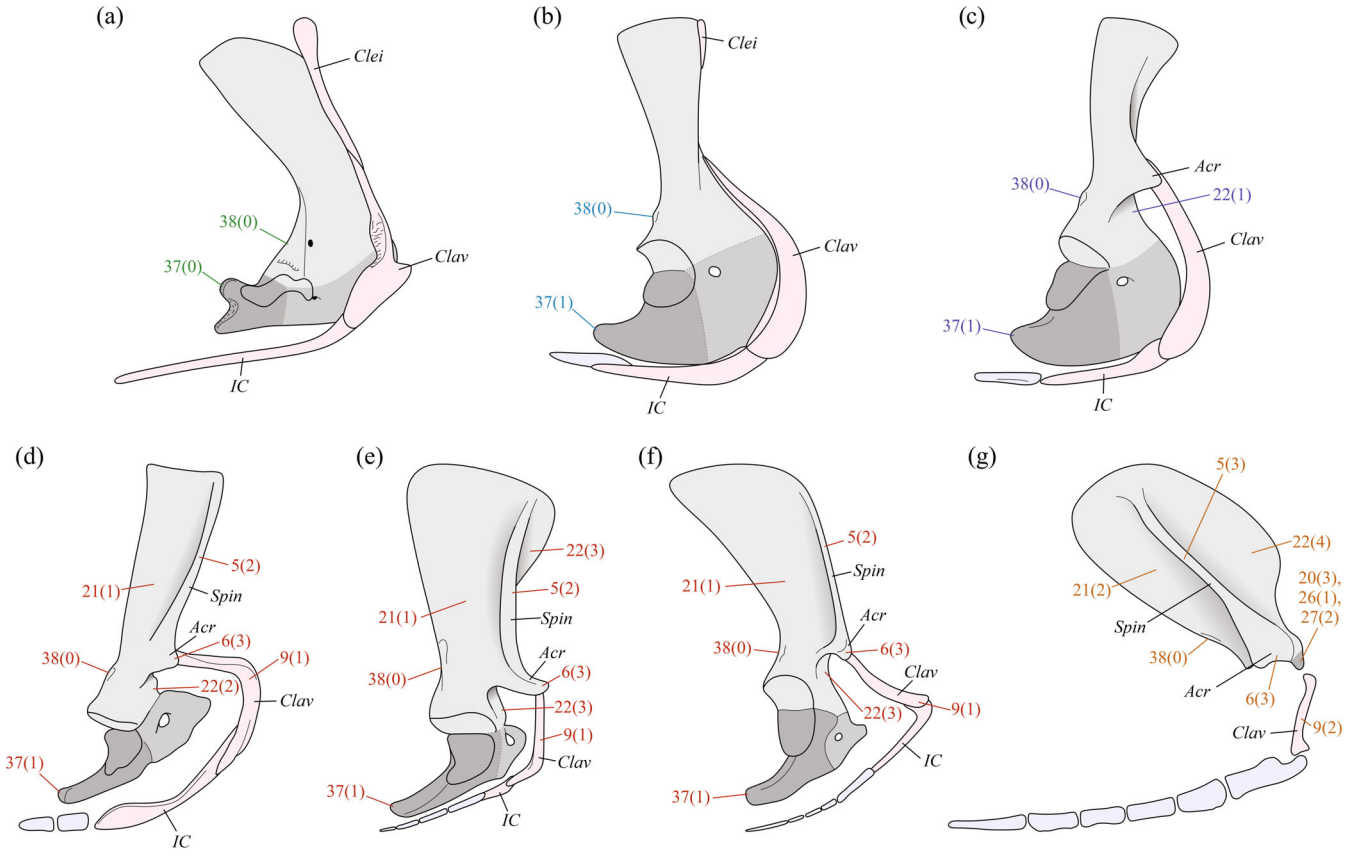

FIGURE 3 Summary of the evolution of pectoral girdle morphology within Synapsida. (a) "Pelycosaur". (b) Therapsid. (c) Bidentalian dicynodont. (d) Eucynodont. (e) Tritylodontid mammaliamorph. (f) Mammaliaform. (g) Therian. Pectoral girdles shown in lateral view (not to scale); dark gray = metacoracoid, medium gray = procoracoid, light gray = scapula. Light pink bones are dermal elements, light purple bones are sternal elements. Individual girdles are not necessarily based on a single taxon, but rather are indicative of the stage in synapsid evolution that they represent, and as such are based on numerous literature sources and first-hand observation of numerous specimens. In this and subsequent figures, features corresponding to muscle character–state combinations with explicit osteological correlates are indicated, with the font and line color used indicative of the major taxonomic group (cf. Figure 1).

of a single "ventral" surface. These surfaces are recognized such that the humerus is horizontally oriented, directed laterally away from the body, and with the axis of elbow flexion–extension being horizontal (see also Brocklehurst et al., 2022). In such a disposition, two additional surfaces are recognized to complete the "anatomical compass"—anterior and posterior, corresponding to "lateral" and "medial" in the mammalian literature. In the twisted humeri of basal amniotes, anterior and posterior surfaces curve about the surface of the bone proximodistally. Terms describing attachments on the radius and ulna are used as if the two bones were articulated naturally, and with the antebrachium oriented vertically and its extensor surface pointing forwards; this gives anterior, posterior, medial (radial-ward) and lateral (ulnar-ward) aspects. Lastly, terms describing attachments on the manus assume that the entire manus is straightened out and oriented horizontally with the digits pointing forward; this gives dorsal, ventral (plantar-ward), medial (digit I-ward), and lateral (digit V-ward) aspects. Note that these terms of reference do not necessarily correspond to an in-life relative positioning of the humerus, antebrachium, or manus. Nomenclature of the individual elements of the scapulocoracoid follows Vickaryous and Hall (2006).

On another terminological note, the muscles involved have typically received different names in the herpetological versus mammalian literature, even if there is no doubt as to homology (abbreviations outlined in Table 1). Given this historical precedent and the profound anatomical transformation that occurred along the mammalian stem lineage, use of a single name for a given muscle will hamper communication. No one name will work well for all purposes; using a herpetological name for a cynodont may be confusing for mammal specialists, and likewise using a mammalian name for a "pelycosaur" may be confusing for early amniote specialists. As a compromise, the muscle is initially referred to using its herpetological name, but

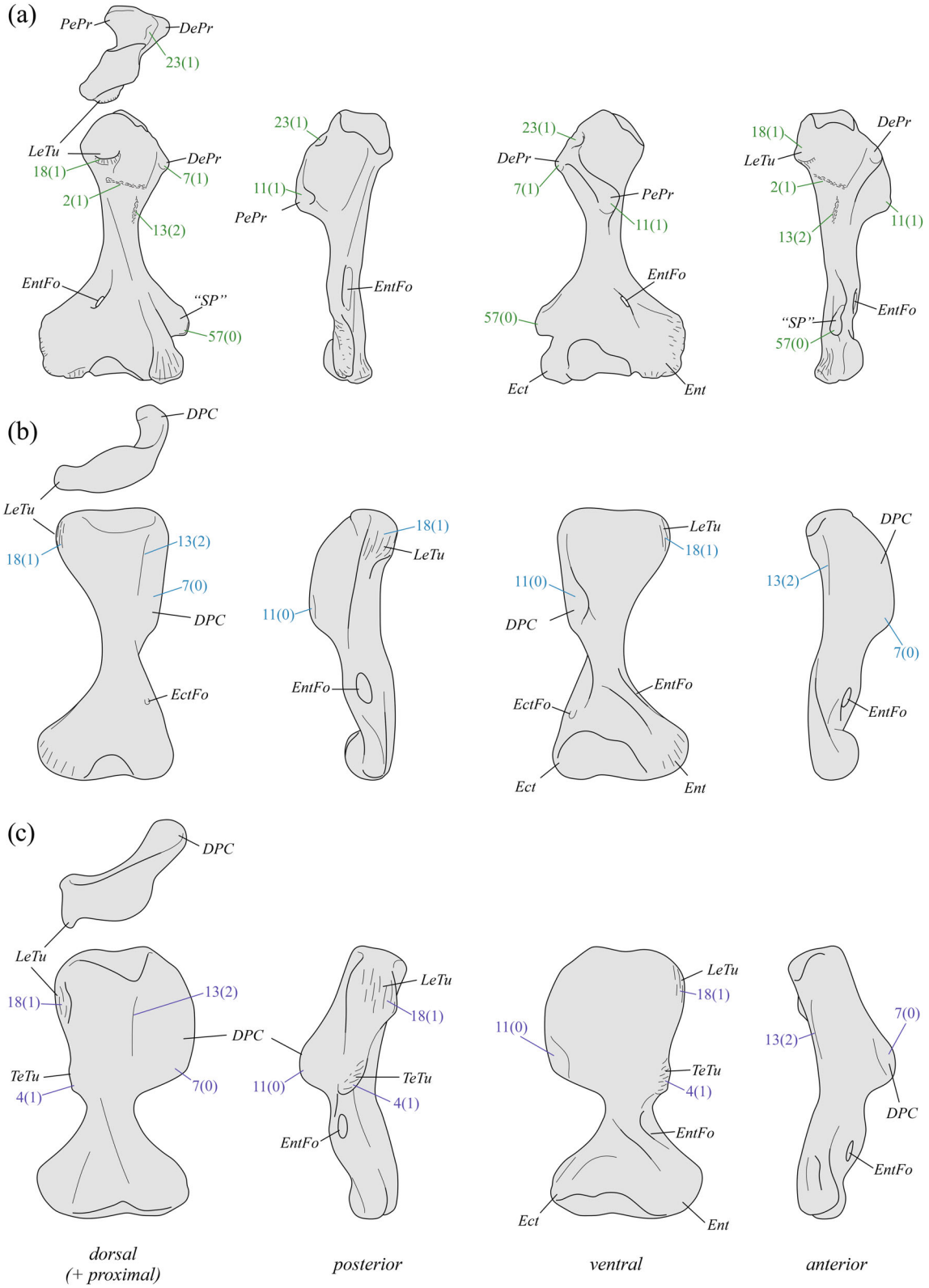

FIGURE 4 Summary of the evolution of humeral morphology within Synapsida. (a) "Pelycosaur". (b) Therapsid. (c) Bidentalian dicynodont. (d) Eucynodont. (e) Therian. Individual humeri (not to scale) are not necessarily based on a single taxon, but rather are indicative of the stage in synapsid evolution that they represent, and as such are based on numerous literature sources and first-hand observation of numerous specimens.

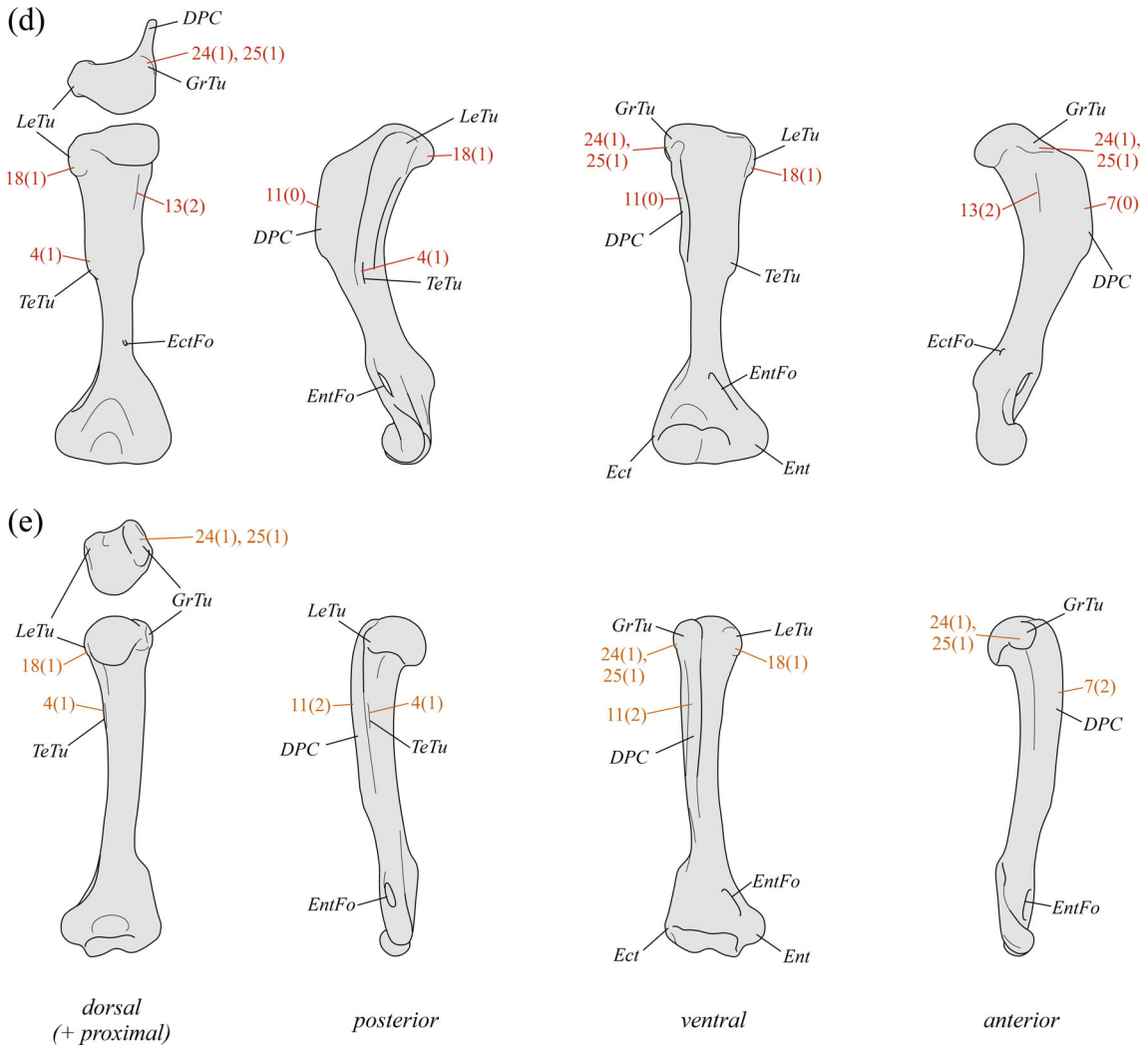

FIGURE 4 (Continued)

when it exhibits a more "mammalian" manifestation, the mammalian name is used instead. So, for example, when the triceps coracoideus shifts its origin onto the latissimus dorsi, it "becomes" the dorsoepitrochlearis. This approach does not distinguish between plesiomorphic and apomorphic states, providing a neutral means to communicate character evolution.

Schematic summaries of changes in gross osteology from basal synapsids through to crown mammals are presented for the pectoral girdle (Figure 3), humerus (Figure 4), antebrachium (Figure 5), and manus (Figure 6). These provide a broader skeletal context for the subsequent figures that focus on the evidence for specific muscles, and also illustrate major trends in skeletal transformation on the line to mammals. Abbreviations used for key anatomical landmarks in the text and figures are as follows: Acr = acromion, BicFos = bicipital fossa, Clav = clavicle, Clei = cleithrum, DePr = deltoid process, DPC = deltopectoral crest, Ect = ectepicondyle, EctFo = ectepicondylar foramen, Ent = entepicondyle, EntFo = entepicondylar foramen, Ext = scarring of digital extensor origins, Flex = scarring of digital flexor origins, GrTu = greater tuberosity, Hum = humerus, I–V = digits I–V, IC = interclavicle, LeTu = lesser tuberosity, Olec = olecranon, PePr = pectoral process, Pis = pisiform, "SP" = "supinator" (brachioradialis) process, Spin = scapular spine, TeTu = teres tuberosity. In all figures, bones are illustrated from the right side of the body.

3.1 | Latissimus dorsi (LD, Figures 4 and 7): Characters 1 and 2

1. Origin

0. Dorsal fascia and/or neural spines of thoracic/dorsal vertebrae posterior to scapula

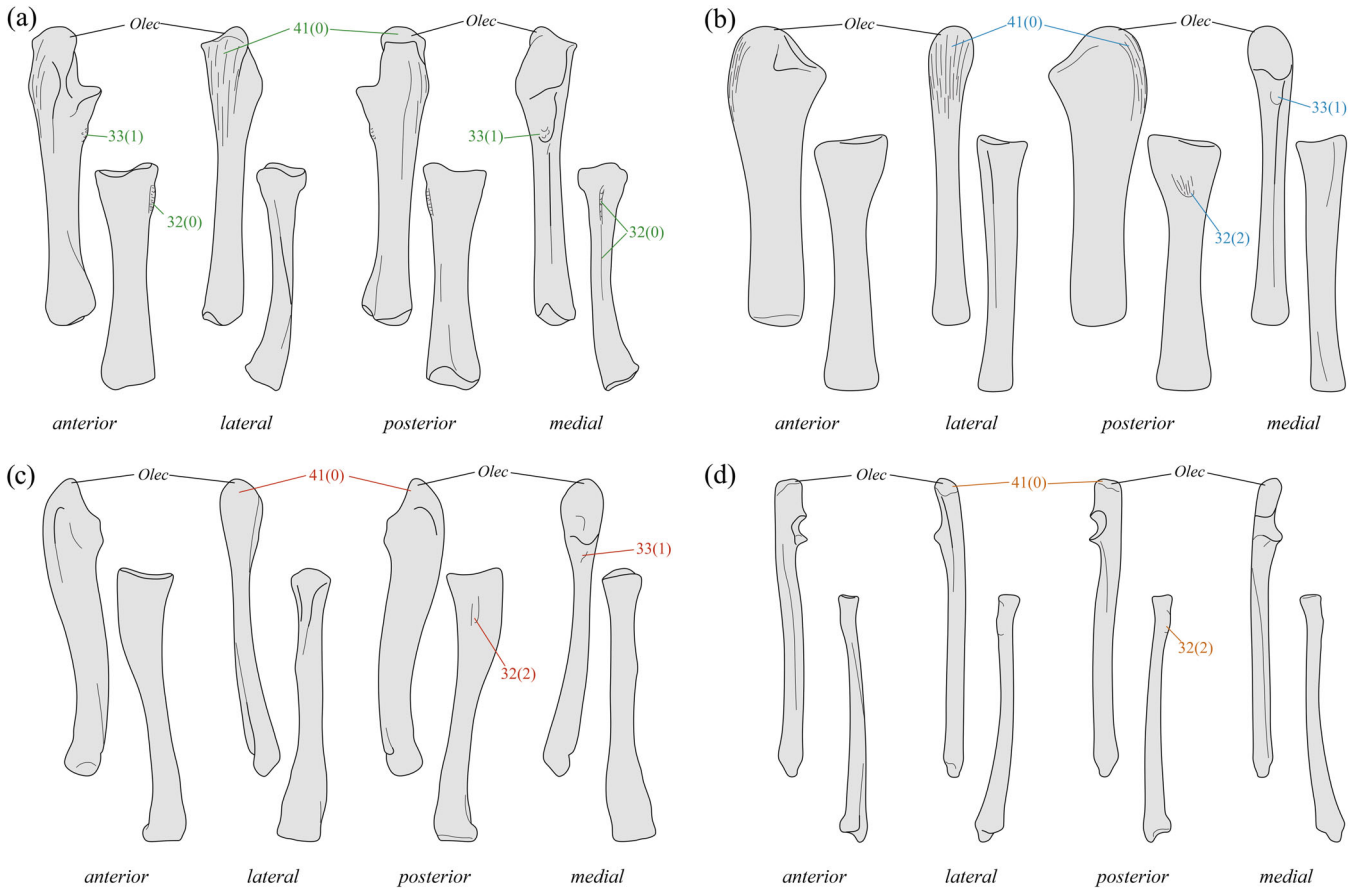

FIGURE 5 Summary of the evolution of antebrachial morphology within Synapsida. (a) "Pelycosaur". (b) Therapsid. (c) Eucynodont. (d) Therian. Each panel shows the ulna (upper row) and radius (lower row). Individual bones (not to scale) are not necessarily based on a single taxon, but rather are indicative of the stage in synapsid evolution that they represent, and as such are based on numerous literature sources and first-hand observation of numerous specimens.

1. As (0), with second discrete attachment to lateral surface of ribs
2. As (0), with subdivision from lateral aspect of posterodorsal scapula

2. Insertion

0. Dorsal aspect of proximal humerus, posterior to insertions of deltoids, and supracoracoideus [tubercle, rugosity, or sulcus]
1. Dorsal aspect of proximal humerus, posterior to insertions of deltoids, and supracoracoideus [transverse line of scarring]
2. Proximal tendon of origin of triceps scapularis
3. Posterior aspect of humeral entepicondyle or adjacent shaft [linear tubercle]

Remarks—Romer (1922) interpreted a roughened transverse line on the humerus of various "pelycosaurs" (e.g., Figure 7b) as demarcating the boundary between the insertion of the LD (proximally) and the origins of the humeral triceps heads (distally), corresponding to state 1. Later (Romer & Price, 1940), he re-interpreted the locus of LD insertion to be a pronounced tubercle positioned more proximally on the humerus, which he previously interpreted as for the subscapularis (SSc, see character 18 below); the SSc now was deemed to insert on the posteroproximal apex of the humerus instead. However, extensive first-hand observations provide greater support for his original interpretation. First, while the transverse line may terminate posteriorly near the large tubercle in "pelycosaurs," they are well separated in captorhinids (and some diadectomorphs), and indeed the transverse line terminates posteriorly in its own tubercle (Figure 7a; Holmes, 1977). This argues for the insertion of two separate muscles in early amniotes, away from the corner of the bone. Second, well-preserved "pelycosaur" humeri show that the articular surface of the caput extends right to the posterior corner of the bone, such that any scarring textures here are more likely for joint capsule attachment. Thus, the transverse line is

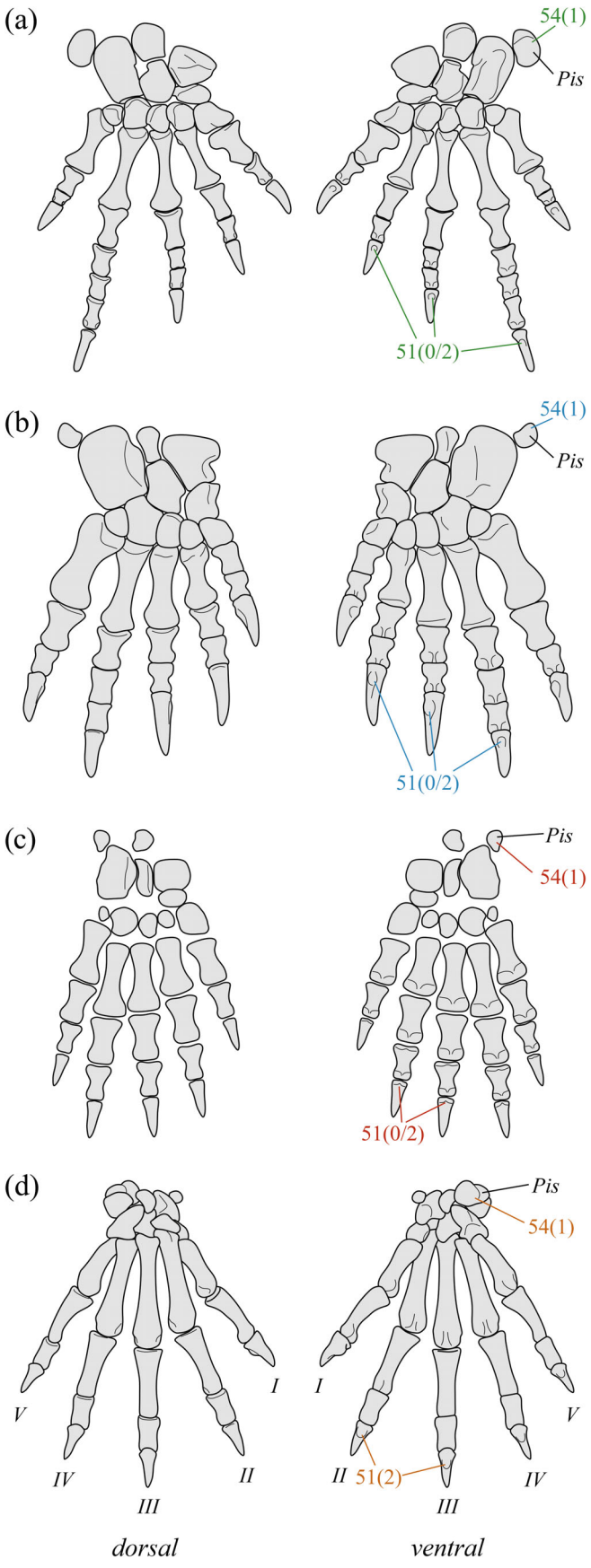

considered as denoting the insertion of the LD, with the SSc inserting on the pronounced tubercle; this tubercle is hence homologous to the lesser tuberosity (LeTu) of mammals and may be referred to as such.

In contrast to "pelycosaurs," the proximal surface of therapsid humeri is usually devoid of unambiguous osteological indicators of LD insertion. Probable exceptions include at least one specimen of the tapinocephalid *Moschops* with a broad, rugose pit near midshaft (Figure 7c), some gorgonopsians that possess an ill-defined pit on the posterior aspect of the humerus, just proximal to midshaft (Figure 7e–g), and some specimens of the cynognathian *Diademodon* (Figure 7n), which possess a ridge superficially similar to the condition in "pelycosaurs." The basal probainognathian *Trucidocynodon* also possesses two well-defined, ridge-like scars on the proximal dorsal humerus (Figure 7o), topologically similar to the condition in *Diademodon*, suggesting that the posterior of the two is for insertion of the LD (De Oliveira et al., 2010). Lastly, eutherocephalians frequently exhibit an ovoid pit on the mid-dorsal surface of the humerus (Figure 7h–m), which is somewhat more distally positioned compared to "pelycosaurs." Previously, Kemp (1980a) and Lai et al. (2018) interpreted a small process on the posterior humerus of cynognathian cynodonts as denoting the insertion of the LD, but strong evidence argues in favor of the teres major inserting here instead (see character 4).

3.2 | Teres major (TMA, Figures 4 and 8): Characters 3 and 4

3. Origin

0. Absent
1. Lateral aspect of posterodorsal scapula
2. Lateral aspect of expanded posterodorsal scapula, with postscapular fossa [posterodorsal angle expanded and distinct fossa present]

Remarks—The homology of the TMA among amniotes has recently been clarified through the embryological

FIGURE 6 Summary of the evolution of manual morphology within Synapsida. (a) "Pelycosaur". (b) Therapsid. (c) Cynodont. (d) Therian. Each panel shows the manus in dorsal (left) and ventral (right) view. Individual mani (not to scale) are not necessarily based on a single taxon, but rather are indicative of the stage in synapsid evolution that they represent, and as such are based on numerous literature sources and first-hand observation of numerous specimens. Among other things, note the increasing mediolateral symmetry of the manus in more crownward taxa.

work of Smith-Paredes et al. (2022). Whereas the TMA of therians (at least) develops from the same embryonic mass as the SSc, the same-named muscle of crocodylians and testudines develops from the same mass as the LD; thus, the TMA of mammals and archelosaurs are not homologous. Within lepidosaurs, a TMA-like muscle has

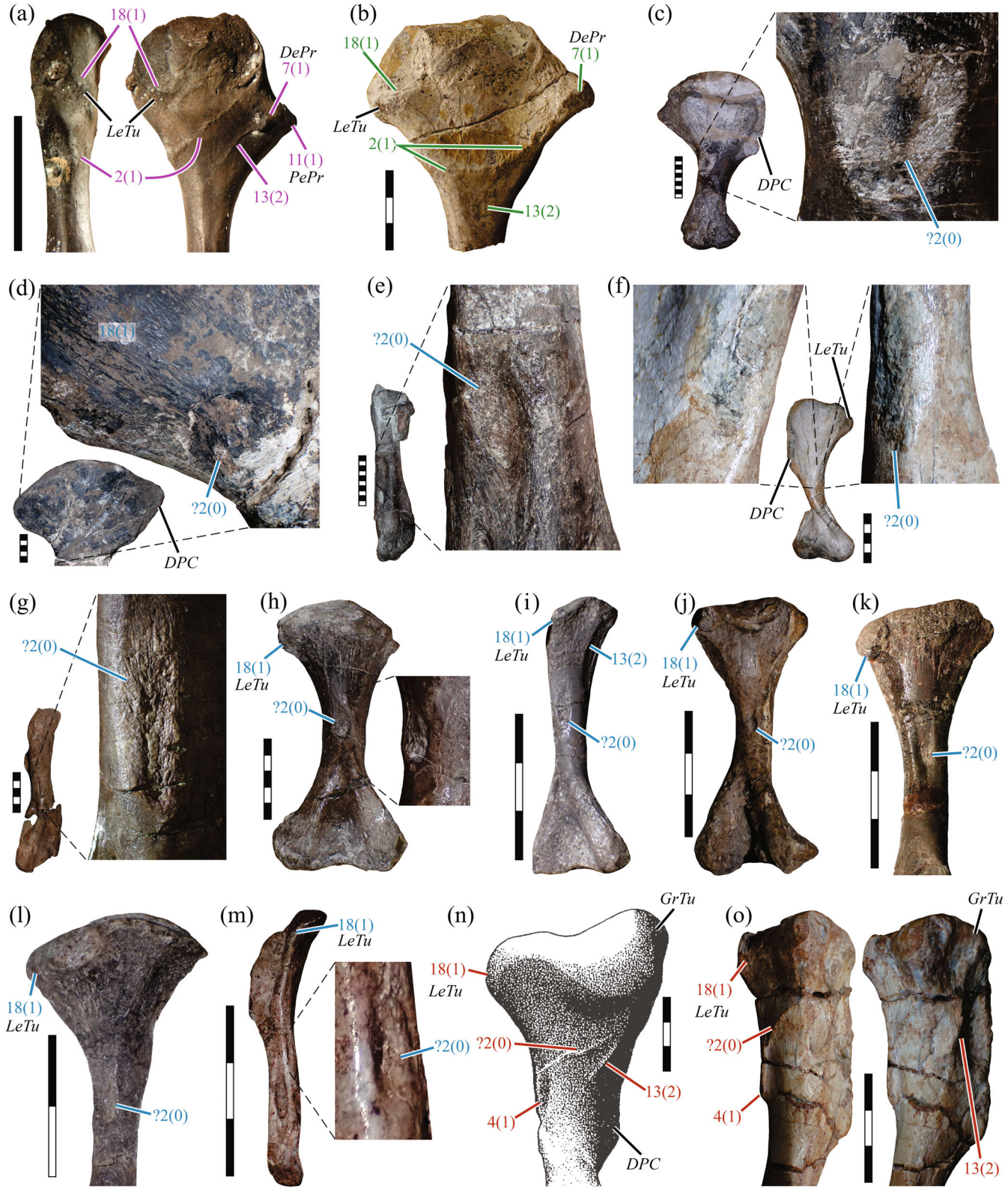

FIGURE 7 Legend on next page.

only been reported in the agamid *Uromastyx* (Lécuru, 1968), where it inserts separately and posteriorly to the LD. In the context of the present synapsid-focused study, crocodylians and squamates are coded as state 0 here (and for the following character) for they lack a "mammalian" TMA; the archelosaur condition is only recognized through character 1 (state 2) above. State 2 of the present character is created to accommodate the morphology observed in several fossorial extant mammals, as well as *Cynognathus* and some tritylodontids (Jenkins, 1971; Sues & Jenkins, 2006). Although a postscapular fossa is lacking, the scapular blade of the eutherocephalian *Promoschorhynchus* bears distinctive scarring on the lateral aspect of much of its posterior half, terminating ventrally in a shallow pit (Figure 8a). This scarring may indicate attachment of a TMA-like muscle, or alternatively represent a modified origin of the deltoideus scapularis (see character 5 below).

4. Insertion

0. Absent
1. Posterior aspect of proximal humerus, distal to LeTu [linear ridge, tubercle, or tuberosity]

Remarks—A ridge or other linear scar is present on the posteroproximal humerus of epicynodonts, distal to and in line with the LeTu, and this basic manifestation can be traced continuously through more derived synapsids to therians (Figure 8b–o). In extant therians, this scar is associated primarily with the insertion of the TMA (state 1, often being termed the "teres tubercle" or "teres tuberosity," TeTu), and in some Mesozoic mammals its apomorphic enlargement coincides with an expanded posterodorsal scapula surface or development of a postscapular fossa (e.g., Hu, 2006; Luo & Wible, 2005; Martin, 2005). These observations strongly argue for the identification of state 1 in epicynodonts and more derived taxa. Remarkably, a virtually identical structural arrangement is also observed in many dicynodonts, including the basal form *Eodicynodon*, wherein the TeTu tends to be more developed and more heavily scarred on the humerus' ventral surface, and forms a dorsally everted lip (Figure 8p–w; "pinna-like process" of DeFauw, 1986). Maximum likelihood ASR posits the transition to state 1 as having occurred close to the base of Therapsida (Supporting Information Appendix S4), but nondicynodont anomodonts lack any indication of scarring on the proximal humerus comparable to that in dicynodonts or epicynodonts (Brinkman, 1981; Cisneros et al., 2015; Fröbisch & Reisz, 2011), as do all other noncynodont therapsids. The absence of phylogenetic continuity implies nonhomology between the scars in epicynodonts and dicynodonts, and in turn nonhomology between the muscles that inserted on them (but see Discussion).

Given the common developmental origin of the TMA and SSc in extant therians, it would be expected that when the two first differentiated in synapsid evolution, their insertions on the humerus would have been immediately adjacent to each other. The humeri of some cynodonts and dicynodonts, although possessing a distinct TeTu and LeTu, also possess a ridge spanning between the two scars (Figure 8b,c,e,i–m,q,r,u,v), approximating what might be expected as the transitional condition. This morphology is consistent with an incomplete separation of TMA and SSc masses in these taxa, and further supports the identification of the TeTu as the attachment point for the TMA in cynodonts, and a TMA-like muscle in dicynodonts. Extant monotremes also display a similar condition, where the TeTu is connected to an expanded LeTu by a well-developed ridge, almost to the point that the two structures form part of a single flange of bone (Figure 8n).

The distinction of putative TMA scarring from the insertion of the SSc is clear in these fossils, but

FIGURE 7 Osteological evidence of latissimus dorsi musculature attachment to the humerus in synapsids. (a) USNM PAL 643598 cf. *Captorhinus* (Captorhinidae) in posterior (left) and dorsal (right) views. (b) MCZ VPRA-1314 *Dimetrodon limbatus* (Sphenacodontia) in dorsal view. (c) AMNH FARB 5553 *Moschops capensis* (Tapinocephalidae) in anterodorsal view. (d) SAM-PK-9149 *Jonkeria truculenta* (Titanosuchidae) in dorsal view. (e) NMQR 4000 *Inostrancevia africana* (Kammerer et al., 2023) in posterior view. (f) SAM-PK-K1676 Gorgonopsia indet, whole bone and left inset in ventral view, right inset in posterior view. (g) UMZC T.883 Gorgonopsia indet. in posterior view. (h) NMQR 3351 *Moschorhinus kitchingi* (Eutherocephalia) in dorsal view, inset in anterodorsal view. (i) BP/1/3973 *Olivierosuchus parringtoni* (Botha-Brink et al., 2014; Eutherocephalia) in dorsal view. (j) NMQR 3375 *Theriognathus microps* (Eutherocephalia) in dorsal view. (k) GPIT-PV-117121 *Silphoictidoides ruhuhuensis* (Eutherocephalia) in dorsal view. (l) SAM-PK-K11515 *Scaloposaurus constrictus* (Eutherocephalia) in dorsal view. (m) NMQR 3189 *Microgomphodon oligocynus* (Eutherocephalia) in posterior view. (n) NMQR 1205 *Diademodon tetragonus* (Cynognathia) in dorsal view; this illustration, modified from Jenkins (1971), is a composite based on multiple specimens (hence scale is approximate only). (o) UFRGS-PV-1051-T *Trucidocynodon riograndensis* (basal probainognathian) in dorsal view, illuminated from different directions. Unless otherwise indicated, all scale bars in this and the following figures are in increments of centimeters.

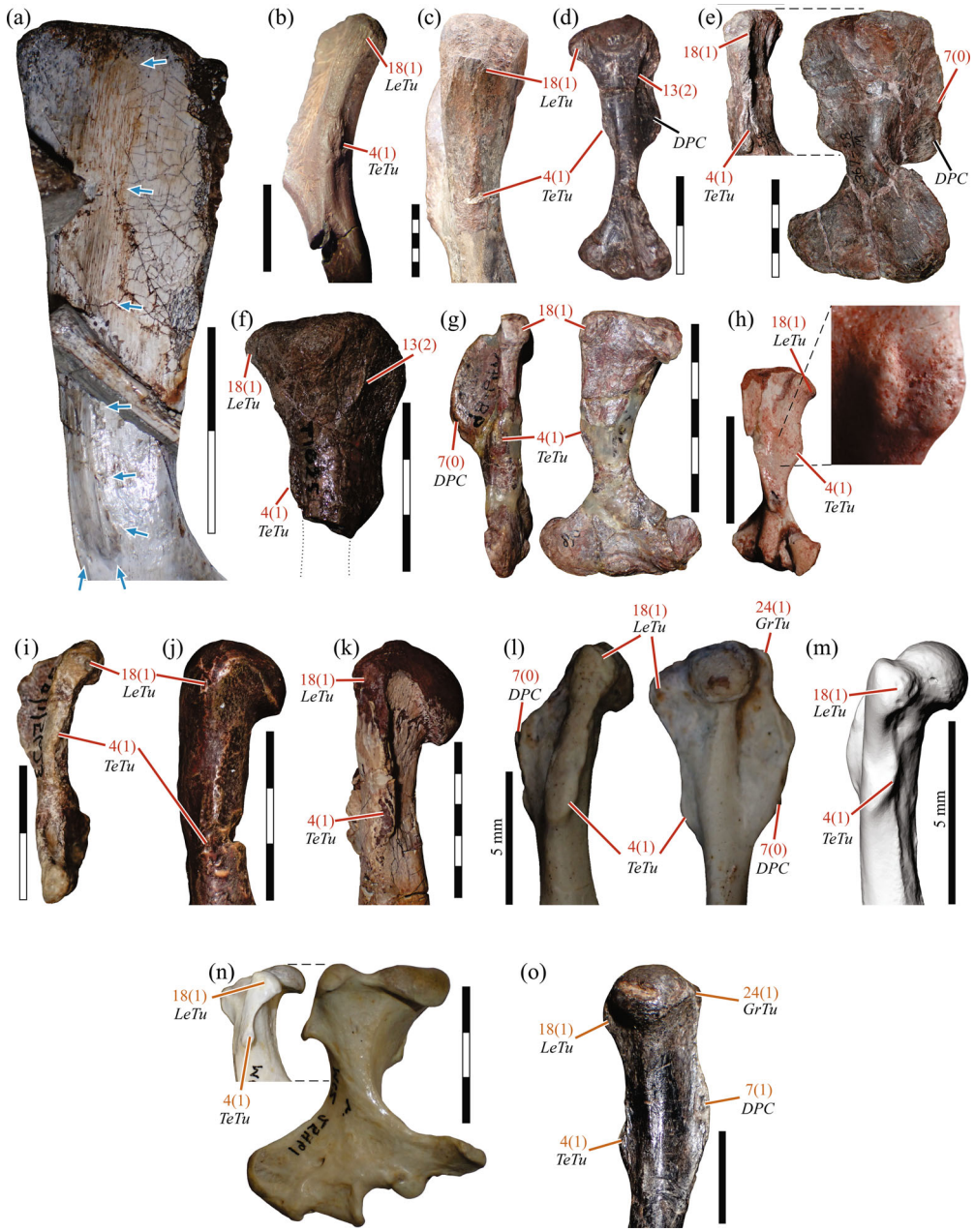

FIGURE 8 Osteological evidence of teres major musculature attachment in synapsids. (a) SAM-PK-K10014 *Promoschorhynchus* cf. *P. platyrhinus* (Eutherocephalia) scapula in lateral view, arrows delimit possible origin. (b) UMZC T.823 *Galesaurus planiceps* (Epicynodontia) humerus in posterior view. (c) NHMUK PV R.3772a *Cynognathus* sp. (Cynognathia) in posterior view. (d) MCZ VPRA-3691 *Massetognathus pascuali* (Cynognathia) humerus in dorsal view. (e) MCZ VPRA-4503 *Exaeretodon argentinus* (Cynognathia) humerus in posterior (left) and dorsal (right) views. (f) UMZC T.1025 Traversodontidae indet. (Cynognathia) humerus in dorsal view. (g) MCZ VPRA-4002 *Chiniquodon theotonicus* (basal probainognathian) humerus in posterior (left) and dorsal (right) views. (h) UFRGS-PV-599-T *Irajatherium hernandezi* (Tritheledontidae) humerus in ventral view; note that this specimen is remarkable in possessing two putative tuberosities for muscular attachment, with other specimens possessing only a single tuberosity (Guignard et al., 2019b). (i) BP/1/5623 *Pachygenelus monus* (Tritheledontidae) humerus in posterior view. (j) BP/1/5671 *Tritylodon longaevus* (Tritylodontidae) humerus in posterior view. (k) MCZ VPRA-8812 *Kayentatherium wellesi* (Tritylodontidae) humerus in posterior view. (l) UFRGS-PV-1043-T *Brasilodon quadrangularis* humerus in posterior (left) and dorsal (right) views. (m) MCZ VPM-19940 *Eozostrodon parvus* (Mammaliaformes) humerus in posterior view; render of digital model acquired via X-ray micro-computed tomographic scanning (Skyscan 1273 [Bruker, U.S.A.] 90 kV, 300 μA, 288 ms exposure time, 1 mm aluminum filter, 23.8 μm isotropic voxel resolution). (n) MCZ 25461 *Tachyglossus aculeatus* (Monotremata) humerus in posterior (left) and dorsal (right) views. (o) MACN-N 09 *Vincelestes neuquenianus* (cladotherian, i.e., stem therian) humerus in dorsal view. (p) NMQR 3154 *Eodicynodon oosthuizeni* (Dicynodontia) humerus in ventral view. (q) NHMUK PV R.4067 *Oudenodon bainii* (Dicynodontia) humerus in posterior (left) and dorsal (right) views. (r) GPIT-PV-60755 *Rhachiocephalus magnus* (Dicynodontia) humerus in ventral (left) and posterior (right) views. (s) NHMUK PV R.37080 *Kitchinganomodon crassus* (Dicynodontia) humerus in ventral view. (t) GPIT-PV-60766 *Daptocephalus leoniceps* (Dicynodontia) humerus in posterior (left) and ventral (inset) views. (u) NHMUK PV R.37374 Dicynodontia indet. humerus in posterior view. (v) NMQR 3940 *Lystrosaurus mccaigi* (Dicynodontia) humerus in posterior view. (w) GPIT-PV-117203 *Lystrosaurus* sp. (Dicynodontia) humerus in ventral view. See also Figures 7 and 10.

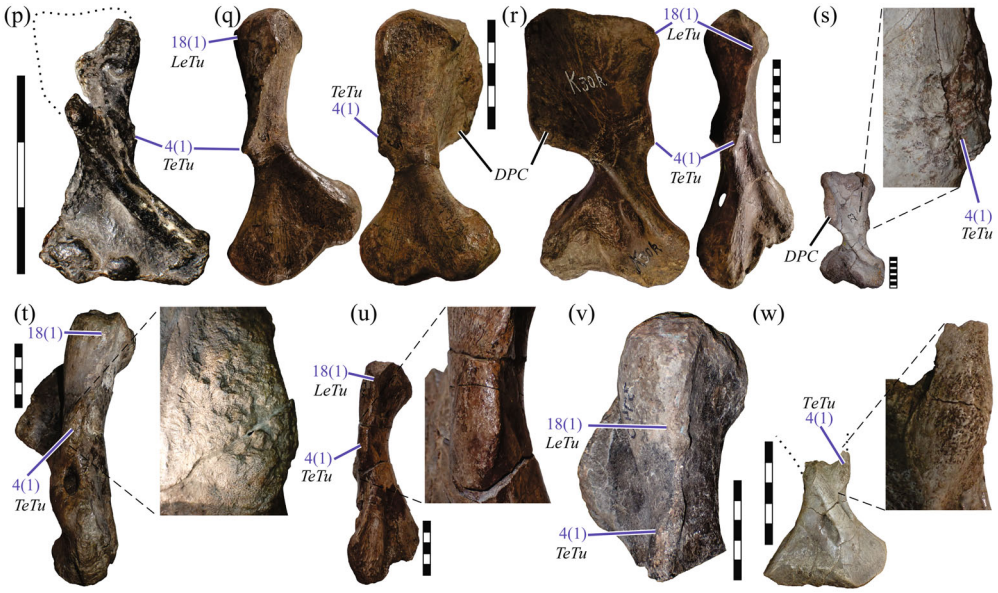

FIGURE 8 (Continued)

distinguishing it from potential scarring of the LD insertion is less straightforward. Among extant tetrapods, while the LD can leave an indication of its attachment, it frequently does not, in spite of its ubiquitous presence. Numerous prior studies of dicynodonts have interpreted the posterior margin of the proximal humerus as the site of insertion of the LD, including on the TeTu when present (e.g., Angielczyk et al., 2009; DeFauw, 1986; King, 1981a, 1981b; Ray, 2006; Ray & Chinsamy, 2003; Walter, 1988b; Watson, 1917), yet as outlined above osteological and developmental evidence better supports inferring the insertion of a TMA-like muscle instead. In the present study, a scar on the posterior to dorsal aspect of the proximal humerus of a given therapsid is conservatively presumed to indicate insertion of the LD, which can be confidently inferred to have existed. Only when strong evidence for a TMA exists should this be considered the more likely candidate. Such evidence includes phylogenetic continuity (traceability) through to the TeTu of crown mammals, osteological association with the LeTu, and the presence of multiple discrete scars (e.g., De Oliveira et al., 2010; Jenkins, 1971). Currently, compelling evidence for a TMA or TMA-like muscle only exists within dicynodonts and epicynodonts.

3.3 | Deltoideus group (Figures 3, 4, and 9): Characters 5–9

5. Deltoideus scapularis (DSc) origin

0. Much of lateral surface of dorsal scapula and/or suprascapula
1. Lateral anterodorsal scapula [thickened, laterally reflected anterodorsal margin]
2. Anterior margin of scapula [most of anterior margin is laterally reflected]
3. Posterior margin of scapular spine (= deltoideus spinalis, DSp) [thickened scapular spine located posterolateral to anterior margin of scapula]

Remarks—The traditional interpretation of DSc evolution within synapsids (e.g., Gregory & Camp, 1918; Guignard et al., 2019b; Jenkins, 1971; Lai et al., 2018; Romer, 1922) is that its origin tracked the anterior margin of the scapular blade: as the margin became laterally reflected and moved posteriorly (forming the scapular spine), so too did the DSc, becoming the DSp of therians. Based on developmental evidence, Smith-Paredes et al. (2022) posited an alternative hypothesis of more radical transformation of origin sites, involving a spatial disassociation between muscle and bone for multiple muscles. Abundant fossil evidence and the anatomy of extant monotremes do not support some aspects of this hypothesis, but are more consistent with the traditional interpretation; this is explored in full in the Discussion after all the fossil evidence has been documented first.

The scapular blade of eutherocephalians lacks any indication of a laterally reflected anterior margin, yet many taxa exhibit a longitudinal median ridge running along much of the blade's lateral surface (Figure 9h,i; Attridge, 1956; Botha-Brink & Modesto, 2011; Fourie, 2013; Fourie & Rubidge, 2007; King, 1996). This ridge may indicate the boundary between the DSc (posteriorly) and the trapezius (anteriorly) in eutherocephalians. No muscle scarring texture has been observed on the ridge in any specimen thus far examined, but this may be due to their generally small size.

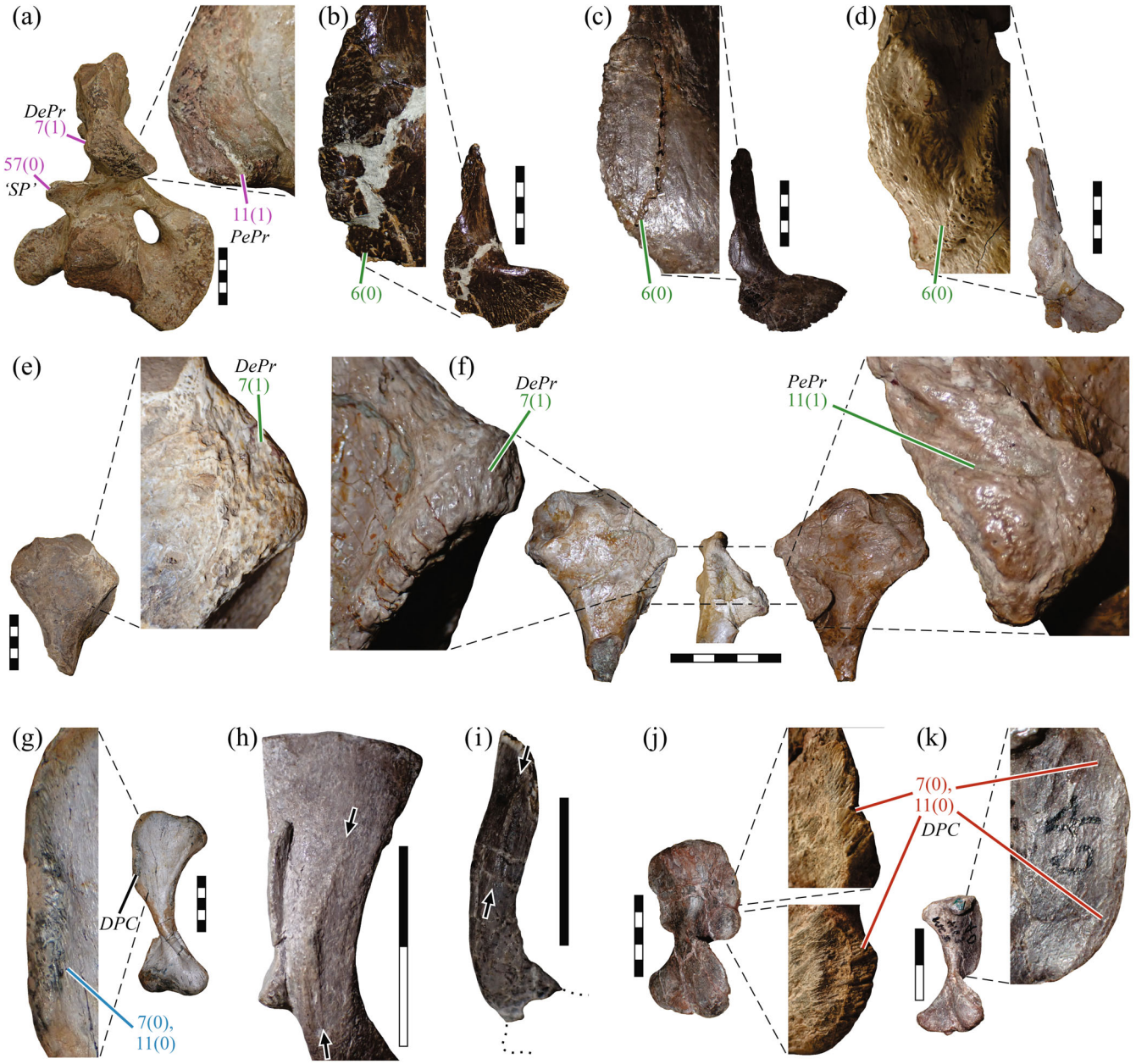

FIGURE 9 Osteological evidence of deltoid and pectoral musculature attachment in synapsids. (a) AMNH FARB 4380 *Diadectes* sp. (Diadectomorpha) humerus in ventral view (inset in posteroventral view). (b) MCZ VPRA-4316 *Edaphosaurus boanerges* (Edaphosauridae) clavicle in ventrolateral view. (c) UCMP 83489 *Sphenacodon ferox* (Sphenacodontia) clavicle in ventrolateral view. (d) MCZ VPRA-1367 *Dimetrodon milleri* (Sphenacodontia) clavicle in ventrolateral view. (e) AMNH FARB 4082 *Secodontosaurus obtusidens* (Sphenacodontia) humerus in dorsal view. (f) MCZ VPRA-1367 *Dimetrodon milleri* humerus in (left to right) dorsal, anterior, and ventral views. (g) SAM-PK-K1676 Gorgonopsia indet. humerus in ventral view. (h) SAM-PK-11515 *Scaloposaurus constrictus*. (Eutherocephalia) scapular blade in lateral view. (i) SAM-PK-K11522 *Tetracynodon* sp. (Eutherocephalia) scapular blade in anterolateral view. (j) MCZ VPRA-4503 *Exaeretodon argentinus* (Cynognathia) humerus in anterodorsal view. (k) MCZ VPRA-4163 *Chiniquodon theotonicus* (basal probainognathian) humerus in dorsal view. Arrows in (h) and (i) indicate longitudinal scapular ridge.

6. Deltoideus clavicularis (DCl) origin

0. Lateral aspect of clavicle and interclavicle
1. Anterior end of procoracoid [all dermal girdle elements absent]
2. Anterolateral aspect of ventral scapula [clavicles absent]
3. Ventrolateral acromial process of scapula (= deltoideus acromialis, DAc) [acromial process and infraspinous fossa]

Remarks—In squamates, the origin extends around to the dorsal and anterior surfaces of the clavicle, and can be

situated more on the medial side of the bone, to produce a complex folded morphology to the muscle (Russell & Bauer, 2008). However, this does not manifest in a different structure to the clavicle itself, and so at an osteological level is indistinguishable from the condition in *Sphenodon*; both are coded as state 0 here.

The clavicles of "pelycosaurs" and some stem amniotes bear a spatulate flange on the posterolateral margin of the ascending process, which is directed posteriorly (e.g., Berman & Sumida, 1990; Holmes, 1977; Romer & Price, 1940). This flange is especially well developed in sphenacodontids, where it is lobate and heavily scarred on its lateral (external) surface (Figure 9b–d); it likely served at least part of the origin of the DCl in these animals (Romer & Price, 1940).

Traditionally, the DAc of mammals has been considered intimately tied with the DCl (Diogo et al., 2016), but Smith-Paredes et al. (2022) demonstrated that the DCl of therians is derived from the supracoracoideus mass, not the deltoid mass, and suggested the DAc to be a therian apomorphy. In the revised transformational hypothesis considered here, the DAc of extant mammals has a one-to-one correspondence with the DCl of nonmammals (Table 1), having undergone a dorsal shift in origin, onto the scapula, as it was displaced by a dorsally expanding supracoracoid mass (see Discussion). Given that an acromion and infraspinous fossa are well-supported osteological correlates of a dorsally shifted and differentiated supracoracoideus (see character 22 below), their presence is therefore also indicative of a dorsally shifted DCl mass (state 3). This transformation would have occurred prior to *Procynosuchus*, the basalmost cynodont with an infraspinous fossa and acromion (Broom, 1947), but a comparable condition is also observed in the Permian dicynodont *Dicynodontoides* (Cox, 1959) and in Triassic kannemeyeriiform dicynodonts, where a shallow "infraspinous fossa" and posteriorly shifted acromion occur (see below).

7. DSc insertion

0. Anterodorsal aspect of deltopectoral crest (DPC) of humerus, on or near apex [singular DPC with localized apex]
1. Anterodorsal aspect of proximal humerus, on tubercle, distinct from ventral process for pectoralis attachment ["deltoid process," scarring; may continue distally on linear ridge]
2. Anterodorsal aspect of entire length of DPC of humerus [DPC ridge-like]
3. Anterior proximal humerus, proximal to and separate from DPC

Remarks—Among extant tetrapods, the anteroproximal humerus bears a single major eminence, the "deltopectoral crest," to which the deltoideus and pectoralis musculature attach. (Crocodylians are an exception: state 3.) However, exactly what constitutes a "deltopectoral crest" is somewhat nebulous when stem and early crown amniotes are taken into consideration, where the putative insertions for both muscle groups form their own distinct eminences, connected by a bridge of bone. This more complex structure, or just the bridge itself, has previously been referred to as the "deltopectoral crest" (e.g., Brinkman & Eberth, 1983; Fox & Bowman, 1966; Holmes, 1977; Romer, 1922, 1956; Romer & Price, 1940; Sumida, 1997; White, 1939), as has a comparable structure in temnospondyls (e.g., Pawley, 2007; Pawley & Warren, 2006; Romer, 1922). In the context of synapsid evolution, distinct eminences for deltoid and pectoral attachment are recognizable throughout "pelycosaurs" (Romer & Price, 1940), wherein they may be termed the "deltoid process" and "pectoral process" respectively (state 1). The apex of the deltoid process is typically continued distally for a short distance by a sharp ridge that may also be scarred (Figure 9e,f). With the transition to therapsids, this region of the humerus is structurally simplified to form a single blade-like expansion (Bishop et al., 2023; state 0); it more closely approximates the structure in extant nonmammals and may be more reasonably termed a "deltopectoral crest."

8. DCl insertion

0. Anterodorsal aspect of humerus, adjacent to or in common with DSc
1. Anterodorsal aspect of humerus, well separated from DSc

9. "Clavicular deltoid" division of supracoracoideus

0. Absent
1. Present, originating from ventral aspect of clavicle and interclavicle, and inserting adjacent to DSc and DCl on DPC of humerus
2. Present, originating from ventral clavicle only (interclavicle absent), and inserting adjacent to DSc and DCl on DPC of humerus

Remarks—As noted above, developmental evidence indicates that the DCl of therians is derived from the supracoracoideus mass, and hence not homologous with the DCl of nonmammals (Smith-Paredes et al., 2022); although yet to

be verified, it is presumably the same case for monotremes. The present character accounts for this. Unambiguous osteological correlates of subdivision of the "clavicular deltoid" from the SPC mass are absent, but as noted above a dorsal shift in the SPC mass can be reasonably correlated with the appearance of an acromion and supraspinous fossa. In such a scenario, the "clavicular deltoid" probably appeared around the origin of Cynodontia, although maximum likelihood ASR suggests a later origin (Supporting Information Appendix S4). The loss of a distinct interclavicle as it was incorporated into the sternal complex in stem therians (Bendel et al., 2022; Brent et al., 2023) probably coincided with a restriction of the origin of the "clavicular deltoid" to the clavicle only (state 2), as observed in extant Theria.

3.4 | Pectoralis (PECT, Figures 4 and 9): Characters 10 and 11

10. Origin

0. Ventral surface of sternal complex (including interclavicle, when present) and anterior abdominal musculature
1. As (0), but also extends anteriorly to ventral surface of clavicle
2. As (0), but also extends onto ventral aspect of thoracic ribs

Remarks—Although the PECT of most amniotes has multiple subdivisions, these are apparently highly variable across (and sometimes within) taxa, and the recognition of various heads has in the past varied depending on the author. This hampers attempts to equate different heads across the broad phylogenetic groups considered here. Additionally, recent embryological evidence indicates that part of the pectoralis of therians (and possibly a more inclusive group) is derived from the supracoracoideus mass, and thus not homologous to the pectoralis of nonmammalian tetrapods (Smith-Paredes et al., 2022). Until a comprehensive evaluation of the homologies of all the PECT heads across extant tetrapods is conducted, this study refrains from attempting to codify variation in PECT subdivision. From a purely functional perspective, the feature of greater importance is where the muscle(s) originate and insert.

11. Insertion

0. Apex and/or posteroventral aspect of DPC of humerus [singular DPC with localized apex]
1. Anteroventral aspect of proximal humerus, on large pectoral process, distinct from dorsal process for deltoideus attachment [scarring and/or unfinished bone]
2. Entire length of DPC of humerus, on ventral to posteroventral aspect [DPC ridge-like]

Remarks—Reiterating the remarks noted above for the deltoideus musculature (character 7), a distinct process for PECT attachment may be recognized in stem and early crown amniotes, including "pelycosaurs" (state 1), which is subsequently remodeled into a simpler deltopectoral crest in therapsids (state 0).

3.5 | Scapulohumeralis anterior (SHA, Figures 4 and 10): Characters 12 and 13

12. Origin

0. Middle to anterior part of lateral surface of ventral scapula and dorsal procoracoid
1. Lateral surface of posteroventral procoracoid
2. Lateral surface of ventral scapula, dorsal to glenoid and ventrolateral to triceps scapularis origin (=teres minor, TMI)
3. Absent

Remarks—The SHA of lepidosaurs has traditionally been considered the homologue of the mammalian TMI (Diogo et al., 2016; Romer, 1944). However, as part of their alternative hypothesis of shoulder muscle homologies and evolution, Smith-Paredes et al. (2022) posited that the DSc of nonmammals is homologous to the TMI of therians, and that the SHA is an apomorphy for Lepidosauria. Yet, a SHA-like muscle has been recognized in the basal salamander *Andrias* (Miner, 1925), where it has a comparable insertion and innervation to the SHA of *Sphenodon*, and also appears to have been observed in *Necturus* (Wilder, 1912, p. 392). It is possible that this muscle also exists in other salamanders but has hitherto been overlooked, potentially because the small size of many taxa renders it inseparable from the overlying DCl.

By framing the location with respect to the triceps scapularis and glenoid, state 2 tacitly accounts for both the autapomorphic condition in monotremes and the condition in therians.

In their study of the cynognathian cynodont *Massetognathus*, Lai et al. (2018) recognized a scar at the base of the lateral scapula, dorsal to the glenoid, and suggested this to denote the origin of the TMI. The "mottled" surface texture and location of this feature (Figure 10ai) is consistent with attachment of such a muscle (state 2), but extensive first-hand examination of available material shows this manifestation to be exceedingly rare among cynodonts (or indeed, therapsids) studied to date. Guignard et al. (2019b) suggested that a tubercle at the posterolateral base of the scapula in the tritheledontid

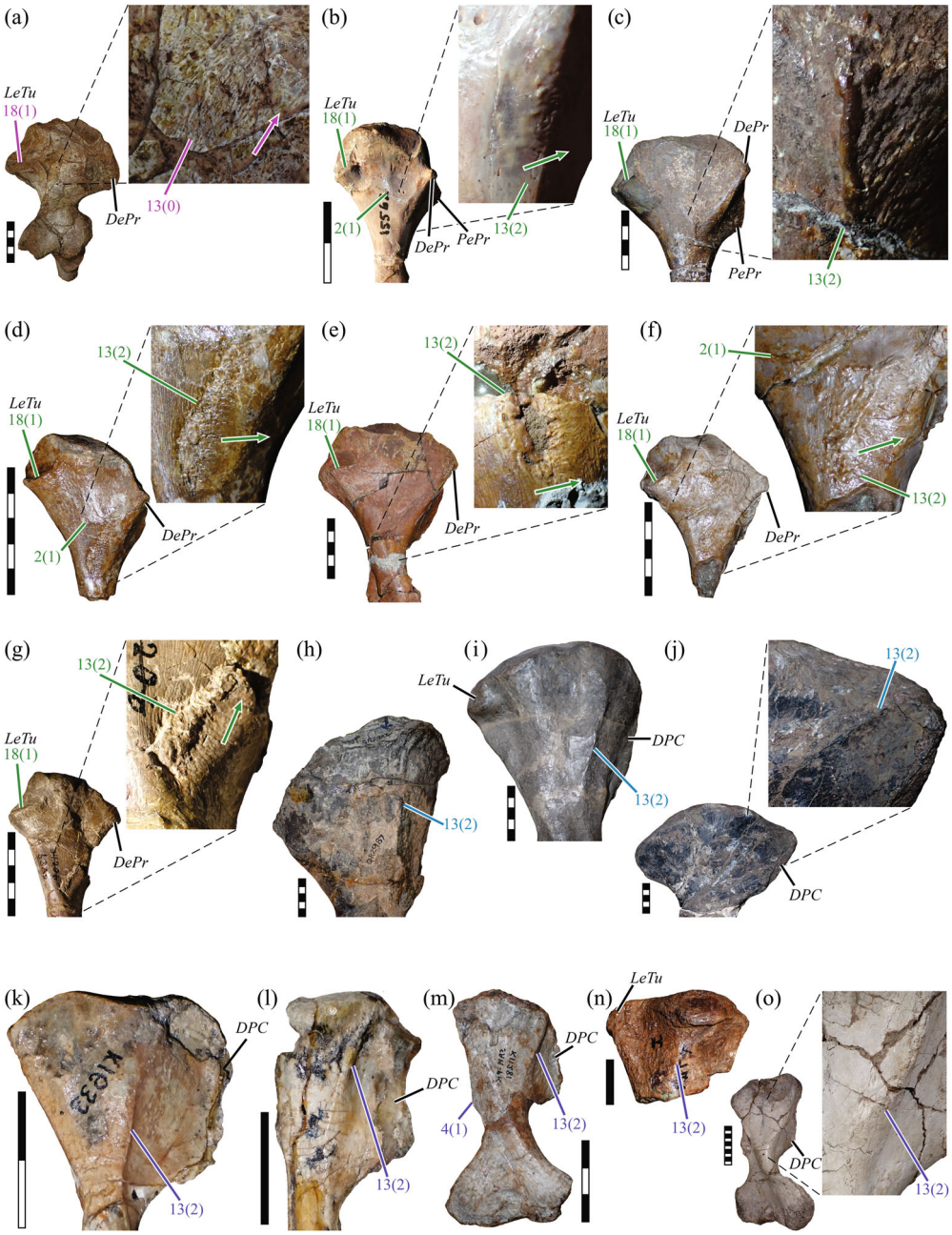

FIGURE 10 Osteological evidence of scapulohumeralis anterior musculature attachment to the proximal humerus in synapsids. (a) AMNH FARB 4709 *Diadectes* sp. (Diadectomorpha). (b) USNM V 15562 *Varanosaurus* sp. (Ophiacodontidae). (c) AMNH FARB 4141 *Ophiacodon retroversus* (Ophiacodontidae). (d) MCZ VPRA-2944 *Secodontosaurus* sp. (Sphenacodontia). (e) AMNH FARB 4037a *Dimetrodon giganhomogenes* (Sphenacodontia). (f) MCZ VPRA-1367 *Dimetrodon milleri* (Sphenacodontia). (g) UCMP 83544 *Sphenacodon ferox* (Sphenacodontia). (h) NMQR 2987 *Tapinocaninus pamelae* (Tapinocephalidae). (i) AMNH FARB 5222 *Moschops capensis* (Tapinocephalidae). (j) SAM-PK-9149 *Jonkeria truculenta* (Titanosuchidae). (k) SAM-PK-K1633 *Diictodon feliceps* (Dicynodontia). (l) USNM PAL 410241 cf. *Robertia* (Dicynodontia). (m) SAM-PK-K11281 *Brachyprosopus* sp. (Dicynodontia). (n) UMZC T.747 *Dicynodontoides nowacki* (Dicynodontia). (o) NHMUK PV R. R.37080 *Kitchinganomodon crassus* (Dicynodontia). (p) AMNH FARB 2240 *Lycaenops ornatus* (Gorgonopsia). (q) SAM-PK-2342 *Aelurognathus tigriceps* (Gorgonopsia). (r) BSPG 1934-VIII-28 *Gorgonops* sp. (Gorgonopsia). (s) GPIT-PV-31579 "*Scymnognathus*" *parringtoni* (Gorgonopsia). (t) SAM-PK-K1676 Gorgonopsia indet. (u) UMZC T.883 Gorgonopsia indet. (v) SAM-PK-K7809 *Glanosuchus macrops* (Scylacosauridae). (w) SAM-PK-K12051 *Alopecognathus* sp. (Scylacosauridae). (x) SAM-PK-K11200 Scylacosauridae indet. (y) BP/1/3973 *Olivierosuchus parringtoni* (Eutherocephalia). (z) NHMUK PV R.5755 *Theriognathus microps* (Eutherocephalia). (aa) UCMP 40467 *Mirotenthes digitipas* (Eutherocephalia). (ab) BP/1/2294 *Ictidosuchus intermedius* (Eutherocephalia). (ac) NMQR 3745 *Tetracynodon* sp. (Eutherocephalia). (ad) SAM-PK-1395 *Thrinaxodon liorhinus* (Cynodontia). (ae) NMQR 860 *Galesaurus planiceps* (Cyndontia). (af), NMQR 1205 *Diademodon tetragonus* (Cynognathia). (ag) NHMUK PV R.3772a *Cynognathus* sp. (Cynognathia). (ah) UCMP 42749 *Cynognathus* sp. (Cynognathia). (ai) MCZ VPRA-3691 *Massetognathus pascuali* (Cynognathia), inset shows muscle attachment to base of lateral scapula. (aj) UMZC T.905 *Cricodon metabolus* (Cynognathia). (ak) NHMUK PV R.36995 *Luangwa drysdalli* (Cynognathia). (al) PVL 4426 *Andescynodon mendozensis* (Cynognathia). (am) MCZ VPRA-4017 *Probainognathus jenseni* (basal probainognathian). (an) BP/1/5623 *Pachygenelus monus* (Tritheledontidae). (ao) BP/1/5671 *Tritylodon longaevus* (Tritylodontidae). All humeri are shown in approximately dorsal view (parallel to plane of proximal end), except (ai), which is shown in approximately anterior view. See also Figures 7 and 8. Arrows in (a), (b), and (d)–(g) indicate the "trend" of muscle scarring on the bone.

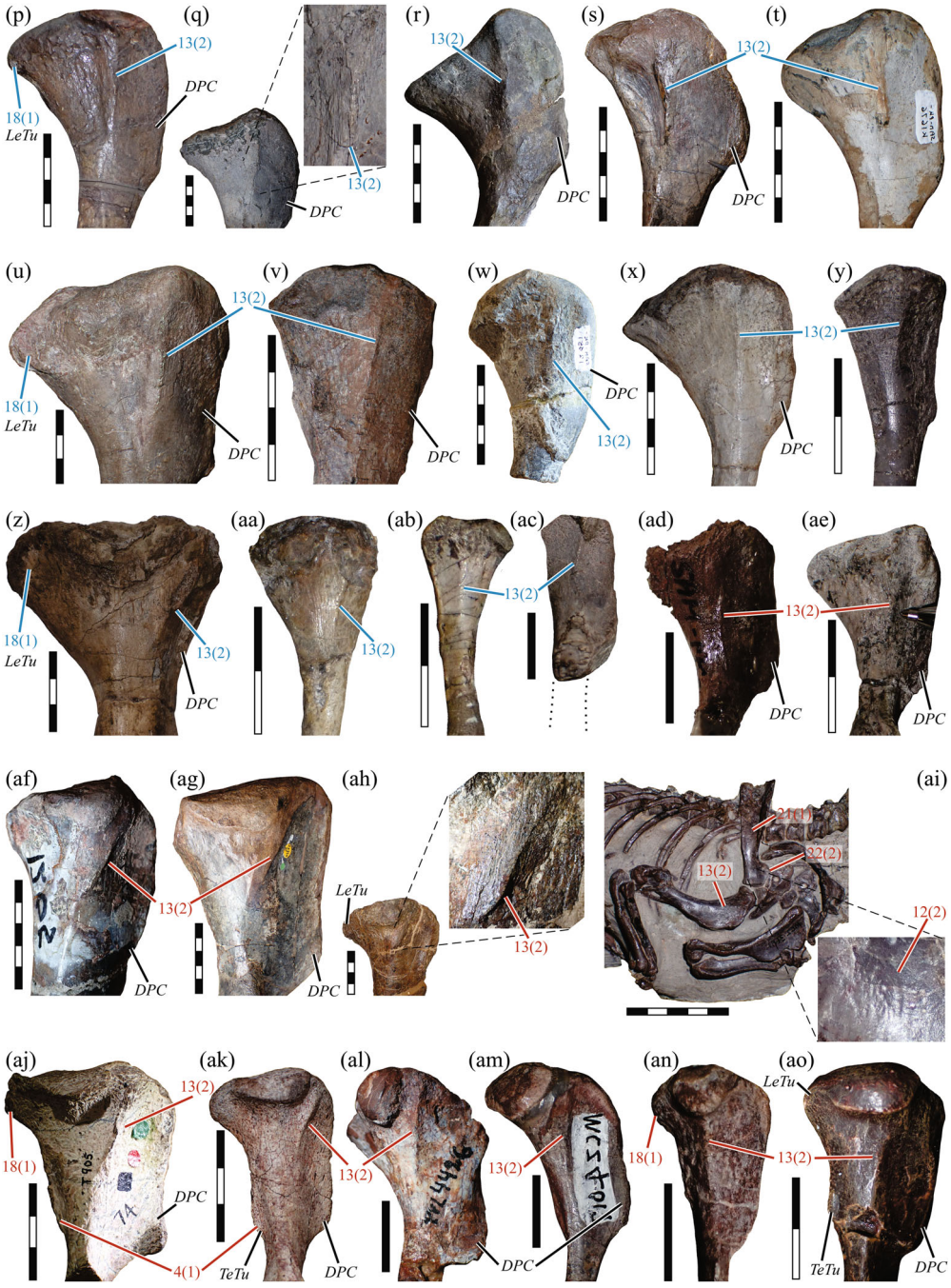

FIGURE 10 (Continued)

Riograndia was for attachment of the TMI, but this is morphologically more consistent with the widely observed scar for the triceps scapularis instead (see character 38 below).

13. Insertion

0. Dorsal surface of proximal humerus
1. Posterodorsal proximal humerus, adjacent and distal to LeTu
2. Anterodorsal proximal humerus, adjacent and posterodistal to insertions of SPC and deltoids (=TMI) [longitudinal ridge or patch of scarring]
3. Absent

Remarks—In monotremes, the TMI is well developed and passes deep to the triceps scapularis on the way to its insertion, just like the SHA in squamates. In therians, the TMI is very small; it is sometimes absent as a distinct muscle, its fibers becoming inseparable from those of the infraspinatus.

Abundant fossil evidence indicates that, rather than being restricted to Lepidosauria (Smith-Paredes et al., 2022), a SHA-like muscle was extensively distributed across basal amniotes and nonmammalian synapsids. Well-preserved "pelycosaur" humeri characteristically bear a longitudinal patch of scarring toward the anterior side of the proximal dorsal surface, approximately at the level of the distal base of the "pectoral process" (Figure 10b–g). It is always located anterior and distal to the transverse line of scarring for the LD, and posteriorly offset from the ridge leading proximally toward the "deltoid tubercle." Evidently influenced by the superficially similar position of a scar on the humerus of crocodylians, Romer and Price (1940) interpreted the "pelycosaurian" scar as denoting the origin of a brachialis, a distally directed muscle. However, microscopic examination shows that the texture of scarring is typically directed anteriorly to anteroproximally (or alternatively, when the scarring forms a pit, the pit "faces" anteroproximally), arguing against such an interpretation. With the SSc, LD, deltoids, and supracoracoideus (see character 23 below) all "accounted for" by other consistently recognizable osteological correlates, the scar in question indicates the presence of an additional, anteriorly directed, dorsally positioned muscle; a SHA-like muscle is the best candidate. A similarly sited patch of scarring is also observed in various stem amniotes, although it need not be as localized in spatial extent (Figures 7a and 10a; see also Holmes, 1977; Romer, 1956).

In therapsids, a longitudinal ridge or patch of scarring is also typically present on the anterior side of the proximal dorsal surface, also separate from the DPC (and greater tuberosity, where present). However, it differs from the scar of "pelycosaurs" in two aspects: it is usually more proximodistally elongate, and it tends to be more proximally positioned, frequently reaching up almost to the level of the articular surface of the caput. This scar has previously been documented in a handful of Permian dicynodonts (Angielczyk et al., 2009; King, 1981b), gorgonopsians (Sigogneau-Russell, 1989), a therocephalian (Fourie & Rubidge, 2009), nonmammalian cynodonts (de Oliveira et al., 2010; Gaetano et al., 2017; Jenkins, 1971; Lai et al., 2018), the docodont mammaliaform *Haldanodon* (Martin, 2005), and the eutriconodont theriimorph *Repenomamus* (Hu, 2006). Previous authors have unanimously interpreted it as demarcating the attachment of the homologue of the TMI, as it is located in the same general position as the insertion of the TMI in extant therians. Extensive first-hand observation confirms that this scar is widely distributed throughout therapsids and cynodonts, occupying a consistent position on the humerus (Figures 7n,o and 10h–ao). The straightforward transformation from a distal position in "pelycosaurs" to a proximal position in therapsids, and the occurrence of a similar scar in an intermediate-form humerus (Bishop et al., 2023), supports homology between the scarring in both groups. Thus, scarring can be traced continuously from stem amniotes through to theriimorphs, supporting the hypothesis of homology between the SHA and TMI.

3.6 | Scapulohumeralis posterior (SHP): Characters 14 and 15

14. Origin

0. Absent
1. Lateral to posterolateral aspect of scapula, dorsal to origin of triceps scapularis

Remarks—This muscle only occurs in extant saurians, and is probably a saurian (or sauropsid) apomorphy; it is hence tangential in the context of the present synapsid-focused work. It is nevertheless included here should future studies seek to expand the present analysis to include more amniote taxa. Even then, uncertainty remains as to whether the SHP is truly homologous across all extant saurians. Topology, development (Romer, 1944; Smith-Paredes et al., 2022), and the variable degree to which this muscle is differentiated from the SSc (Russell & Bauer, 2008) suggests that in squamates it is a derivative of the subcoracoscapularis mass. Likewise, in archosaurs the SHP shares innervation and developmental history with the SSc (Meers, 2003; Smith-Paredes et al., 2022). However, innervation patterns suggest that the SHP is more similar to the SHA in *Sphenodon* (Miner, 1925).

15. Insertion

0. Absent
1. Posterodorsal to posterior aspect of proximal humerus, posterior to SHA insertion.

3.7 | Subcoracoscapularis group (Figures 4 and 11): Characters 16–19

16. Subscapularis (SSc) origin

0. Medial surface to posterior margin of ventral scapula and posterodorsal margin of metacoracoid
1. Medial surface of much of scapula (and suprascapula, when present)
2. Lateral surface of posterior scapula and posterior scapular margin [posterior subscapular fossa]

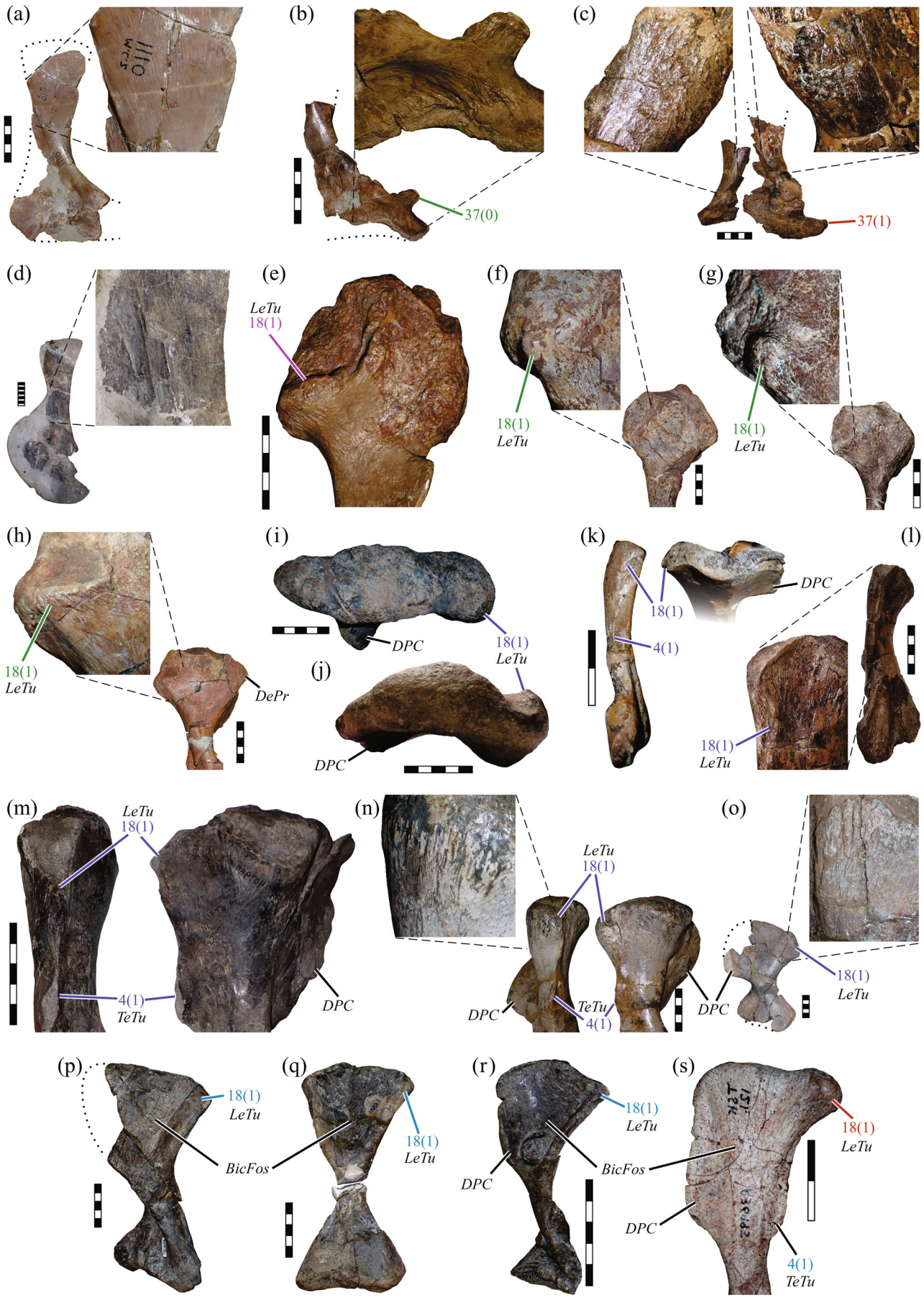

FIGURE 11 Legend on next page.

Remarks—In some squamates, the origin extends around to the posterior lateral scapula, but this is not accounted for explicitly here, as it bears much similarity to the SHP already codified above.

From an osteological perspective, the conditions in monotremes and fossorial therians are indistinguishable from one another (state 2): both possess a fossa on the lateral scapula, posterior to a ridge running dorsal from the triceps scapularis origin, but one is occupied by the SSc (monotremes) the other by the TMA (fossorial therians). Consequently, in the absence of other evidence, it is not possible to unambiguously identify the muscle attached to a posterior scapular fossa in extinct synapsids (e.g., *Cynognathus*). Only with additional evidence from the humerus—such as a TeTu separate from a putative LD insertion—would it be possible to infer the presence of a well-developed TMA, favoring it as the likely candidate that occupied the postscapular fossa (e.g., Hu, 2006).

Multituberculates often possess a distinctive linear scar on the anteromedial aspect of the ventral scapula, running back from the coracoid process, which was interpreted by Kielan-Jaworowska and Gambaryan (1994) as marking part of the origin of the subscapularis. Similarly, the dicynodont *Kannemeyeria* possesses a comparably sited tubercle on the medial scapula (Govender et al., 2008), as do some specimens of the cynodont *Cynognathus* (Figure 11c), whereas more diffuse scarring is apparent in some dinocephalian scapulae (Figure 11d). A long ridge is also present on the medial surface of the scapula in the basal therocephalian *Simorhinella* (Abdala et al., 2014). Whether these scars denote the attachment of the SSc remains ambiguous, however; it is also possible that the sterno/costocoracoideus equivalent ("subclavius") may have attached here instead (in a comparable fashion to extant monotremes: Gambaryan et al., 2015), or may alternatively mark an extended origin of the coracobrachialis or biceps brachii, in the case of multituberculates.

17. Subcoracoideus (SCo) origin

0. Absent
1. Much of inner (dorsal/medial) surface of coracoid element(s)

Remarks—It is not clear if the SCo of extant sauropsids (lepidosaurs and birds) is indeed homologous to the same-named muscle of monotremes, despite the similarity in their gross topology. In the former, the muscle is innervated by the subcoracoscapular nerve along with the SSc (Baumel et al., 1993; Lécuru, 1968; Miner, 1925), whereas in monotremes the innervation is different (McKay, 1894), quite so according to Howell (1937), who recognized a more ventral nerve supply in association with the coracobrachialis in *Ornithorhynchus*. Due to the sparse distribution of a SCo-like muscle across extant tetrapods, and the absence of clear osteological correlates, character inference within nonmammalian synapsids is currently ambiguous using both maximum likelihood and parsimony approaches (Supporting Information Appendix S4). Previous attempts at reconstructing early amniote pectoral musculature have relied on geometric, rather than phylogenetic, inference and have reached conflicting conclusions regarding the manifestation of the SCo (Holmes, 1977; Jenkins, 1971; Romer, 1922). Further work, such as embryological study, could help clarify the situation.

18. SSc insertion

0. Posterior aspect of proximal half of humerus
1. Posterior to posterodorsal aspect of proximal humerus, on LeTu [tubercle or protuberance]

Remarks—A LeTu is widespread among tetrapods, and it can be recognized in several stem tetrapod taxa as well

FIGURE 11 Osteological evidence of subcoracoscapularis musculature attachment in synapsids. Panels (a)–(d) illustrate potential indicators of origin on the scapulocoracoid, (e)–(s) illustrate insertions on the humerus. (a) MCZ VPRA-1110 *Dimetrodon booneorum* (Sphenacodontia) in medial view. (b) MCZ VPRA-1367 *Dimetrodon milleri* (Sphenacodontia) in medial view. (c) UCMP 42749 *Cynognathus* sp. (Cynognathia) left and right scapulocoracoids in medial view; in right inset the acromion has been digitally removed to aid clarity. (d) AMNH FARB 5553 *Moschops capensis* (Tapinocephalidae) in medial view. (e) MCZ VPRA-1035 *Diadectes tenuitectus* (Diadectomorpha) in dorsal view. (f) AMNH FARB 4006 *Lupeosaurus kayi* (Edaphosauridae) in dorsal view. (g) MCZ VPRA-3417 *Edaphosaurus* sp. (Edaphosauridae) in dorsal view. (h) AMNH 4037a *Dimetrodon giganhomogenes* (Sphenacodontia) in dorsal view. (i) SAM-PK-915 Anteosauridae indet. in proximal view (dorsal to top). (j) GPIT-PV-60755 *Rhachiocephalus magnus* (Dicynodontia) in proximal view (dorsal to top). (k) SAM-PK-K1633 *Diictodon feliceps* (Dicynodontia) in posterior (left) and proximal (right, ventral to top) views. (l) NHMUK PV R.37374 Dicynodontia indet. in posterodorsal view. (m) USNM PAL 407984 *Oudenodon bainii* (Dicynodontia) in posterior (left) and dorsal (right) views. (n) USNM V 24645 *Daptocephalus leoniceps* (Dicynodontia) in posterior and dorsal views. (o) MCZ VPRA-3455 *Dinodontosaurus brevirostris* (Dicynodontia) in ventral view. (p) CGS MJF 21 Lycosuchidae indet. in ventral view. (q) SAM-PK-11557 Scylacosauridae indet. in ventral view. (r) BP/1/6229 Scylacosauridae indet. in ventral view. (s) NHMUK PV R.36995 *Luangwa drysdalli* (Cynognathia) in ventral view. See also Figures 7, 8, 10, and 13.

(Bishop, 2014; Coates, 1996; Otoo et al., 2021). It is especially prominent in "pelycosaurs" and other early amniotes, where it forms a dorsally oriented prominence set distal to the articular surface of the caput (Figures 7a,b, 10a–g, and 11e–h; Romer & Price, 1940). Within therapsids, it has shifted proximally to occupy the posterodorsal corner of the humerus, but it is usually poorly developed, often only recognized by the presence of a localized thickening of bone and muscle scarring (Figure 11i–s). The LeTu of dicynodonts is characteristically well developed, often forming a dorsally everted lip near its posterodorsal apex (Figure 11j,k). As noted above, within epicynodonts and dicynodonts the LeTu may be partially connected to a more distally situated TeTu by a ridge of bone.

19. SCo insertion

0. Absent
1. Immediately adjacent to or with insertion of SSc on proximal humerus.

3.8 | Supracoracoideus (SPC, Figures 3, 4, 12, and 13): Characters 20–25

20. Origin of "head 1"

0. Ventral to anteroventral margin of coracoid
1. Lateral surface of much of coracoid (pro- and/or metacoracoid) anterior to glenoid
2. Dorsal (inner) through to anteroventral aspect of procoracoid
3. Absent [pro-/metacoracoid lost, only coracoid process remains]

Remarks—One of the more profound changes to the musculoskeletal system during synapsid evolution was the dorsal migration, expansion, and differentiation of the ancestral SPC, to form the infra- (ISP) and supraspinatus (SSP) muscles of mammals (Cheng, 1955; Gregory & Camp, 1918; Jenkins, 1971; Kemp, 1982; Romer, 1922, 1962; Smith-Paredes et al., 2022; Watson, 1917). In the context of the current study, delineating the differences in origins, insertions, and muscular divisions in a tractable framework is not straightforward. The present character encompasses the variation in SPC origin among extant nonmammals, and simultaneously accounts for the three-headed condition observed in extant monotremes; it is important to note that this character takes a taxic approach to homology only. Some studies have hypothesized that the condition in monotremes represents a transitional morphology (state 2; e.g., Diogo et al., 2016; Fahn-Lai et al., 2020), implying that SPC evolution was one of trifurcation, not bifurcation (see also Smith-Paredes et al., 2022), and that the third head was subsequently lost on the line to therians. Here, characters 20–25 are intentionally agnostic with respect to this particular transformational hypothesis: by effectively treating the SPC mass as three discrete units, this permits "head 1" to be both (a) the original precursor mass that gave rise to the SSP and ISP and (b) a distinct entity that persisted for much of synapsid evolution, lost only in Theria. Thus, recognition of osteological correlates and ASR can provide an objective assessment of the likely scenario of SPC evolution. As state 2 is only observed in extant monotremes, maximum likelihood ASR not surprisingly suggests that evolution toward the condition in therians probably did not involve a tripartite configuration (i.e., 1 → 3; Supporting Information Appendix S4).

In this synapsid-focused study, the present character focuses on the principal locus of origin only, ignoring minor variations within specific taxa. It also ignores the tripartite condition in crocodylians (Meers, 2003) or the bipartite condition in some squamates (Russell & Bauer, 2008); Fahn-Lai et al. (2020) recognized a third "acromial" head of the deltoideus mass in the teiid *Salvator*, but further observations and comparison to the literature suggest that this was actually the dorsal division of a bipartite SPC.

21. Infraspinatus (ISP) origin

0. Absent, not divided
1. Lateral surface of scapula [laterally reflected anterior margin, fossa between anterior margin and triceps scapularis origin]
2. Posterior half of lateral surface of scapula, bounded anteriorly by scapular spine and posteriorly by triceps scapularis origin [scapular spine shifted posteriorly, and infraspinous fossa]

Remarks—This study follows the conventional presumption that the scapular spine of theriimorphs is homologous to the anterior scapular margin of nontheriimorphs (Jenkins, 1971; Luo, 2015; Romer, 1922), although see Sánchez-Villagra and Maier (2003) for an alternative interpretation. State 1 tacitly accommodates the autapomorphic condition in monotremes; state 2 tacitly accounts for the autapomorphic condition in fossorial therians.

22. Supraspinatus (SSP) origin

0. Absent, not divided
1. Anterior procoracoid and anteroventral scapula [acromion process on anterior to anterolateral scapula, with distinct recess on scapula anteroventral to acromion]

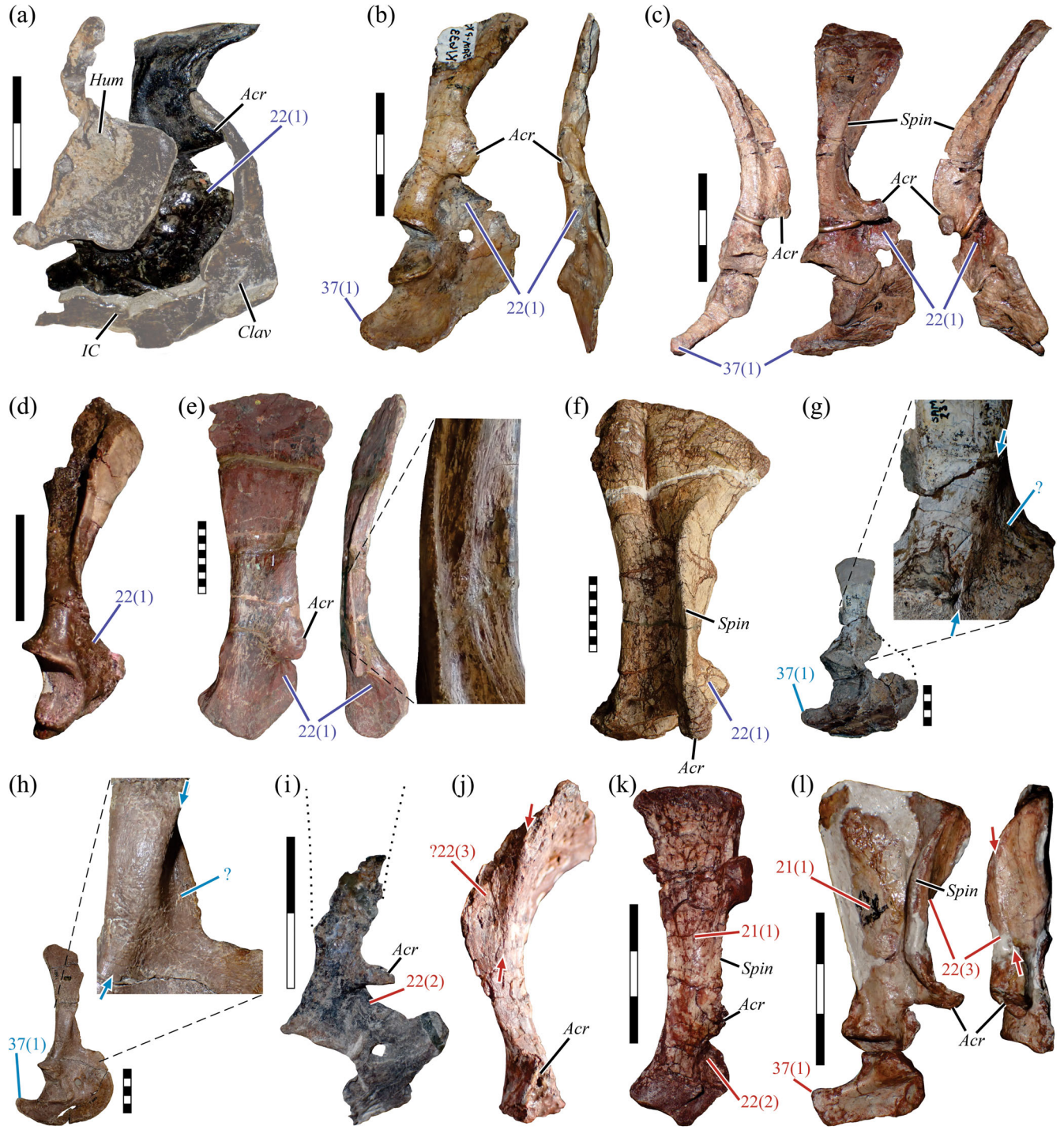

FIGURE 12 Osteological evidence of infra- and supraspinatus musculature attachment to the pectoral girdle in synapsids. (a) NMQR 2911 *Eodicynodon oosthuizeni* (Dicynodontia) in lateral view; humerus (Hum), clavicle (Clav), and interclavicle (IC) lightened to aid clarity. (b) SAM-PK-K1633 *Diictodon feliceps* (Dicynodontia) in lateral (left) and anterior (right) views. (c) UMZC T.747 *Dicynodontoides nowacki* (Dicynodontia) in (left to right) posterior, lateral, and anterior views; note the strongly laterally reflected acromion and anterior margin. (d) GPIT-PV-117035 *Kawingasaurus fossilis* (Dicynodontia) in lateral view; acromion not preserved in this specimen. (e) NHMUK PV R.3762 *Kannemeyeria simocephalus* (Dicynodontia) scapula in lateral (left) and anterior (right) views. (f) MCZ VPRA-1688 *Stahleckeria potens* (Dicynodontia) scapula in lateral view. (g) SAM-PK-2342 *Aelurognathus tigriceps* (Gorgonopsia) in lateral view. (h) UMZC T.883 Gorgonopsia indet. in lateral view. Arrows in (g) and (h) denote broad ridge bounding a fossa on the anteroventral scapula and anterior coracoid. (i) MCZ VPRA-4016 *Massetognathus pascuali* (Cynognathia) in lateral view. (j) PVL 4423 *Andescynodon mendozensis* (Cynognathia) scapula in anterior view. Distinctively among cynognathians, the acromion is greatly reduced in size and there exists a faint ridge (between arrows) dividing the anterior scapular surface into a medial (for trapezius?) and lateral (for SSP?) region. (k) MCZ VPRA-3616 *Chiniquodon* sp. (basal probainognathian) scapula in lateral view. (l) BP1/5167 *Tritylodon longaevus* (Tritylodontidae) in lateral and anterior views; arrows demarcate faint ridge dividing the anterior scapular surface into a medial (for trapezius?) and lateral (for SSP?) region.

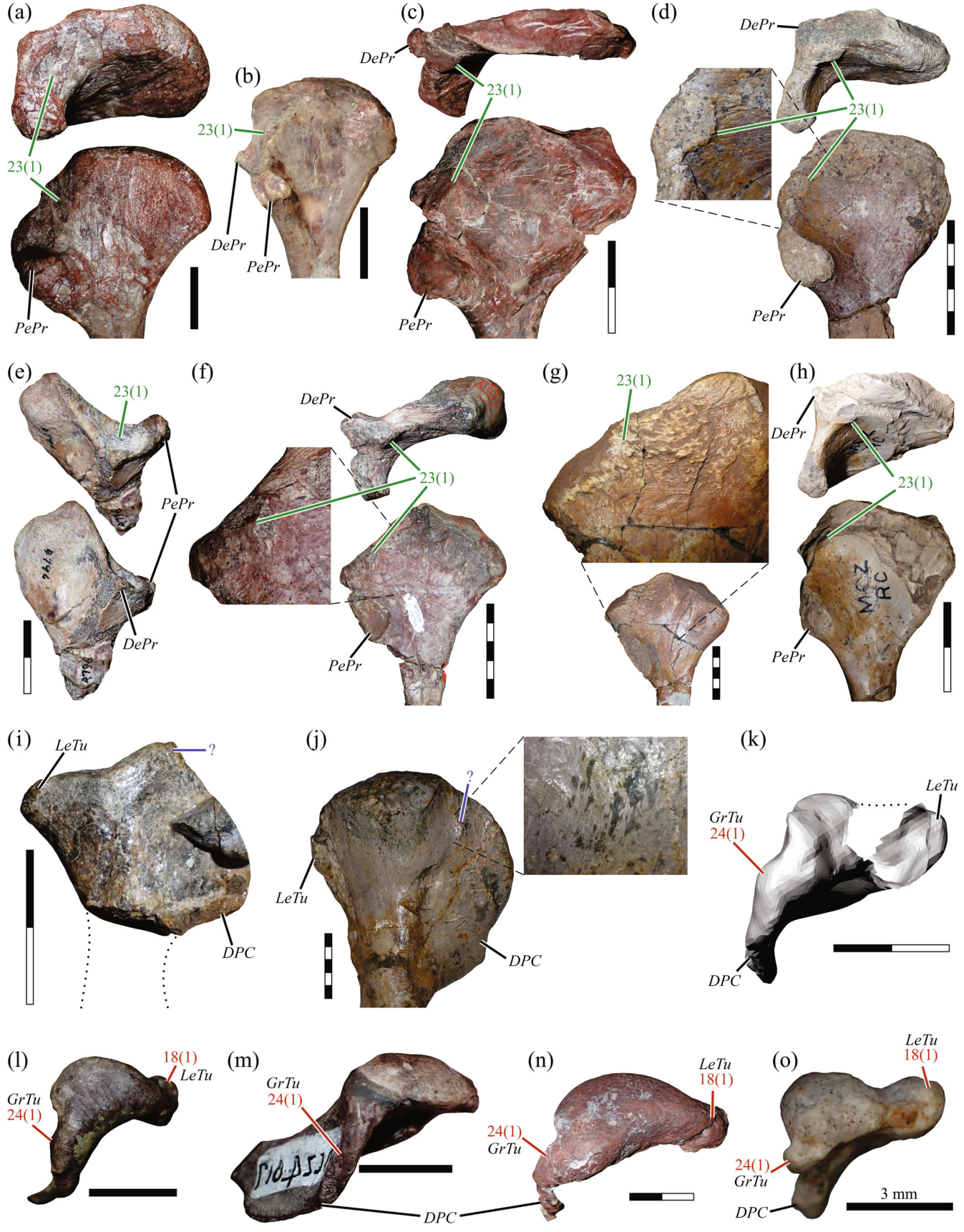

FIGURE 13 Legend on next page.

2. Anterior to anteromedial procoracoid, anterior to acromion process [small acromion process on anteroventral scapula, approximately in line with plane of anterior margin of coracoid, small recess centered on procoracoid]
3. Anteromedial aspect of scapula [procoracoid reduced or absent, large acromion process forming ventral archway; may also present recess on anteromedial scapula, medial to laterally reflected anterior margin]
4. Lateral aspect of anterior scapula [acromion process and laterally reflected margin more posteriorly positioned, forming scapular spine and supraspinous fossa]

Remarks—States 2–4 encapsulate a transformational hypothesis (see also Sun & Li, 1985) whereby the presence of an acromion—here taken to mean a localized, raised process of bone—implies that the clavicle no longer articulated with the scapulocoracoid along its full length, opening up a mediolateral passage between the clavicle and scapula. The appearance of an acromion (state 2) signifies the differentiation of the SSP (and shifting of the DCl origin; see character 8); the reduction of the procoracoid and widening of the passage into a ventral archway (state 3) signifies the enlargement of the SSP and migration onto the anteromedial scapula, as observed in extant monotremes; the posterior shift of the laterally reflected margin to form a scapular spine and supraspinous fossa marks the final stage in the transformation (state 4). These states were left unordered in the phylogenetic analyses, but ASR nevertheless suggests the likely sequence of evolution along the stem lineage was $0 \rightarrow 2 \rightarrow 3 \rightarrow 4$ (Supporting Information Appendix S4), supporting the transformational hypothesis.

State 1 accounts for the condition observed in dicynodonts, which also possess an acromion on the anteroventral scapula (Figure 12a–f). Although superficially similar to state 2, it exists as a separate state to account for the lateral displacement of the acromion and anterior margin in more derived taxa, particularly kannemeyeriiforms. Some forms indeed present a modestly reflected anterior scapular margin, paralleling the condition observed in cynodonts (Figure 12c,d,f), yet the acromion remains relatively small and the procoracoid is well developed. More basal anomodonts lack any indication of an acromion or anteroventral recess (Brinkman, 1981; Fröbisch & Reisz, 2011). Interestingly, large gorgonopsians can also exhibit a distinct fossa on the anteroventral scapula and anterior procoracoid, bounded posteriorly by a broad ridge running from the anterior margin of the base of the scapular blade toward the glenoid (Figure 12g,h; Boonstra, 1934; Pravoslavev, 1927). A near-identical morphology also exists in some scylacosaurid therocephalians (Boonstra, 1964). Unlike cynodonts and dicynodonts, however, gorgonopsians and scylacosaurids lack an acromion process, and the clavicle remained appressed to the scapulocoracoid for its entire length (as observed in articulated specimens, for example, SAM-PK-9344 *Aelurognathus microdon*, AMNH FARB 2240 *Lycaenops ornatus*). Considering the condition in basal anomodonts and noncynodont therapsids more broadly (lacking any osteological indicators of states 1–4), dicynodonts and cynodonts are superficially convergent with one another, so it remains uncertain whether the SPC of dicynodonts underwent structural subdivision [producing infraspinatus (ISP)- and SSP-like muscles], or simply a topographic expansion.

23. Insertion of "head 1"

0. Proximal DPC of humerus, from anteroventral to posteroventral aspect
1. Proximoventral aspect of bony bridge running between deltoid and pectoral processes [discrete scarring, separate from both processes]
2. Apex of deltopectoral crest
3. Absent

Remarks—Among various stem and early crown amniotes, there is frequently an irregularly shaped scar situated between the otherwise discrete processes for deltoid

FIGURE 13 Osteological evidence of supracoracoideus (including infra- and supraspinatus) musculature attachment to the humerus in synapsids. (a) MCZ VPRA-1926 *Varanops* sp. (Varanopidae) in ventral and proximal view. (b) USNM V 15562 *Varanosaurus* sp. (Ophiacodontidae) in ventral view. (c) MCZ VPRA-6289 *Ophiacodon mirus* (Ophiacodontidae) in ventral and proximal views. (d) MCZ VPRA-5958 *Ophiacodon retroversus* (Ophiacodontidae) in ventral and proximal views. (e) AMNH FARB 4796 *Nitosaurus jacksonorum* (? Edaphosauridae) in dorsal and proximal views. (f) MCZ VPRA-4906 *Sphenacodon ferocior* (Sphenacodontia) in ventral and proximal views. (g) AMNH FARB 4037a *Dimetrodon giganhomogenes* (Sphenacodontia) in ventral view. (h) MCZ VPRA-7044 *Dimetrodon natalis* (Sphenacodontia) in ventral and proximal views. (i) NMQR 3153 *Eodicynodon oosthuizeni* (Dicynodontia) in dorsal view (see also Figure 10k,l). (j) USNM V 24645 *Daptocephalus leoniceps* (Dicynodontia) in anterodorsal view. (k) RC 92 *Procynosuchus delaharpeae* (Cynodontia) in proximal view; render of digital model acquired via a GoSCAN 20 laser surface scanner (Creaform, USA). (l) MCZ VPRA-3691 *Massetognathus pascuali* (Cynognathia) in proximal view. (m) MCZ VPRA-4017 *Probainognathus jenseni* (basal probainognathian) in proximal view. (n) MCZ VPRA-8812 *Kayentatherium wellesi* (Tritylodontidae) in proximal view. (o) UFRGS-PV-1043-T *Brasilodon quadrangularis* in proximal view. All proximal views are shown with dorsal to the top, except (e), where ventral is to the top.

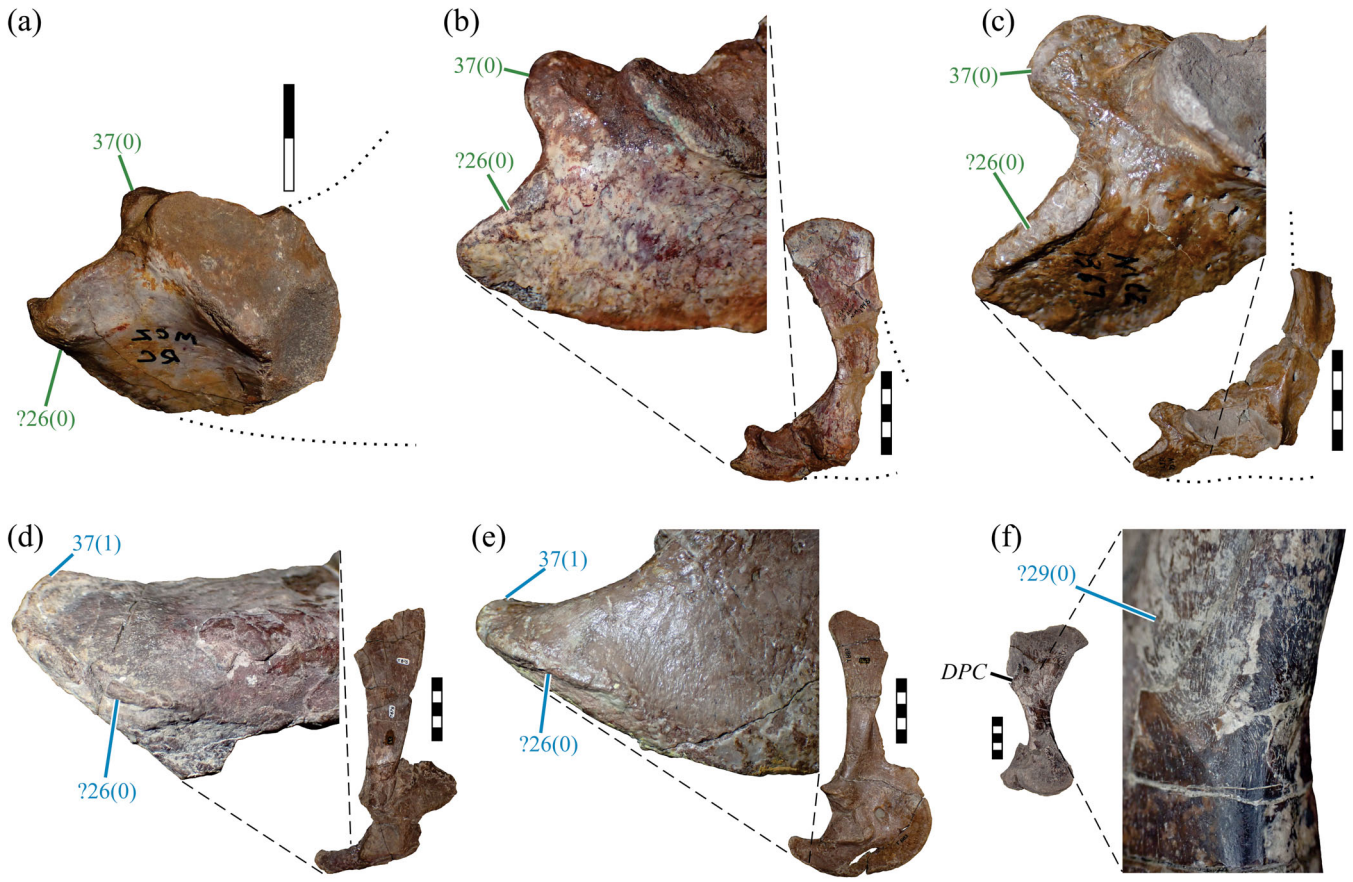

FIGURE 14 Osteological evidence of coracobrachialis musculature attachment in synapsids. (a) MCZ VPRA-4830 *Ophiacodon retroversus* (Ophiacodontidae) coracoid in lateral view. (b) MCZ VPRA-1946 *Sphenacodon ferocior* (Sphenacodontia) scapulocoracoid in lateral view. (c) MCZ VPRA-1367 *Dimetrodon milleri* (Sphenacodontia) scapulocoracoid in lateral view. (d) UMZC T.878 *Sycosaurus nowaki* (Gorgonopsia) scapulocoracoid in lateral view. (e) UMZC T.883 Gorgonopsia indet. scapulocoracoid in lateral view. (f) UMZC T.1278 Gorgonopsia indet. humerus in ventral view, showing scarring texture potentially indicative of attachment of the CBB on the posteroventral aspect.

and pectoral muscle attachment (state 1). This scar is always on the proximoventral aspect of the humerus (i.e., never purely terminal in location), and was previously interpreted as denoting the insertion of the SPC (Fox & Bowman, 1966; Holmes, 1977; Romer, 1922; Romer & Price, 1940). A similar topological relationship, somewhat between but proximal to deltoid and pectoral insertions, is also generally observed among extant salamanders and lepidosaurs, as well as monotremes (Gambaryan et al., 2015; Regnault et al., 2020). The manifestation of this scar within "pelycosaurs" is variable. In some specimens, it may be little more than a local thickening of the bone, but in well-ossified specimens (even of small species) it typically forms a broad, rugose tubercle (Figure 13c,d,f,g,h). However, in varanopids, the ophiacodontid *Varanosaurus*, some caseids (e.g., *Casea*), and the putative edaphosaurid *Nitosaurus*, the scar occurs as a hollow instead (Figure 13a,b,e), which may be well-excavated to create two ridges running between the deltoid and pectoral processes (Brinkman & Eberth, 1983). The somewhat ventral disposition of the scarring suggests that the attaching SPC had a more plesiomorphic configuration in these animals, originating from more ventral parts of the pectoral girdle (cf. character 20). Paralleling the evolution of deltoid and pectoral attachments, the transition to therapsids involved the loss of a discrete site of scarring as a simplified and singular deltopectoral crest was formed.

24. ISP insertion

0. Absent
1. Proximal aspect of greater tuberosity (GrTu) on humerus [tuberosity distinct from DPC and caput]

Remarks—The GrTu is an unambiguous osteological correlate of the insertions of the ISP and SSP in extant mammals, but elsewhere among extant tetrapods a distinct process for the SPC mass is absent. Considering the morphology and phyletic distribution of scars on the anteroproximal humerus of stem and early crown amniotes (see characters 7, 11, and 23), scarring for the SPC is

recognizable in "pelycosaurs" on the *ventral* proximal humerus, but it is invariably absent (or at least, cannot be unambiguously recognized) in noncynodont therapsids. A tuberosity or bump is observed on the *terminal* humerus in cynodonts, distinct from the articular surface of the caput (Figure 13k–o), and this can be easily traced through to the GrTu of crown mammals. From a mechanobiological perspective, the appearance of a terminally positioned GrTu in cynodonts, coincident with a restructuring of the scapular blade, is consistent with the appearance of more dorsally pulling musculature that would have changed the direction of forces on the humerus, altering the local bone loading regime. Maximum likelihood ASR suggests that the transition to state 1 occurred toward the base of therapsids (Supporting Information Appendix S4), but the consistent absence of a GrTu in noncynodont therapsids does not support this.

25. SSP insertion

0. Absent
1. Anterior aspect of GrTu on humerus [tuberosity distinct from DPC and caput]

3.9 | Coracobrachiales (Figures 3, 4, and 14): Characters 26–29

26. Coracobrachialis longus (CBL) origin

0. Lateral to ventrolateral aspect of posteriormost metacoracoid, near apex
1. Medial aspect of coracoid process of scapula [coracoid process present, coracoids absent]
2. Absent

Remarks—Well-preserved metacoracoids of "pelycosaurs" and gorgonopsians occasionally bear an elevated region of rugose bone texture, on the lateral surface of the apex, where individual striations face laterally (Figure 14a–e). This likely demarcates the primary attachment of at least the CBL in these taxa.

27. Coracobrachialis brevis (CBB) origin

0. Lateral aspect of posterior coracoid, anterior to CBL origin
1. Lateral aspect of middle to anterior coracoid
2. Medial aspect of coracoid process of scapula [coracoid process present, coracoids absent]

28. CBL insertion

0. Caudal (medial) aspect of distal humerus, proximal to entepicondyle
1. Absent

29. CBB insertion

0. Ventral aspect of proximal humerus, in fossa between DPC anteriorly and posterior margin
1. Posterior aspect of proximal humerus, distal to lesser tuberosity

Remarks—The proximal humerus of most synapsids typically possesses a broad "bicipital fossa" on its ventral aspect (Figure 11p–s; see also Figure 14f), which likely served as the locus of insertion of the CBB. However, this fossa sometimes only exists by virtue of the DPC (anteriorly) and a thickened LeTu, and is better considered a "spandrel" (Gould & Lewontin, 1979), rather than an unambiguous osteological correlate of muscle attachment in its own right.

3.10 | Biceps brachii (BICB, Figures 5, 15, and 16): Characters 30–33

30. Number of heads

0. One
1. Two

Remarks—In salamanders, a BICB does not exist per se, but is topologically and functionally replaced by the single-headed "coracoradialis proprius." The exact homology of this muscle with respect to the BICB of extant amniotes remains to be fully resolved, although the proximal muscle mass at least appears to be homologous to part of the amniote BICB (Diogo et al., 2016; Diogo & Tanaka, 2012; Miner, 1925). For the purposes of the present study, the coracoradialis proprius will be treated as the homologue of the BICB of amniotes. Embryological evidence suggests that what has historically been termed the brachialis in crocodylians is actually the short head of the BICB (Smith-Paredes et al., 2022).

31. Origin

0. Lateral aspect of posteroventral coracoid, ventral (superficial) to CBB origin

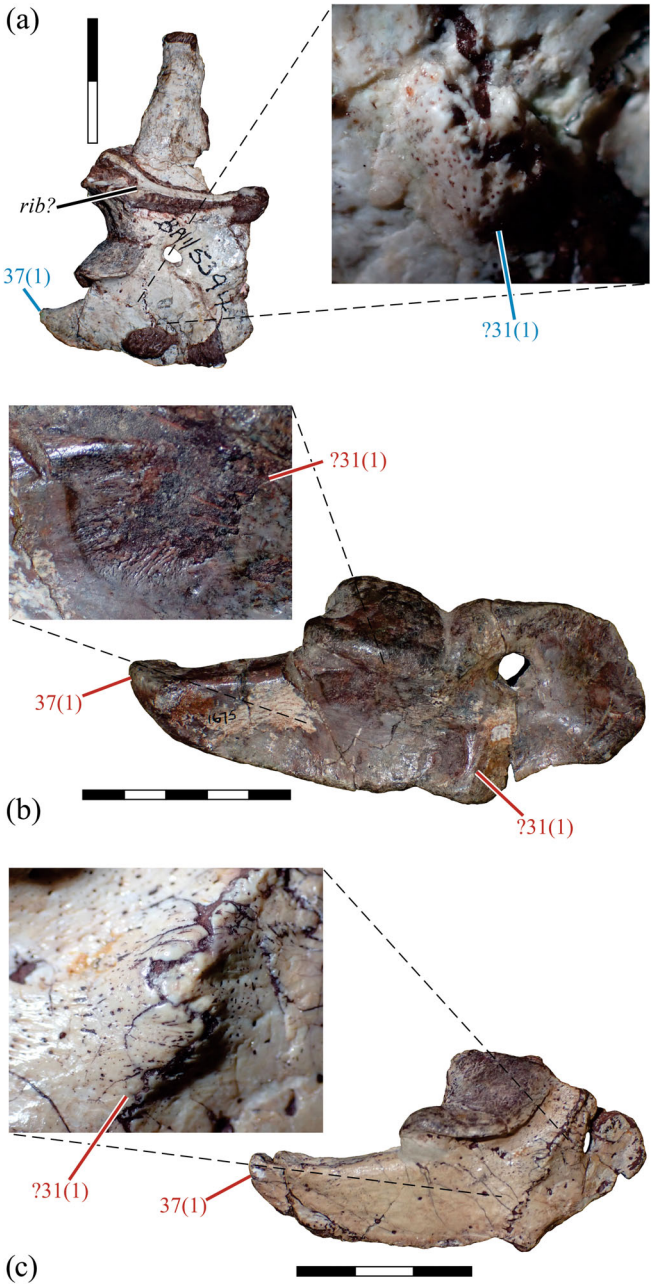

FIGURE 15 Rare osteological evidence of biceps brachii attachment to the pectoral girdle in theriodonts. (a) BP/1/5394 *Regisaurus jacobi* (Eutherocephalia) scapulocoracoid in lateral view. (b) BP/1/1675 cf. *Cynognathus* (Cynognathia) coracoid plate in lateral view. (c) MCZ VPRA-8812 *Kayentatherium wellesi* (Tritylodontidae) coracoid plate in lateral view.

1. Lateral to ventrolateral aspect of coracoid (pro- and/or meta-), anterior to CBB origin [tubercle sometimes present]
2. Lateral aspect of (meta)coracoid, anterior to CBB origin [tubercle], and anteroventral humeral shaft
3. Lateral aspect of coracoid process of scapula and anterodorsal lip of glenoid [coracoid process present, coracoids absent, supraglenoid tubercle]

Remarks—The condition in the monotreme *Ornithorhynchus*, whereby the long head encroaches onto the interclavicle and its short head originates posteriorly to the CBB, is evidently autapomorphic for this taxon and not accounted for in the above codification. The coracoids of one specimen of cf. *Cynognathus* bear a dorsoventrally oriented ridge between two fossae, the posterior one of which also bears a low, broad scar ventral to the glenoid (Figure 15b; Jenkins, 1971). Additionally, the eutherocephalian *Regisaurus* and the tritylodontid *Kayentatherium* both possess a distinct tubercle straddling the metacoracoid–procoracoid suture (Figure 15a,c). These features may denote the attachment of the BICB. Lai et al. (2018) interpreted a smooth-surfaced depression on the lateral procoracoid as denoting the origin of the BICB in one specimen of the cynognathian cynodont *Massetognathus*. Yet the coracoids of most cynodonts, which are small and delicate, are liable to taphonomic deformation, complicating interpretations of subtle topographic features.

32. Insertion on radius

0. Medial aspect of proximal shaft [scar]
1. Lateral to posterolateral aspect of proximal shaft
2. Posterior aspect of proximal to middle shaft [tubercle, pit or scar]

Remarks—The radius of stem and early crown amniotes, including "pelycosaurs," is characterized by a well-developed, longitudinally oriented scar on the medial margin of the proximal third of the bone (state 0; Figure 16a,c,e,f), likely demarcating the insertion of the BICB. Remarkably, this scar is continued distally by a fine, rugose ridge down most of the remaining length of the bone's medial aspect, suggesting a distally extensive insertion of the BICB (or brachialis, see below). It is also worth noting that the scar for insertion of the BICB is located distal to midshaft in the anteosaurid dinocephalian *Titanophoneus* (Orlov, 1958). In concert with the generally short proportions of the antebrachium, large pectoral process, and large entepicondyle of "pelycosaurs," this paints a picture of a stocky forelimb in these animals, where the "crook" to the elbow was only modestly developed. This was probably the case in other early crown and stem amniotes as well, given the generally conservative forelimb osteology across all groups.

Scarring denoting the insertion of the BICB also occurs on the radius of most therapsids and cynodonts, but importantly, it is located on the bone's posterior surface instead, and lacks any distal continuation (Figure 16h–k,m,o,q–t,v). This change in the locus of insertion potentially affected forearm mobility or force/moment-producing capacity, but what these effects might be must await quantitative mechanistic testing.

FIGURE 16 Legend on next page.

33. Insertion on ulna

0. Absent
1. Medial to posterior aspect of proximal shaft [tubercle, scar, or depression/pit]

Remarks—The ulna of "pelycosaurs" typically bears a small longitudinal scar on the bone's medial margin, immediately distal to the articular surface (state 1; Figure 16b,d,g); unlike the radius, it is not continued distally by additional scarring. A similarly sited scar is also observed in some therapsid and cynodont ulnae (Figure 16l,n,p,t).

3.11 | Brachialis (BRA): Characters 34–36

34. Origin

0. Anterior aspect of humeral shaft; variable proximodistal extent, and possible encroachment onto more dorsal or ventral aspects
1. Anterodorsal surface of proximal humerus, separating deltoid insertions anteriorly from triceps humeralis origins posteriorly

Remarks—Romer (1922) considered that the plesiomorphic condition for tetrapods was for the BRA to originate from the ventral humerus only, ventral to the "anterior dorsoventral line"; in turn, the occupation of a more dorsal aspect of the humerus would be a more mammalian trait (Gambaryan et al., 2015; Regnault et al., 2020). While the origin of the ventral humerus was indeed probably plesiomorphic for tetrapods as a whole (Bishop, 2014; Molnar et al., 2018), the development of a waisted humeral diaphysis in crown tetrapods would have removed the bony "wall" precluding its dorsal encroachment, so there is no reason to expect a ventrally restricted origin in early amniotes. Indeed, in *Sphenodon*, the muscle has encroached onto the dorsal surface of the DPC (Miner, 1925; Osawa, 1897). Considering the robust and twisted structure of stem and early crown amniote humeri, especially larger taxa where the ventral space between the pectoral process and distal condyles was limited, encroachment of the BRA onto a more dorsal aspect of the proximal humerus may have been inescapable.

Recent embryological work has demonstrated that what has historically been termed the "humeroradialis" of crocodylians is homologous to the BRA of other amniotes (Smith-Paredes et al., 2022), casting doubt on its homology with the same-named muscle of *Sphenodon* (which also possesses a BRA). It is possible that the doubly-innervated "humeroradialis" of *Sphenodon* is neomorphic or otherwise not homologous to any muscle in other tetrapods (Russell & Bauer, 2008).

35. Insertion on radius

0. Medial aspect of proximal shaft
1. Lateral to posterolateral aspect of proximal shaft
2. Posterior aspect of proximal shaft [sometimes a tuberosity]
3. Absent

36. Insertion on ulna

0. Posterior aspect of proximal shaft
1. Medial aspect of proximal shaft

Remarks—Often the BRA shares its insertion with the BICB among extant taxa, but when the two are separate in their attachments, the BRA is typically proximal to the BICB.

FIGURE 16 Osteological evidence of biceps brachii attachment to the antebrachium in synapsids. (a) MCZ VPRA-2045 *Archeria crassidisca* (Embolomeri, stem amniote) radius in medial view. (b) MCZ VPRA-1366 *Ophiacodon uniformis* (Ophiacodontidae) ulna in proximal view. (c) MCZ VPRA-1203 *Ophiacodon retroversus* (Ophiacodontidae) radius in anterior (left) and medial (right) views. (d) MCZ VPRA-4319 *Edaphosaurus boanerges* (Edaphosauridae) ulna in posterior view. (e) MCZ VPRA-5063 *Dimetrodon booneorum* (Sphenacodontia) radius in anterior (left) and medial (right) views. (f) UCMP 83566 *Sphenacodon ferox* (Sphenacodontia) radius in anterior view. (g) MCZ VPRA-5421 *Dimetrodon limbatus* (Sphenacodontia) ulna in medial (left) and posterior (right) views. (h) AMNH FARB 5222 *Moschops capensis* (Tapinocephalidae) radius in posterior (left, partially occluded by ulna) and medial views. (i) AMNH FARB 5611 *Jonkeria truculenta* (Titanosuchidae) radius in posterior view. (j) USNM PAL 299746 *Daptocephalus leoniceps* (Dicynodontia) radius in posterior view. (k) PVL 3465 *Acratophorus argentinensis* (Dicynodontia) radius in posterior view. (l) MCZ VPRA-3455 *Dinodontosaurus brevirostris* (Dicynodontia) ulna in anterior view. (m) UFRGS-PV-0509-T *Jachaleria candelariensis* (Dicynodontia) radius in posterior view. (n) NMQR 3939 *Moschorhinus kitchingi* (Eutherocephalia) ulna in medial (left) and posterior (right) views. (o) NMQR 1207 *Cynognathus crateronotus* (Cynognathia) radius in posterior view. (p) BP/1/1675 cf. *Cynognathus* ulna in anterior view (inset in anteromedial view). (q) PVL 2461 *Exaeretodon* sp. (Cynognathia) radius in posterior view. (r) PVL 4677 *Probainognathus jenseni* (basal probainognathian) radius in posterior view. (s) MCZ VPRA-3616 *Chiniquodon* sp. (basal probainognathian) radius in posterior view. (t) MCZ VPRA-8812 *Kayentatherium wellesi* (Tritylodontidae) ulna (left, medial view) and radius (right, posterior view). (u) MCZ 25461 *Tachyglossus aculeatus* (Monotremata) radius and ulna in posterior view. (v) MACN-N 01 *Vincelestes neuquenianus* (cladotherian) radius in posterior view.

3.12 | Triceps group (Figures 3, 5, and 17–19): Characters 37–41

37. Triceps coracoideus (TRIC) origin

0. Posterodorsal margin of (meta)coracoid, at the level of the glenoid [angle, tubercle, or tuberosity]
1. Via ligamentous band on inner (medial) surface girdle, running from coracoid/sternum ventrally [scar, well below level of glenoid] to scapula dorsally
2. Lateral aspect of distal LD prior to the latter's insertion into humerus (=dorsoepitrochlearis, DEP)

Remarks—Romer (1922) and Diogo et al. (2016) homologized the TRIC of nonmammalian tetrapods with the DEP of mammals, a hypothesis recently supported by the embryological data of Smith-Paredes et al. (2022). Whereas the muscle in *Sphenodon* has a direct connection to the metacoracoid (state 0), in squamates it typically originates indirectly, via the sternoscapular ligament (state 1; Romer, 1922; Russell & Bauer, 2008), and crocodylians exhibit a comparable arrangement as well. Early amniotes, including "pelycosaurs," characteristically bear a well-developed process posterodorsal to the glenoid, which has long been interpreted as the site of TRIC attachment (Romer, 1922). Surface striations on the apex of this process are directed laterally, not posteriorly, supporting this inference (Figure 17a). This process is lost in therapsids, in tandem with the progressive reduction of the coracoid plate as a whole, but the posterior apex of the metacoracoid remains locally thickened to form a subtle tuberosity, suggesting that it served as the attachment for the TRIC (Figure 17b–g).

From an osteological perspective, states 0 and 1 are indistinguishable, as both are manifested by scarring on the posterior end of the (meta)coracoid. Yet they form part of a probable transformation scenario within synapsids ($0 \rightarrow 1 \rightarrow 2$), supported by the results of ASR (Supporting Information Appendix S4). As the (meta)coracoid progressively reduced in size and moved anteroventrally, the TRIC shifted its origin from a direct connection to the coracoid to an indirect ligamentous one, and then finally to the LD, presumably to maintain an appropriate line of action with respect to the shoulder, upper arm and elbow joint. In this scenario, the presence of a scar on the posterior coracoid of a given fossil taxon only argues against state 2. The direct connection to the coracoid in *Sphenodon* demonstrates that modest reduction and migration of the coracoid does not guarantee a shift in TRIC origin onto soft tissues; a more dramatic change to coracoid morphology, such as seen in crocodylians, is required. Following this reasoning, it is likely that the condition in "pelycosaurs" is indicative of a direct attachment. Moreover, it might not have been until the posterior extent of the coracoid was considerably reduced at around crown Mammalia that the shift to state 2 occurred, as even basal mammaliaforms possess a long posterior coracoid process (Jenkins & Parrington, 1976). Maximum parsimony would dictate that the DEP of therians and monotremes are homologous, implying that the shift to state 2 was indeed around crown Mammalia; in contrast, maximum likelihood ASR does not detect a shift until later, around Theriiformes (Supporting Information Appendix S4).

38. Triceps scapularis (TRIS) origin

0. Posterior margin of scapula, just dorsal to the glenoid [scarring]
1. Dorsoventrally oriented ridge along lower half of lateral surface of scapula, dorsal to glenoid but anterior to the posterior margin

Remarks—The condition in monotremes (state 1) can easily be reconciled with the uniformity observed elsewhere among crown tetrapods by a "pronation" twist or shearing of the scapula, which also brings the SSc origin partly onto the lateral surface. The origin of the TRIS in nonmammalian synapsids is easy to recognize, due to its consistent topology and well-developed scarring textures varying from positive to negative relief (Figure 18). At least one specimen of the therocephalian *Lycosuchus* exhibits a massively developed projection for TRIS attachment (Figure 18o), similar to the enlarged process in the dinocephalian *Anteosaurus* (Figure 18e; Boonstra, 1955).

39. Triceps humeralis medialis (TRIM) and lateralis (TRIL) origin

0. Much of dorsal surface of humerus, as well as the anterior and posterior aspects of the shaft; posterior to BRA origin and anterior to CBL insertion; TRIL generally anterior to TRIM

Remarks—There is a broad diversity in the topological relationships between these two muscles' origins and those of neighboring muscles. Compounded by the division of the humeralis mass into three heads in crocodylians and monotremes (which obfuscates homologization across taxa), this precludes a succinct, tractable codification for all of crown tetrapods. The description for the above lone state captures the essential commonalities across tetrapod groups, which may be supplemented with

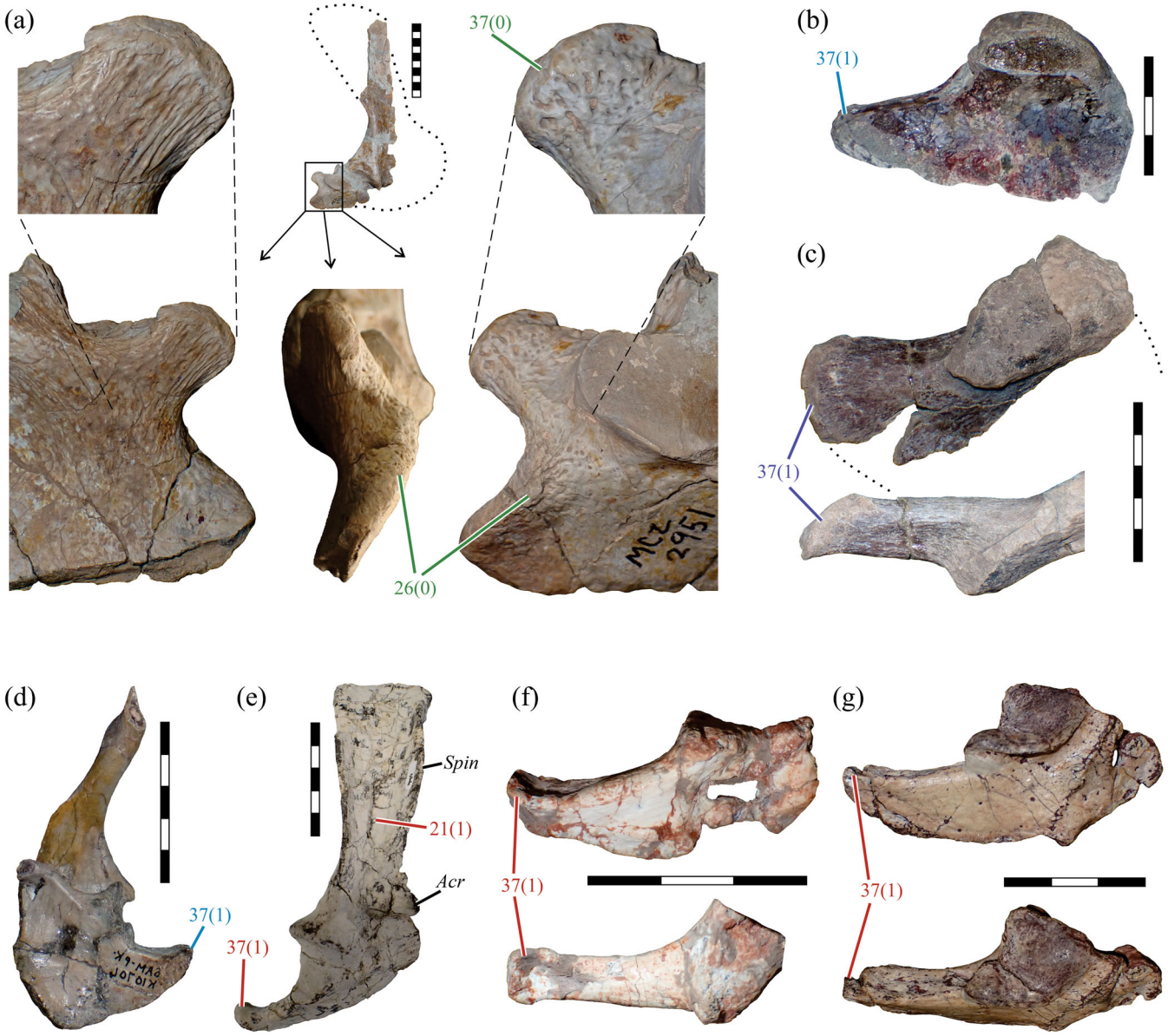

FIGURE 17 Osteological evidence of triceps coracoideus attachment to the pectoral girdle in synapsids. (a) MCZ-VPRA 2951 *Dimetrodon limbatus* (Sphenacodontia) scapulocoracoid; whole bone shown in lateral view, with enlarged insets shown in (left to right) medial, posterior, and lateral views. (b) SAM-PK-K252 *Hipposaurus boonstrai* (Biarmosuchia) metacoracoid in lateral view. (c) MCZ VPRA-3455 *Dinodontosaurus brevirostris* (Dicynodontia) metacoracoid in lateral (top) and dorsal (bottom) views. (d) SAM-PK-K10704 *Ictidosuchoides* sp. (Eutherocephalia) scapulocoracoid in medial view. (e) FMNH PR 2444 *Menadon besairei* (Cynognathia) scapulocoracoid in lateral view. (f) UFRGS-PV-1051-T *Trucidocynodon riograndensis* (basal probainognathian) coracoid plate in lateral (top) and dorsolateral (bottom) views. (g) MCZ VPRA-8812 *Kayentatherium wellesi* (Tritylodontidae) coracoid plate in lateral (top) and dorsal (bottom) views. See also Figures 12, 14, and 15.

osteological evidence on a case-by-case basis should it present itself.

40. TRIC insertion

0. Via common insertion with other triceps heads on olecranon process of ulna
1. Proximal ulna and/or fascia of forearm flexor muscles (=DEP)

41. Insertion of other triceps heads

0. Via common tendon on olecranon process of ulna [olecranon process, scarring]

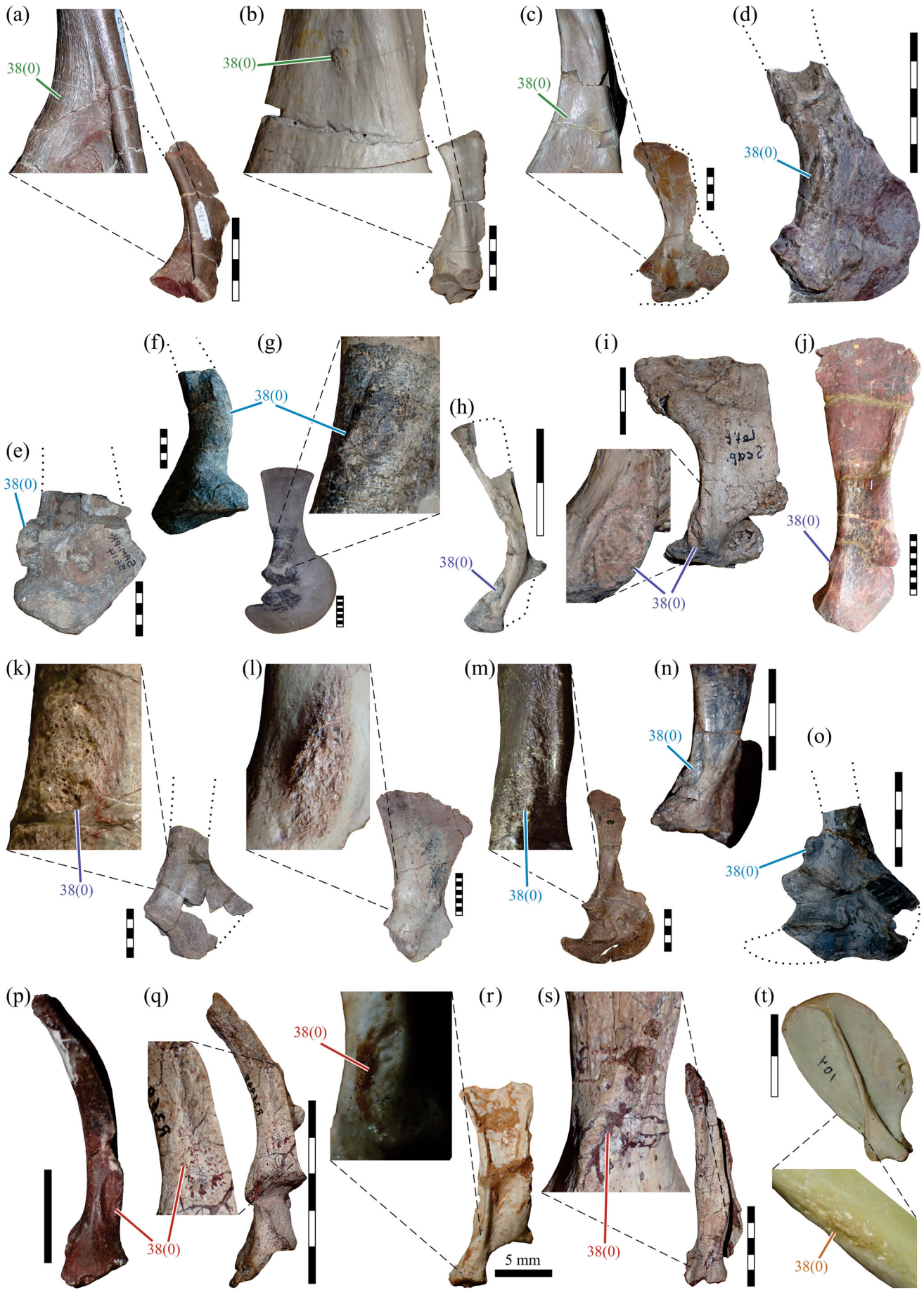

FIGURE 18 Legend on next page.

1. Via separate, but immediately adjacent, insertions onto olecranon process of ulna [anteroposteriorly expanded olecranon process]

Remarks—The olecranon process (Figure 19) is a highly consistent, unambiguous osteological correlate for the triceps group as a whole, but it often is not preserved due to poor skeletal ossification, particularly among noncynodont therapsids. Nevertheless, even in those taxa where an ossified process is absent, the proximal ulna is capped with unfinished bone, indicating that it would have continued proximally into a fibrocartilaginous process. In addition, the lateral margin of the proximal ulna is frequently scarred with longitudinal striations (Figure 19a–d,g,h), indicative of the extension of connective tissue from the olecranon down onto the main body of the bone. Mammals generally have a better-developed process relative to their nonmammalian ancestors, although two notable exceptions are aberrant fossorial taxa (Cluver, 1978; Cox, 1972) and derived kannemeyeriiform dicynodonts (Camp & Welles, 1956; Ray, 2006; Sulej & Niedźwiedzki, 2018). In the latter, the olecranon typically manifests as a separate and robust ossification, which in mature individuals becomes fused to the main body of the ulna (Figure 19e). Such "traction epiphyses" (Barnett & Lewis, 1958) and the functional or evolutionary implications of their development have remained little studied in nonmammalian synapsids.

3.13 | Pronator teres (PRTE): Characters 42–44

42. Number of heads

0. Absent
1. One
2. Two
3. Three

Remarks—This character accommodates the pronator accessorius (PRAC), a probable apomorphy of lepidosaurs (but see Burch, 2014). Although the PRAC originates more deeply than the PRTE, including from the ulna when a third head exists (state 3), its consistent insertion immediately proximal to the PRTE suggests that they are probably developmentally related. The PRTE is absent in salamanders, but a PRTE-like muscle is usually present in anurans (Abdala & Diogo, 2010), suggesting that the PRTE may in fact be synapomorphic to crown tetrapods, rather than just amniotes.

43. Origin

0. Absent
1. Posteroventral aspect of entepicondyle on humerus, proximal to the origins of all other flexor muscles
2. Ventral aspect of entepicondyle on humerus, deep to the origins of all other flexor muscles
3. Posterior aspect of entepicondyle on humerus, and ventral apex of entepicondyle (deep to other muscle origins)
4. Posterior aspect of entepicondyle on humerus, ventral apex of entepicondyle (deep to other muscle origins), and posterolateral aspect of proximal ulna

44. Insertion

0. Absent
1. Much of medial and posterior aspects of radial shaft, distal to insertion of BRA and/or BICB and/or humeroradialis (when present)

Remarks—In lepidosaurs, the PRAC tends to insert more proximally and laterally to the PRTE.

FIGURE 18 Osteological evidence of triceps scapularis attachment to the pectoral girdle in synapsids. (a) MCZ VPRA-4895 *Ophiacodon mirus* (Ophiacodontia) scapula in lateral view (inset in posterior view). (b) AMNH FARB 4046 *Secodontosaurus obtusidens* (Sphenacodontia) scapula in posterolateral view. (c) MCZ VPRA-1110 *Dimetrodon booneorum* (Sphenacodontia) scapulocoracoid in lateral view (inset in posterior view). (d) SAM-PK-8950 *Hipposaurus boonstrai* (Biarmosuchia) scapula in posterolateral view. (e) SAM-PK-5614 *Anteosaurus magnificus* (Anteosauridae) scapula in lateral view. (f) SAM-PK-5014 *Jonkeria truculenta* (Titanosuchidae) scapula in posterior view. (g) AMNH FARB 5551 *Moschops capensis* (Tapinocephalidae) scapulocoracoid in lateral view. (h) USNM V 22981 *Emydops* sp. (Dicynodontia) scapula in posterolateral view. (i) NHMUK PV R.37005 *Euptychognathus* sp. (Dicynodontia) scapula in lateral view (inset in posterior view). (j) NHMUK PV R.3762 *Kannemeyeria simocephalus* (Dicynodontia) scapula in lateral view). (k) MCZ VPRA-3455 *Dinodontosaurus brevirostris* (Dicynodontia) scapula in lateral view (inset in posterior view). (l) UFRGS-PV-0287-T *Jachaleria candelariensis* (Dicynodontia) scapula in lateral view (inset in posterior view). (m) UMZC T.883 Gorgonopsia indet. scapulocoracoid in lateral view (inset in posterior view). (n) GPIT-PV-31579 "*Scymnognathus*" *parringtoni* (Gorgonopsia) scapulocoracoid in posterolateral view. (o) SAM-PK-12185 *Lycosuchus* sp. (Lycosuchidae) scapulocoracoid in lateral view. (p) TM 4025 *Thrinaxodon liorhinus* (Cynodontia) scapula in posterior view. (q) NHMUK PV R.36995 *Luangwa drysdalli* (Cynognathia) scapulocoracoid in posterior view. (r) UFRGS-PV-1379-T *Riograndia guaibensis* (Tritheledontidae) scapula in lateral view (inset in posterior view). (s) MCZ VPRA-8812 *Kayentatherium wellesi* (Tritylodontidae) scapula in posterior view. (t) MCZ 104 *Didelphis marsupialis* (Theria) scapula in lateral view.

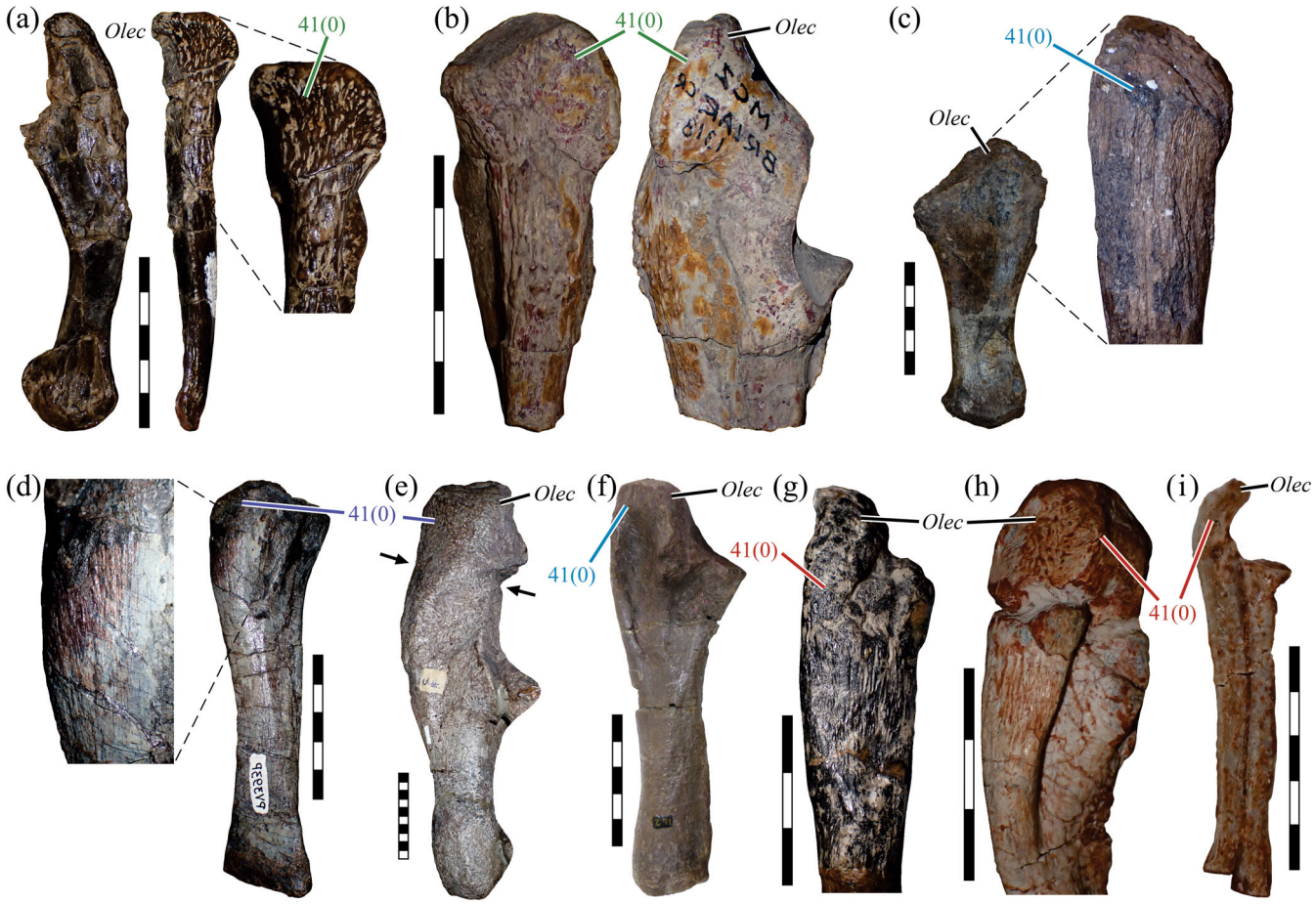

FIGURE 19 Osteological evidence of triceps insertion in synapsids. (a) MCZ VPRA-4319 *Edaphosaurus boanerges* (Edaphosauridae) ulna in posterior (left) and lateral (right) views. (b) MCZ VPRA-1318 *Dimetrodon booneorum* (Sphenacodontia) ulna in lateral (left) and anterior (right) views. (c) AMNH FARB 5322 *Moschops capensis* (Tapinocephalidae) ulna in posterior view (inset in lateral view). (d) UFRGS-PV-0393-P *Tiarajudens eccentricus* (basal anomodont) ulna in anterior view (inset in lateral view). (e) PVL 3807 *Ischigualastia jenseni* (Dicynodontia) ulna in anterior view; arrows indicate boundary between the main body of the bone and the fused "traction epiphysis" of the olecranon. (f) UMZC T.883 Gorgonopsia indet. ulna in anterior view. (g) PVL 2467 *Exaeretodon* sp. (Cynognathia) ulna in lateral view. (h) UFRGS-PV-1051-T *Trucidocynodon riograndensis* (basal probainognathian) ulna in anterolateral view. (i) SAM-PK-K359 *Erythrotherium parringtoni* (Mammaliaformes) ulna and radius in anterior view. See also Figure 16.

3.14 | Flexor carpi radialis (FCR): Characters 45 and 46

45. Origin

0. Posterior aspect of entepicondyle on humerus, proximal to origin of flexor digitorum longus
1. Posteroventral aspect of entepicondyle on humerus, deep to origin of flexor digitorum longus
2. Absent

46. Insertion

0. Medial and posterior aspect of radius, and medial and ventral aspect of radiale
1. Ventral aspect of radiale
2. Ventromedial aspect of base of metacarpal I
3. Ventral aspect of base of metacarpal II, and possibly also III
4. Absent

Remarks—The above codification reflects the main locus of muscle attachment on the carpus, and ignores a certain level of clade-specific nuance.

In their embryological study, Smith-Paredes et al. (2022) interpreted the therian FCR as deriving from the "central superficial lobe," rather than the "radial lobe" as observed in nonmammals; this would indicate nonhomology across the two groups. However, they also recognized *two* PRTE muscles (or at least two subdivisions to that muscle), both deriving from the radial lobe. Yet the PRTE

is ubiquitously singular in extant mammals, and the disposition of the two lobes, as illustrated (their extended data figs 9 and 10), compares favorably with the disposition of the PRTE and FCR as illustrated in previous myological studies (Stein, 1981, fig. 6; Carry et al., 1993, fig. 1). Furthermore, Smith-Paredes et al. did not account for all therian forearm flexor muscles in their revised homology scheme (extended data Figure 2), most notably lacking the flexor digitorum superficialis; the superficial digital flexor of nonmammals was observed to originate from the central lobe. These incongruences probably stem from a case of mistaken identity, and a revised interpretation of the results of Smith-Paredes et al. (2022) is proposed: (a) the therian FCR does indeed develop from the radial lobe, lateral to the PRTE, as it does in nonmammals, and (b) the flexor digitorum superficialis of therians is homologous with the superficial digital flexor of nonmammals, developing from the central superficial lobe.

3.15 | Flexor digitorum longus (FDL, Figures 6 and 20): Characters 47–51

47. Number of heads in superficial layer

0. One
1. Two

Remarks—Burch (2014) recognized two principal divisions of this muscle across saurians (superficial and deep), which can be reasonably recognized in all crown tetrapods. The superficial layer primarily gains origin from the humerus, whereas in the deep layer, it is primarily from the ulna. For the most part, the former corresponds to the "central superficial lobe" observed in development by Smith-Paredes et al. (2022). The exact homology between the various heads of the FDL across amniotes (and salamanders), and even within mammals, still remains to be clarified, due to variation in the number of heads and attachment topologies, as well as limited understanding of monotreme development. It is also probable that part of the FDL mass in mammals is actually homologous with part of the flexor carpi ulnaris (FCU) mass in sauropsids, in particular, the palmaris longus (Diogo et al., 2016; Smith-Paredes et al., 2022). Notwithstanding these uncertainties, it seems likely that at least the division between superficial and deep portions of the FDL (topographically central) mass is consistent across all groups.

48. Number of heads in deep layer

0. One
1. Two
2. Three
3. Four

Remarks—This character ignores additional deep heads in squamates and crocodylians that originate from the carpals, distal to the wrist joint.

49. Origin of superficial layer

0. Posterior to posteroventral aspect of entepicondyle of humerus, proximal to flexor carpi ulnaris origin
1. Distoventral aspect of entepicondyle of humerus, distal and deep to flexor carpi ulnaris origin

Remarks—The entepicondyle serves as the principal site of origin of all forearm flexor muscles, including the FDL. Although it may bear scarring (particularly prominent in "pelycosaurs"; Figure 20a–d), such scars do not clearly or consistently delimit the attachments of separate muscles, rendering it practically impossible to reconstruct attachment sites and areas precisely.

50. Origin of deep layer

0. Posterior surface of ulnar shaft
1. Distoventral aspect of entepicondyle on humerus, and posterior aspect of olecranon and proximal ulna [medial and lateral ridges]
2. Posteroventral aspect of entepicondyle on humerus, and posterior aspect of radius and proximal ulna

Remarks—This character ignores additional deep heads in squamates and crocodylians that originate from the carpals, distal to the wrist joint.

A longitudinal depression on the posterior aspect of the proximal ulna is widespread among cynodonts and therocephalians at least (Figure 16h,j–l), echoing the manifestation observed in monotremes (state 1; Figure 16u). The monotreme condition may hence be characteristic for a more inclusive group.

51. Insertion

0. Superficial and deep heads unite into common plantar aponeurosis, which sends tendons to the ventral base of the terminal phalanges [flexor tubercles]
1. Superficial and deep heads unite into common flexor tendon, which inserts on ventral aspect of penultimate phalanges of digits I–III
2. Superficial heads insert on palmar fascia and middle phalanges of digits II–IV, while deep heads unite into

common palmar aponeurosis (deep to and separate from palmar fascia) that sends tendons to base of terminal phalanges [flexor tubercles]

Remarks—Similar to character 46, the above codification reflects the main locus of muscle attachment and topology, glossing over some of the finer nuances or variations observed in extant taxa. For example, sometimes the FDL does not insert on the phalanges of all digits, or possesses additional insertions elsewhere; these are ignored for the sake of creating a tractable scheme, useable at the broad phyletic scale considered here. Flexor tubercles are commonly observed throughout nonmammalian synapsids (Figure 20e,f,i), but they alone do not inform which state is present.

3.16 | Flexor carpi ulnaris (FCU, Figures 6 and 21): Characters 52–54

52. Number of heads

0. One
1. Two

Remarks—Smith-Paredes et al. (2022) reported that the palmaris longus of therians, a superficial digital flexor, actually develops from the "ulnar lobe," and hence is at least partly homologous with the FCU of nonmammals. The situation in monotremes remains to be clarified. Rather than attempting to account for this result in the current character, the palmaris longus is considered above under the superficial layer of the FDL, where it is functionally more similar (reaching to the central manus, well distal to the wrist).

53. Origin

0. Posterodistal aspect of humeral entepicondyle, distal to FDL origin
1. As (0), also extends to lateral aspect of proximal posterior surface of ulna
2. Distal aspect of humeral entepicondyle, superficial to FDL origin, and lateral aspect of proximal posterior surface of ulna

54. Insertion

0. Ventrolateral aspect of ulnare and intermedium
1. Ventral aspect of pisiform [pisiform]

Remarks—The pisiform is the unambiguous osteological correlate of FCU insertion, and its association with the muscle is strongly conserved across extant amniotes. Indeed, it is perhaps the oldest recognizable sesamoid to have evolved in tetrapods, being recorded in various early crown amniotes, as well as some stem taxa such as captorhinids and diadectomorphs (Berman et al., 2004; Holmes, 1977; Williston, 1911). A pisiform is widespread throughout nonmammalian synapsids (Figure 21; Kümmel et al., 2020; Romer & Price, 1940).

3.17 | Epitrochleoanconaeus (EPI, Figure 20): Characters 55 and 56

55. Origin

0. Distal aspect of entepicondyle on humerus, distal to origin of FCU
1. Posterodorsal aspect of entepicondyle on humerus, proximal and dorsal to origin of FCU
2. Absent

Remarks—Although no unambiguous osteological correlate can be identified for this muscle among synapsids, well-ossified "pelycosaur" humeri possess a discrete, distally directed eminence on the distal edge of the entepicondyle, bearing rugose texture (Figure 20b–d, asterisks). Given its distal position and proximity to the ulnar facet, this may well have marked the attachment for the EPI in these taxa.

56. Insertion

0. Posterolateral border of proximal ulna, distal to olecranon process
1. Posterolateral border of distal ulna
2. Posterior aspect of olecranon process of ulna
3. Absent

Remarks—The shift to inserting on the olecranon process on the line to mammals was possibly correlated with the development of a larger, better-ossified process. Expansion of the process would have shifted the triceps insertion (on its apex and lateral border) more proximally, providing room for a more proximal insertion of the EPI.

3.18 | Brachioradialis (BRR, Figures 4 and 22): Characters 57 and 58

57. Origin

0. Anterior aspect of proximal reach of ectepicondyle on humerus, proximal to the origins of all other extensor muscles [crest, process, or scarring]

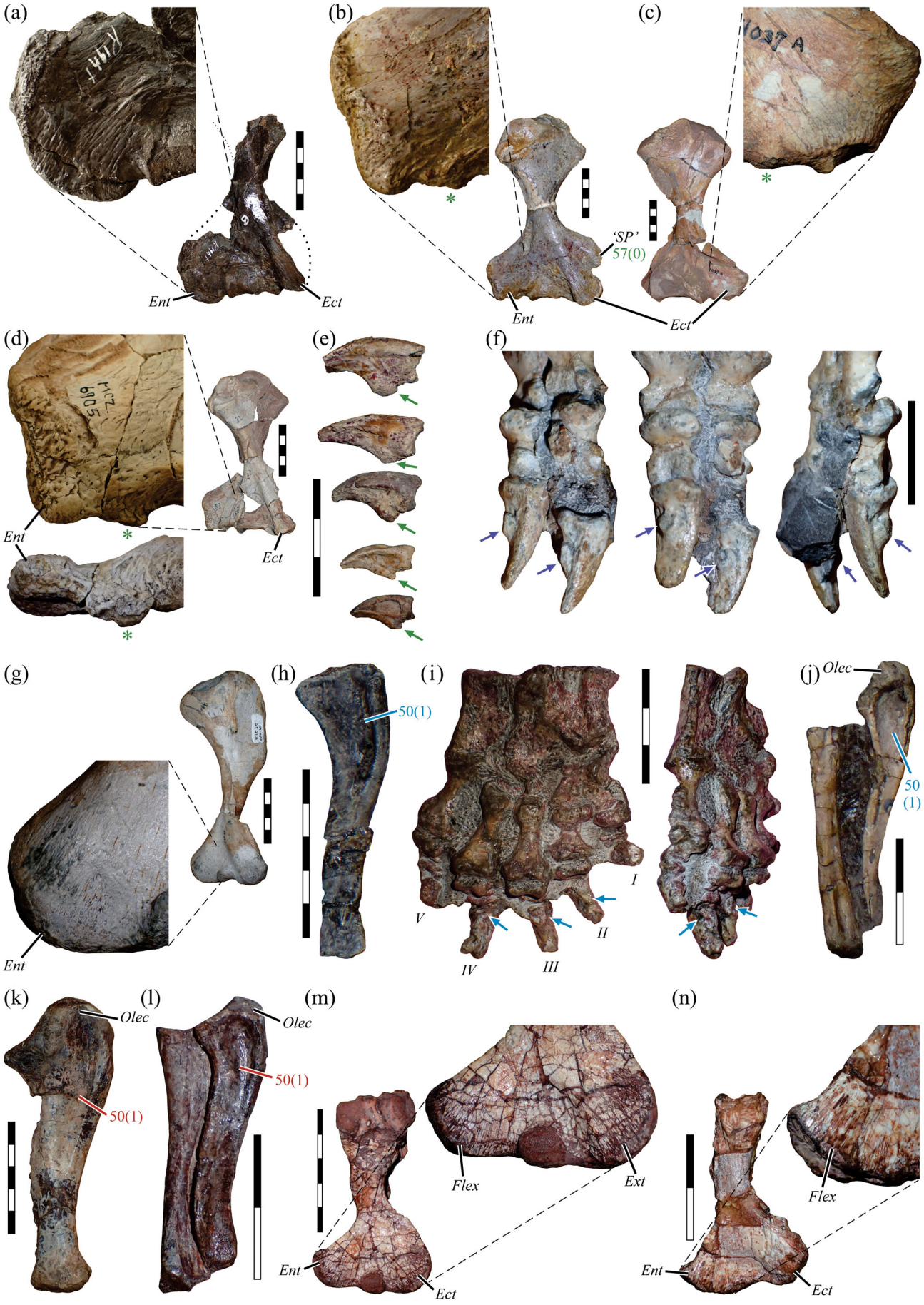

FIGURE 20 Legend on next page.

1. Ventral aspect of ectepicondyle of humerus, deep to origin of (superficial head of) extensor carpi radialis

Remarks—The humerus of stem and early crown amniotes is characterized by a stout process proximal to the ectepicondyle, typically heavily scarred, which has long been referred to as the "supinator process" or "supinator crest" (Figures 4a, 9a, 20b, and 22a–c; Romer, 1922, 1956; Sumida, 1997). As previously remarked, however, this is an unhelpful misnomer, since the BRR is a much more likely candidate to have attached here (Bishop, 2014); indeed, a true supinator muscle is probably a mammalian apomorphy (see character 59). The process of stem and early crown amniotes is more properly termed the "brachioradialis process."

This process subsequently merged with the ectepicondyle on the line to therapsids, enclosing neurovasculature to form the ectepicondylar foramen, which was then lost prior to the origin of mammals (Guignard et al., 2019a). The foramen was also independently formed within *Edaphosaurus* spp. (Figure 22a; Romer & Price, 1940). Since the development of this foramen occurred independent of the development of a similar structure in sauropsids (which persists in extant taxa), it remains uncertain what neurovasculature passed through this foramen, although the radial nerve (as in sauropsids) is a possible candidate.

58. Insertion

0. Medial aspect of radius, especially distal end
1. Medial aspect of radius and metacarpal I
2. Dorsal to medial aspect of radiale (=mammalian scaphoid)

3.19 | Extensor carpi radialis (ECR, Figures 20m and 22): Characters 59–61

59. Number of heads

0. Two
1. Three

Remarks—The ECR musculature of all tetrapods can be divided into superficial and deep head(s). This character incorporates the mammalian supinator (SUP), which is distinct from the "supinator" or "supinator longus" of non-mammalian tetrapods (e.g., Burch, 2014; Meers, 2003; Miner, 1925; Russell & Bauer, 2008), the latter being homologous to the BRR of mammals. Although the grouping of the SUP with the ECR musculature is fairly uncontroversial (Haines, 1939), it remains uncertain as to which head (or heads) in nonmammalian tetrapods is homologous to the SUP. Gross topological relationships suggest that one of the deeper heads may be equivalent to the SUP of mammals, but this requires further investigation.

60. Origin

0. Anterior aspect of ectepicondyle on humerus, immediately distal to BRR origin
1. Antero- and proximoventral aspect of ectepicondyle on humerus, deep to other forearm extensor origins (except BRR)

61. Insertion

0. Anterior aspect of radius, lateral to BRR insertion (deep head/s), and dorsal to medial aspect of proximal carpals, especially the radiale (superficial head)
1. Anteromedial aspect of radial shaft, lateral to BRR insertion (deep head, SUP), and dorsal aspect of base of metacarpals II–III/IV (superficial head/s).

3.20 | Extensor digitorum longus (EDL, Figures 20m and 22): Characters 62–64

62. Number of heads

0. One
1. Three or more

FIGURE 20 Osteological evidence of digital flexor musculature attachment in synapsids. (a) MCZ VPRA-4318 *Edaphosaurus boanerges* (Edaphosauridae) humerus in dorsal view. (b) MCZ VPRA-3357 *Dimetrodon limbatus* (Sphenacodontia) humerus in dorsal view. (c) AMNH FARB 4037a *Dimetrodon giganhomogenes* (Sphenacodontia) humerus in ventral view. (d) MCZ VPRA-6905 *Dimetrodon limbatus* humerus in dorsal view, inset in dorsal (top) and distal (bottom) views. (e) MCZ VP 101776a–e cf. *Dimetrodon* unguals (side unknown). (f) SAM-PK-K1633 *Diictodon feliceps* (Dicynodontia) phalanges and unguals in lateral (left), ventral (middle), and medial (right) views. (g) SAM-PK-K1676 Gorgonopsia indet. humerus in dorsal view. (h) BP/1/6229 Scylacosauridae indet. ulna in posterior view. (i) CGS RS 424 *Glanosuchus macrops* (Scylacosauridae) manus in ventral (left) and ventromedial (right) views. (j) BP/1/2294 *Ictidosuchoides longiceps* (Eutherocephalia) radius and ulna in posterior views. (k) NMQR 2700 cf. *Cynognathus* (Cynognathia) ulna in posterior view. (l) MCZ VPRA-3801 *Massetognathus pascuali* (Cynognathia) radius and ulna in posterior view. (m) MCZ VPRA-3616 *Chiniquodon* sp. (basal probainognathian) humerus in dorsal view. (n) *Prozostrodon brasiliensis* humerus in dorsal view. Arrows indicate flexor tubercles for attachment of the flexor digitorum longus (character 51, state uncertain); asterisks indicate potential site of origin of the epitrochleoanconaeus.

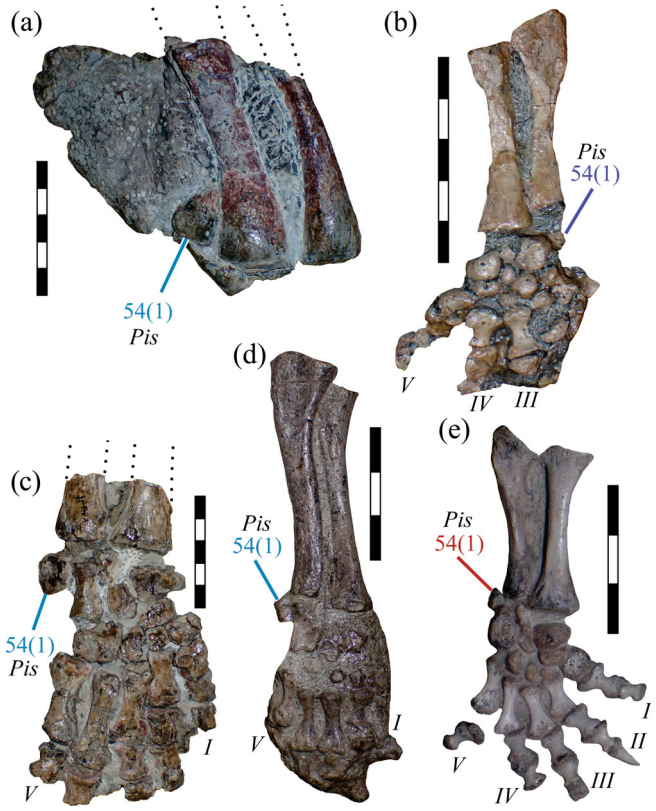

FIGURE 21 The pisiform is an unambiguous correlate of the insertion of the flexor carpi ulnaris, and is widespread throughout synapsids. Some representative therapsid examples are illustrated here (see Romer & Price, 1940 for "pelycosaur" examples). (a) SAM-PK-K252 *Hipposaurus boonstrai* (Biarmosuchia) antebrachium in anterior view; remainder of manus is folded over on the underside of the specimen. (b) CGS T72 *Diictodon feliceps* antebrachium and manus, in posterior/ventral view. (c) SAM-PK-K4441 Gorgonopsia indet. manus in dorsal view. (d) BP/1/3973 *Olivierosuchus parringtoni* (Eutherocephalia) antebrachium and manus in anterior/dorsal view. (e) SAM-PK-K10465 *Galesaurus planiceps* (Cynodontia) antebrachium and manus in anterior/dorsal view.

63. Origin

0. Anterior aspect of ectepicondyle on humerus, between ECR and ECU origins
1. Anterior aspect of ectepicondyle on humerus [extensor digitorum communis/EDC, extensor digitorum lateralis/extensor digtorum longus (EDLa)] and lateral aspect of anterior proximal ulna (extensor digitorum profundus I/EDP1)

Remarks—Although the extensor digitorum profundus has an ulnar origin, suggesting a possible association with the ECU mass instead, its consistent tendency for insertions on the radial side of the manus leads to its grouping here (see also Haines, 1939). The ectepicondyle serves as the principal site of origin of most forearm extensor muscles, including the EDL, and it often exhibits a scarred surface texture in extinct synapsids (Figures 20m and 22), particularly well developed in "pelycosaurs." This texture is typically broad and diffuse, and lacks discrete regions that may unambiguously correlate to specific muscles.

64. Insertion

0. Dorsal aspect of base of metacarpals II–IV
1. Dorsal aspect of base of metacarpal II only
2. Extensor processes of unguals of each digit

Remarks—State 0 captures the fundamental locus of attachment in salamanders and lepidosaurs, ignoring finer nuances of additional attachment to adjacent bones. Interestingly, recent embryological data suggest that the entire set of dorsal hand musculature plesiomorphic to amniotes was lost on the line to therians, being replaced by a translocated part of the ventral hand musculature (Smith-Paredes et al., 2022). It remains to be determined whether this also applies to monotremes, although their therian-like pattern of insertion (state 2) suggests that it may indeed be the case. Irrespective of the origins of this apomorphic condition, the codification outlined here captures the stark contrast in topology between mammals and nonmammals, which is sufficient from a functional perspective at least.

3.21 | Extensor carpi ulnaris (ECU, Figures 20m and 22): Characters 65–67

65. Number of heads

0. One
1. Two

66. Origin

0. Distal aspect of ectepicondyle on humerus
1. Distal aspect of ectepicondyle on humerus, and anterolateral aspect of proximal ulna

67. Insertion

0. Anterolateral aspect of distal ulna, plus lateral carpus and/or metacarpal V
1. Lateral aspect of carpus and proximal metacarpal V
2. Lateral aspect of digit V
3. Anterior aspect of almost entire ulnar shaft

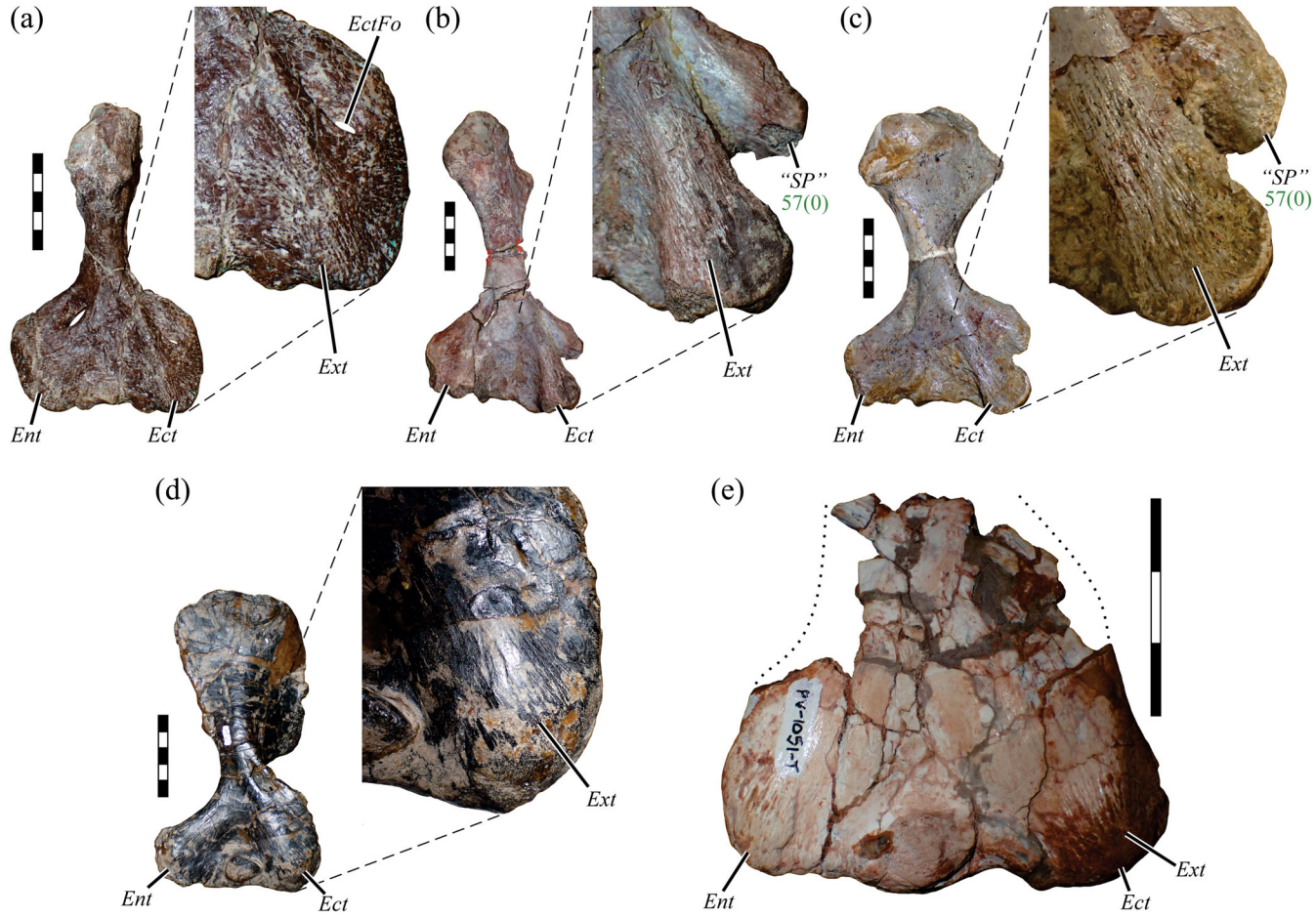

FIGURE 22 Osteological evidence of digital extensor musculature attachment to the humerus in synapsids. (a) MCZ VPRA-3417 *Edaphosaurus* sp. (Edaphosauridae); note how the "supinator" process (SP) is merged with the ectepicondyle (Ect) to form an ectepicondylar foramen (EctFo). (b) MCZ VPRA-4906 *Sphenacodon ferocior* (Sphenacodontia). (c) MCZ VPRA-3357 *Dimetrodon limbatus* (Sphenacodontia). (d) PVL 2554 *Exaeretodon argentines* (Cynognathia). (e) UFRGS-PV-1051-T *Trucidocynodon riograndensis* (basal probainognathian). All humeri are shown in dorsal view.

Remarks—The above codification reflects the main locus of muscle insertion, ignoring some finer nuances of variation within and across groups. In state 0, "carpus" primarily refers to the ulnare and pisiform (when present), whereas in state 1 it refers to the hamate (= distal carpals IV + V; Kümmel et al., 2020). The key point of the codification as constructed here is to capture a distal shift in the insertion within mammals (states 1 and 2).

3.22 | Anconaeus (ANC): Characters 68 and 69

68. Origin

0. Absent
1. Dorsodistal aspect of ectepicondyle of humerus

Remarks—In monotremes, the origin is much more extensive, covering almost the entire dorsal surface of the ectepicondyle. *Sphenodon* possesses an ANC-like muscle that has been named as such by previous workers (Haines, 1939; Miner, 1925; Russell & Bauer, 2008). Yet, it appears closely associated with the ECU in both topology and innervation (Haines, 1939; Osawa, 1897), whereas the ANC of therians is apparently a derivative of the triceps mass (Smith-Paredes et al., 2022, extended data fig. 1), suggesting nonhomology between the two. Study of development in *Sphenodon* would help clarify the matter.

69. Insertion

0. Absent

1. Anterior aspect of proximal ulna, including much of olecranon process

3.23 | Abductor pollicis longus (APL, Figure 23): Characters 70 and 71

70. Origin

0. Dorsal aspect of proximal carpals
1. Anterior aspect of distal ulna
2. Medial aspect of ulnar shaft and anterior aspect of distal radius
3. Medial aspect of proximal anterior ulna and lateral aspect of proximal anterior radius

Remarks—The gorgonopsians *Cyonosaurus longiceps* (e.g., BP/1/4269, SAM-PK-K10428) and *Lycaenops ornatus* (AMNH FARB 2240) bear a broad, elevated scar on the anterolateral aspect of the distal radius (Figure 23b,c). Similarly, the radius of basal eucynodonts (i.e., cynognathians and basal probainognathians) often bears a laterally to anterolaterally projecting crest or flange on its distal half, which opposes a medially projecting flange extending along much of the ulnar shaft (Benoit et al., 2022b; de Oliveira et al., 2010; Jenkins, 1970a, 1971; Liu et al., 2017) (Figure 23d–g). These structures may indicate the attachment of the APL, or alternatively other muscles such as the pronator quadratus (especially for the ulna), but it is not currently possible to recognize discrete, unambiguous osteological correlates for any muscle.

71. Insertion

0. Dorsomedial aspect of base of metacarpal I
1. Dorsal aspect of base of radiale

Remarks—This character captures the principal locus of insertions, ignoring minor variation in possible additional attachments to surrounding bones (e.g., radiale or trapezium) or soft tissues.

3.24 | Pronator quadratus (PRQU, Figure 23): Characters 72 and 73

72. Origin

0. Medial aspect of much of ulnar shaft
1. Posterior aspect of proximal ulna through to medial aspect of distal ulna
2. Absent

73. Insertion

0. Lateral aspect of much of radius
1. As (0), but extending to ventral aspect of medial carpals
2. Absent

Remarks—State 1 focuses on the main locus of insertion, ignoring minor nuances in variable insertions across taxa.

4 | DISCUSSION

Using extensive first-hand observation of fossils and an explicit phylogenetic framework, this study sought to trace the evolution of forelimb musculature from early amniotes through to crown mammals. The identification of homologous (and nonhomologous) structures across disparate extant and extinct taxa has helped clarify several important aspects of how and when the mammalian forelimb was assembled. Frustratingly, interpreting the evolution of musculature distal to the elbow remains hampered by the scarcity of unambiguous and homologous osteological correlates of muscle attachment in the antebrachium and manus of tetrapods. Use of an explicit phylogenetic framework can ease the challenge by providing constraints on the range of inferences, and a means of evaluating the relative support (plausibility) of competing alternative inferences. The anatomical and phylogenetic framework assembled here will also provide a new, more rigorous basis for the future reconstruction of musculature, limb biomechanics, and organismal biology in extinct synapsids (Bishop, Cuff, & Hutchinson, 2021, and references cited therein). In turn, this will help to address questions of postural and functional evolution within Synapsida.

4.1 | Major trends along the stem lineage

The evolution of forelimb musculature on the line to mammals was a complex narrative (Figure 24a,b). The number of state changes at each node of the stem lineage, as inferred from ASR, shows that the pattern of character evolution fluctuated along the stem, with a large concentration of changes at the origin of Therapsida, a more subdued but protracted set of change throughout non-mammalian cynodonts, and a third pulse within Theriiformes (Figure 24b). Assumption of the mono- or paraphyly of Therocephalia does not significantly alter the pattern recovered. Furthermore, there is no

FIGURE 23 Osteological evidence of attachment of deep antebrachial musculature to the radius and ulna in synapsids. (a) UCMP 83566 *Sphenacodon ferox* (Sphenacodontia) radius in lateral (left) and anterior (right) views. (b) SAM-PK-K10428 *Cyonosaurus longiceps* (Gorgonopsia) left and right radii in anterior view (left element mirrored to appear as from right side); note small bulge on distolateral aspect. (c) AMNH FARB 2240 *Lycaenops ornatus* (Gorgonopsia) radius in anterior (left) and anterolateral (right) views; note bulge on distolateral aspect. (d) MCZ VPRA-3812 *Massetognathus pascuali* (Cynognathia) ulna in anterior (left) and medial (right) views. (e) PVL 2467 *Exaeretodon* sp. (Cynognathia) radius in anterior (left) and lateral (right) views. (f) MCZ VPRA-4002 *Chiniquodon theotonicus* (basal probainognathian) radius and ulna in (left to right) anterior, medial, posterior, and lateral views, illustrating opposing flanges of bone. (g) UFRGS-PV-1051-T *Trucidocynodon riograndensis* (basal probainognathian) radius in anterior (left), lateral (right), and anterolateral (inset) views. See also Figure 16p. While these structures possibly served as attachment for the abductor pollucis longus or pronator quadratus (arrows), they cannot at present be unambiguously recognized as osteological correlates for a specific muscle.

significant correlation between the inferred number of state changes at a given node and the proportion of missing data pertinent to that node (Figure 24c; $p = 0.402$, determined using ordinary least squares in PAST 3.01; Hammer et al., 2001), lending credence to the recovered pattern of change. The large anatomical shift associated with the origin of therapsids is not unexpected, given the >30 Ma ghost lineage separating the oldest known well-supported members of Therapsida and their immediate sister group, the sphenacodontid "pelycosaurs" (Angielczyk & Kammerer, 2018; Bishop et al., 2023; Sidor & Hopson, 1998). This reiterates that a critical chapter of synapsid anatomical evolution remains to be understood.

As inferred by the current analyses, major changes in forelimb musculature associated with the origin of therapsids included a shift in the insertion of key shoulder muscles on the proximal humerus, concomitant with a reorganization of proximal humeral structure more generally (characters 2, 7, 11, 18; see also Bishop et al., 2023), a shift in the insertion of the BICB on the radius (character 32), a less direct connection of the TRIC to the metacoracoid (character 37), and a stronger relationship between the FDL origin and ulnar shaft (character 50). Major changes occurring within nonmammalian cynodonts principally revolve around the transformation of deltoid and supracoracoid musculature, affecting the structure of the scapula (characters 5, 6, 21, 22) and

humerus (characters 7, 23–25), in addition to the appearance of a novel muscle, the TMA (character 4). Changes occurring within Theriiformes are related to the reduction or loss of the interclavicle (at least as a large, discrete element; Bendel et al., 2022; Brent et al., 2023) and clavicle, and diminishment of the coracoid plate to form the coracoid process of the glenoid, which modified the origins of the DCl, PECT, BICB, CBB and CBL (characters 9, 10, 31, 26, 27). Other changes possibly include modification of forearm musculature (characters 50, 51, 59, 73), but the scarcity of osteological correlates distal to the elbow warrants caution in this assessment. These results collectively provide partial support for each of the prior macroevolutionary interpretations of Romer (1922; major change occurred in therapsids), Jenkins (1970b, 1971; major change occurred in therapsids and theriiformes), and Kemp (1982; major change occurred in therapsids and advanced cynodonts). More generally, they highlight the nonlinear, mosaic pattern by which modern mammalian traits were accrued, with the reorganization of shoulder anatomy, in particular, occurring in a protracted, step-wise fashion. The functional significance of each of these changes, and of the collective order in which they occurred along the stem lineage, awaits future investigation.

Of note, extant monotremes have frequently featured in considerations of anatomical or functional evolution of synapsid limbs (Brocklehurst et al., 2022; Gregory & Camp, 1918; Haines, 1952; Jenkins, 1970b, 1971; Regnault & Pierce, 2018; Walter, 1988a), due to their phylogenetic position and use of a nonerect limb posture and gait. Notwithstanding these facts, monotremes also possess a suite of musculoskeletal apomorphies, presumably related to their semi-fossorial or semi-aquatic lifestyles (or prior evolutionary histories; Phillips et al., 2009), which may conspire to obfuscate evolutionary interpretation (Haines, 1952; Howell, 1936). To explore this, the phylogenetic analysis and ASR were re-run to the exclusion of monotremes; the proportion of all internal nodes whose state could be reconstructed unambiguously (i.e., likelihood $\geq$0.75; assessed over all characters) increased slightly (Figure 24d). This may suggest that monotremes might contribute more confusion than clarity in interpretations of forelimb anatomical evolution, if not considered with due care. Promisingly, however, the application of an explicit phylogenetic framework, in tandem with a holistic assessment of available fossil data, can help navigate potential pitfalls in this endeavor. Through identifying character polarities, and which states in a given taxon are likely plesiomorphic, apomorphic, or transitional, this can better resolve the likely sequence of character evolution.

4.2 | Evolution of deltoid and scapulohumeral musculature

Through investigation of embryological development among diverse extant species, Smith-Paredes et al. (2022) posited several new hypotheses of homology across the forelimb muscles of crown amniotes. Most hypotheses were accepted and incorporated into the creation of character complexes in the current study, but some aspects were found to be inconsistent with the evidence presented by the fossil record. These concern the homology and history of the deltoideus and scapulohumeral musculature. For the sake of fluency, discussion of the discrepancies was postponed while the evidence itself was documented above; now the issue will be addressed here in full.

Traditionally, the evolution of musculature anterior and dorsal to the shoulder joint of synapsids has been a narrative dominated by the dorsal migration, expansion, and differentiation of the SPC to form the ISP and SSP of therians (Figure 25a) (Cheng, 1955; Diogo et al., 2016; Gregory & Camp, 1918; Jenkins, 1971; Kemp, 1982; Romer, 1922, 1962). In contrast with this major reorganization, the deltoid and SHA musculature were inferred to have undergone minor topological changes only: the DSc origin shifted posteriorly as the anterior scapular blade became laterally reflected to form the scapular spine (DSp); the DCl bifurcated to produce the DCl and DAc; and the SHA reduced and shifted its origin somewhat posteriorly to become the TMI. However, Smith-Paredes et al. (2022) observed the therian DCl to be derived from the SPC mass, implying nonhomology with the homonymous muscle of nonmammals, and suggested that the nonmammal DCl instead is homologous to the DSp of mammals (Figure 25b). In turn, they hypothesized that the DSc of nonmammals is homologous to the TMI of mammals and (crucially) the SHA is apomorphic to lepidosaurs. (Note: both the lepidosaurian SHA and mammalian TMI are derived from the same deltoid division.) Smith-Paredes et al. did not recognize a homologue for the DAc among nonmammalian amniotes, implying that it may be a mammalian neomorph. Under this scenario, the evolution of therian shoulder musculature would have involved the radical transformation of origin sites for multiple muscles, in addition to the SPC, involving considerable spatial disassociation between muscle and bone.

As documented above, abundant fossil evidence records the attachment of a muscle to the proximodorsal humerus of stem and early crown amniotes (including "pelycosaurs"; Figures 7a,b and 10a–g), whose scarring cannot be accounted for by the LD, deltoids, SSc or SPC, which each are evidenced by their own discrete, well-supported osteological correlates. An additional muscle

must therefore have existed. The texture of scarring indicates that this additional muscle is pulled anteriorly, toward the main body of the pectoral girdle. A lepidosaur-like SHA would explain these observations, suggesting that the SHA is a feature of a much more inclusive group. A subtle proximal shift is all that is required to transform this "early amniote" scar into the longitudinal scar that typifies the proximal humerus of therapsids, which can in turn be traced through cynodonts into at least theriimorph mammals (Figures 7n,o and 10h–ao). This proximally shifted scar lies in the same position as the insertion of the TMI in therians, and the simplest explanation is that the scar *is* for the TMI. Collectively, fossil evidence spanning from stem amniotes to

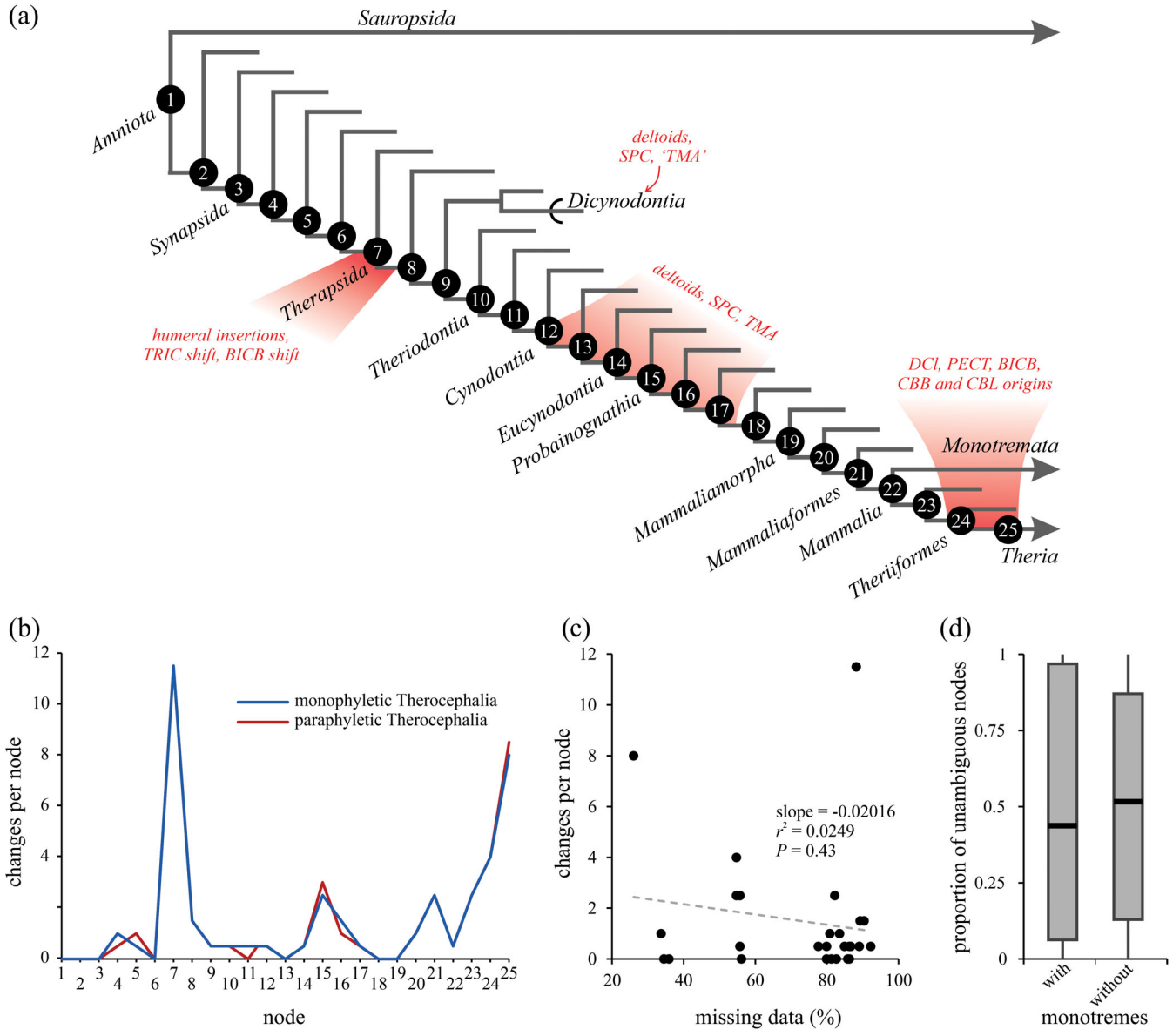

FIGURE 24 Major trends in forelimb muscle evolution along the mammalian stem lineage. (a) Phylogeny of all crown amniote groups examined in this study, with major phases of muscular reorganization indicated. (b) The pattern of character evolution along the mammalian stem lineage, quantified as the number of state changes inferred for each node by maximum likelihood ancestral state reconstruction. Node numbers correspond to those indicated in (a). Values are the average across root-to-tip and tip-to-root sequential comparisons, and are reported for both tree topologies (mono- and paraphyletic Therocephalia). Although the specific numbers should be regarded with some caution, due to the limitations of likelihood-based detection of state change (see Materials and Methods), the general pattern is nonetheless informative. (c) Comparison of the number of state changes for each node on the stem lineage versus the amount of missing data pertinent to that node; the absence of a significant correlation implies that the patterns in (a) and (b) are likely reflective of the true pattern of evolution. (d) Boxplot summary of the proportion of all internal nodes within the phylogeny whose state could be reconstructed unambiguously by maximum likelihood, across all forelimb characters, both with and without the inclusion of monotremes.

crown mammals supports (a) the existence of a SHA in early amniotes (also suggested by a SHA-like muscle in some salamanders; Wilder, 1912; Miner, 1925) and synapsids, and (b) the homology of the lepidosaur SHA with the mammalian TMI, contrasting with the hypothesis of Smith-Paredes et al. (2022).

Further conflicting evidence is presented by the topological arrangement observed in extant mammals, where the paths of the TMI and deltoid musculature are separated by the passage of the ISP; this is particularly obvious in monotremes where the TMI is well developed (Gambaryan et al., 2015; Regnault et al., 2020). Even though the TMI is derived embryonically from the same mass as the deltoids in therians (Cheng, 1955; Smith-Paredes et al., 2022), this spatial relationship renders it difficult to conceive how a gradual phyletic transformation in the adult phenotype—from DSc on the dorsal scapula to TMI on the ventral scapula—could be achieved without the ISP creating an obstruction. Mirroring this issue, the fossil record provides no evidence that illustrates how a shift in origin of the DSc ventrally across the scapular surface could occur, without the dorsally expanding ISP getting in the way. Coincidentally, spatial separation of the DSc and SHA also occurs in lepidosaurs, here created by the passage of the scapulohumeral ligament between the two (Fahn-Lai et al., 2020; Fürbringer, 1900; Jenkins & Goslow, 1983; Landsmeer, 1984).

These conflicting lines of evidence are reconciled here with a new hypothesis (Figure 25c), which largely reiterates the traditional hypothesis except for the "DCl" being derived from the SPC mass in mammals (or at least therians). In this scenario, the "superficial" component of the embryonic deltoid mass always differentiates into two parts, but due to the expansion of the SPC mass in mammals, both parts are confined in their origin to the scapula only, forming the DSp and DAc. The DAc is not a mammalian neomorph, just a relocated DCl, its origin having been dorsally displaced by the SPC mass. It is also suggested that, along the mammalian stem lineage, the transformation of origins was coincident with the development of an acromion, laterally reflected anterior margin and infraspinous fossa, at the base of Cynodontia. The alternative hypothesis proposed here requires far less drastic reorganization of muscle–bone topologies, and presumes a failure of the SHA to differentiate from the deltoid mass in archelosaurs.

4.3 | Convergence between dicynodonts and cynodonts

The reorganization of the synapsid pectoral girdle and its associated musculature, especially the SPC and deltoids, is a textbook example of substantial structural transformation accompanying a major evolutionary transition (Kemp, 1982; Luo, 2015; Romer, 1962). Building upon previous studies (e.g., Jenkins, 1971; Romer, 1922; Sun & Li, 1985), the transformational hypotheses outlined here posit that much of this reorganization can be documented in the mammalian stem lineage from osteological correlates observed in the fossil record, particularly within Cynodontia (cf. characters 5, 6, 21, and 22; Supporting Information Appendix S4). Yet, some of these osteological correlates are also observed in dicynodonts, including the basalmost form *Eodicynodon* (Figure 24a). These animals develop an acromion and recess on the anterior base of the scapular blade, the clavicle ceases to articulate with the scapulocoracoid along its full length, and within therochelonian dicynodonts the anterior scapular margin becomes laterally reflected to form a distinct scapular spine and lateral scapular fossa (Figure 3c). The last two features are particularly accentuated in the aberrant Permian form *Dicynodontoides*, and independently in Triassic kannemeyeriiforms (Figure 12c,f). Given that nondicynodont anomodonts retain a typically therapsid pectoral girdle construction (Brinkman, 1981; Cisneros et al., 2015; Fröbisch & Reisz, 2011), the changes in dicynodont skeletal structure are convergent with those observed in cynodonts. Interestingly, incipient convergence may also have occurred within gorgonopsians and scylacosaurid therocephalians, which possess a ridge that demarcates a shallow fossa on the anterior scapulocoracoid (Figure 12g,h). This structure was not explicitly codified in the present study, but it warrants further investigation.

The superficial similarity between dicynodont and cynodont pectoral girdles, and the present formulation of character complexes, would imply that the dicynodont SPC also underwent topographic expansion, migration, and differentiation, at least in more derived taxa. In reality, however, the structures in dicynodonts are not strictly homologous (failing the test of congruence), rendering it less certain if the full suite of muscular changes occurred. For instance, the SPC may have indeed expanded dorsally to take origin from the anterior surface of the reflected scapular margin (like the mammalian SSP), but could have remained undivided (King, 1981a). It is noteworthy that even in the derived kannemeyeriiforms (e.g., Sulej & Niedźwiedzki, 2018; Walter, 1988b), although the anterior scapular margin and acromion are strongly reflected laterally, the procoracoid remains well developed and a discrete GrTu-like scar on the humerus is absent. The anteroproximal region of the DPC may form a distinct "corner" in some taxa like *Eodicynodon* and *Diictodon* (Figures 10k and 13i), where the SPC would be expected to insert, but a distinct scar resembling the cynodont GrTu is nevertheless absent.

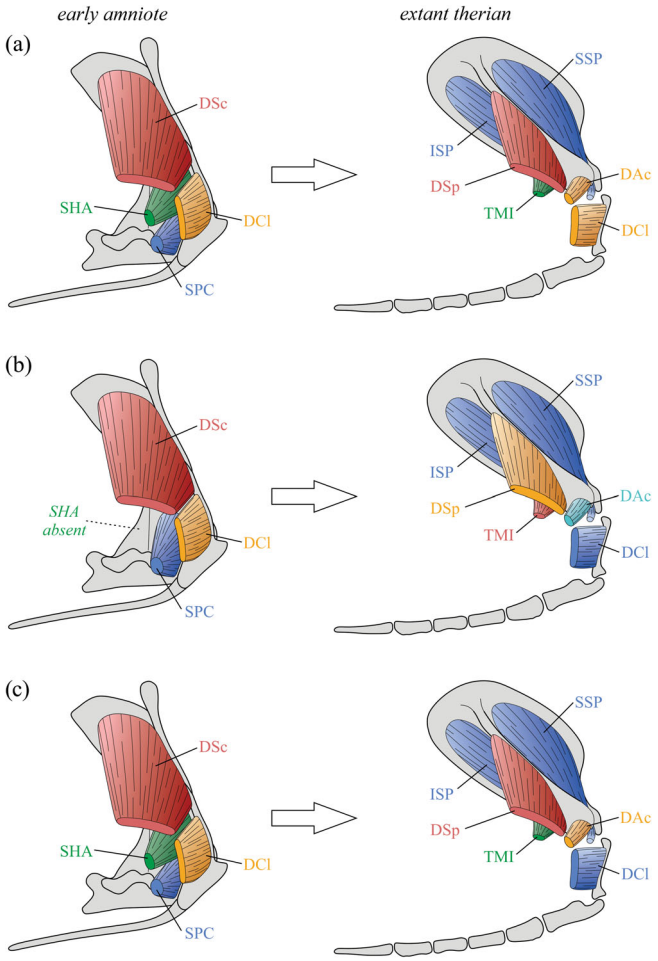

FIGURE 25 Different hypotheses of homology of the deltoid and supracoracoideus musculature from early amniotes (e.g., "pelycosaurs") to extant therian mammals. (a) The traditional hypothesis (e.g., Cheng, 1955; Diogo et al., 2016; Romer, 1922). (b) Novel hypothesis of Smith-Paredes et al. (2022) based on embryology, including the deltoideus acromialis (DAc) as a mammalian neomorph (teal color). (c) Revised hypothesis proposed here that reconciles evidence from embryology and the fossil record. In each panel, colors are used to represent homological correspondences. Note that in (b) and (c) part of the supracoracoideus (SPC) also gave rise to part of the pectoralis major (data not shown here).

A second instance of probable convergence between dicynodonts and cynodonts, hitherto gone unrecognized, is the development of a TeTu on the posterior humerus. In numerous specimens of both dicynodonts and epicynodonts, this tubercle is connected to the LeTu (SSc insertion) proximally via a bridge of bone or other scarring, mirroring the condition in extant monotremes (Figure 8). The TeTu is recognized as the osteological correlate of insertion of the TMA in epicynodonts, and its strikingly similar manifestation in dicynodonts suggests the existence of a TMA-like muscle here as well. A TeTu is not observed in nondicynodont anomodonts, implying that these structures in dicynodonts and epicynodonts are not strictly homologous. Yet, the TMA is a derivative of the subscapular muscle mass in therians (Smith-Paredes et al., 2022), and both dicynodonts and epicynodonts frequently exhibit an osteological connection between the TeTu and LeTu. This suggests that the TeTu in both groups may have arisen via homologous developmental programs (deep homology; Shubin et al., 2009). Common developmental pathways may also have been responsible for convergence in scapular and SPC evolution between the two groups.

Elsewhere in the body, dicynodonts and cynodonts also exhibit instances of convergence in the gross structure of the pelvic girdle, including anterior expansion of the iliac blade, reduction of the postacetabular ilium, reduction and retroversion of the pubis, and a shift of the obturator foramen to lie between the pubis and ischium (Bishop & Pierce, 2023). These skeletal modifications outwardly suggest convergent modifications in hindlimb musculature, although dicynodonts and cynodonts notably departed in femoral osteology (Bishop & Pierce, 2023; Kemp, 1982). Being on the mammalian stem lineage, musculoskeletal transformations within cynodonts have historically received more research focus (as is the case here), but it is noteworthy that each of the above instances of convergence first evolved in mid- to late Permian dicynodonts.

5 | CONCLUSION

Drawing upon the exceptional fossil record of Synapsida, this study has helped clarify the history of mammalian forelimb muscle evolution, identifying those traits that are characteristic of crown mammals, those that have changed leading up to Mammalia, and those that have remained largely unchanged for hundreds of millions of years. Several traits are inferred to have significantly greater antiquity than previously recognized: part of what is traditionally considered as distinctive to mammals has actually been inherited from their (often very) distant ancestors. The evolution of forelimb musculature on the line to mammals was complex, protracted, and nonlinear, with multiple concentrated phases of anatomical transformation and several instances of convergence between disparate clades. Through the present work (and its companion study, Bishop & Pierce, 2023), an understanding of appendicular evolution in Synapsida is now more on par with other major tetrapod groups, such as nonavian dinosaurs (Burch, 2014; Hutchinson, 2001a, 2001b, 2002; Maidment & Barrett, 2011; Otero, 2018).

Taking a fossil-focused approach to investigations of anatomical evolution can better relate taxa that are

morphologically disparate and separated by large expanses of time, especially when it enables the recognition of transitional morphologies that are only preserved in the fossil record. Fossils provide a unique perspective to the development and testing of macroevolutionary hypotheses, beyond what is possible with just extant taxa alone. Yet, previous fossil-based studies of appendicular muscle evolution in synapsids have tended to focus on a few exemplar taxa or specimens, limiting the depth and precision of the inferences that have been made, and rendering them more susceptible to the confounding effects of (unrecognized) apomorphies or homoplasies. The present work builds upon prior studies by evaluating a greatly expanded dataset of fossil evidence, which has facilitated a more comprehensive assessment. In tandem with an explicit phylogenetic framework, this has resulted in a more rigorous detection of homologies and homoplasies, and a more detailed estimation of the sequence of anatomical evolution on the line to mammals. Additionally, this approach has refined interpretations of apomorphies versus retained plesiomorphies in unusual taxa such as extant monotremes, and has highlighted instances of incongruence between fossil data and other lines of evidence (e.g., embryology) that require future scrutiny. Lastly, the development of character–state complexes here will provide a more objective (perhaps even conservative) means for reconstructing anatomy in extinct species, forming a key foundation for future work examining the functional consequences of anatomical changes for posture and locomotion.

AUTHOR CONTRIBUTIONS

Peter J. Bishop: Conceptualization; methodology; data curation; investigation; formal analysis; funding acquisition; writing – original draft; writing – review and editing; visualization; validation; project administration; resources; software. **Stephanie E. Pierce:** Conceptualization; methodology; data curation; investigation; formal analysis; funding acquisition; project administration; writing – original draft; writing – review and editing; visualization; validation; software; supervision; resources.

ACKNOWLEDGMENTS

The research documented in the present paper, and its companion paper, would not have been possible without the efforts of countless individuals who have, over the past century and a half, discovered, collected, prepared, and curated the fossil material studied here. The breadth and depth of insights that can now be gained from such an extensive sample of the fossil record are a testament to the dedication and foresight of these people. It is a pleasure to sincerely thank the curatorial and collections staff of all museums that contributed data to this study, for their hospitality, assistance, and access to material in their care. They include C. Mehling and A. Gishlick (AMNH), S. Jirah, B. Rubidge, and B. Zipfel (BP, RC), O. Rauhut (BSPG), N. Mchunu (CGS), K. Angielczyk, W. Simpson, and A. Stroup (FMNH), I. Werneburg and A. Krahl (GPIT), A. Martinelli, J. Escobar, and M. Ezcurra (MACN), C. Byrd, E. Biedron, M. Omura, S. Johnston and C. Green (MCZ), M. Day (NHMUK), J. Botha and E. Butler (NMQR), P. Ortiz, and R. González (PVL), Z. Skosan and C. Browning (SAM), H. Fourie (TM), P. Holroyd (UCMP), H. Francischini (UFRGS), M. Lowe and R. Stebbings (UMZC), H. Sues, A. Millhouse, and R. Masters (USNM) and C. Sidor (University of Washington, Seattle). The authors benefited from numerous stimulating discussions with many of these people, on various topics, in addition to other colleagues including C. Kammerer, B. Stuart, A. Huttenlocker, M. Van den Brandt, F. Pinheiro, S. Burch, R. Smith, and A. Mann. Many colleagues also generously provided permission to examine and photograph (often unpublished) fossil material in their study or care, or shared photographs or important items of literature. M. Sears and R. Broadfoot (Ernst Mayr Library, Harvard University) also facilitated access to important or obscure literature, and their assistance and skill is gratefully acknowledged. Past and present members of the Pierce Lab are also thanked for their support and feedback, especially R. Brocklehurst and M. Wright for providing laser scans, and T. Simões for assistance with the phylogenetic analyses; T. Barbaro and J. Hughes are also thanked for logistical assistance. The constructive and insightful comments on an earlier version of the manuscript by K. Angielczyk and an anonymous reviewer are also much appreciated, and helped to improve its content and presentation.

FUNDING INFORMATION

This work was financially supported by the United States National Science Foundation (grants DEB-1754459 and EAR-2122115) and the William F. Milton Fund, Harvard University.

CONFLICT OF INTEREST STATEMENT

The authors declare no conflict of interest.

DATA AVAILABILITY STATEMENT

All data relating to this study are provided in the main paper or Supporting Information or are accessioned in registered museum collections (see Materials and Methods).

ORCID

Peter J. Bishop https://orcid.org/0000-0003-2702-0557
Stephanie E. Pierce https://orcid.org/0000-0003-0717-1841

REFERENCES

Abdala, F. (2007). Redescription of *Platycraniellus elegans* (Therapsida, Cynodontia) from the lower Triassic of South Africa and the cladistic relationships of Eutheriodontia. *Palaeontology*, *50*, 591–618.

Abdala, F., Gaetano, L. C., Smith, R. M. H., & Rubidge, B. S. (2019). A new large cynodont from the late Permian (Lopingian) of the south African Karoo Basin and its phylogenetic significance. *Zoological Journal of the Linnean Society*, *186*, 983–1005.

Abdala, F., Kammerer, C. F., Day, M. O., Jirah, S., & Rubidge, B. S. (2014). Adult morphology of the therocephalian *Simorhinella baini* from the middle Permian of South Africa and the taxonomy, paleobiogeography, and temporal distribution of the Lycosuchidae. *Journal of Paleontology*, *88*, 1139–1153.

Abdala, F., Rubidge, B. S., & van den Heever, J. (2008). The oldest therocephalians (Therapsida, Eutheriodontia) and the early diversification of Therapsida. *Palaeontology*, *51*, 1011–1024.

Abdala, V., & Diogo, R. (2010). Comparative anatomy, homologies and evolution of the pectoral and forelimb musculature of tetrapods with special attention to extant limbed amphibians and reptiles. *Journal of Anatomy*, *217*, 536–573.

Abdala, V., & Moro, S. (2006). Comparative myology of the forelimb of *Liolaemus* sand lizards (Liolaemidae). *Acta Zoologica*. *87*, 1–12

Allen, V., Molnar, J., Parker, W., Pollard, A., Nolan, G., & Hutchinson, J. R. (2015). Comparative architectural properties of limb muscles in Crocodylidae and Alligatoridae and their relevance to divergent use of asymmetrical gaits in extant Crocodylia. *Journal of Anatomy*, *225*, 569–582.

Allin, E. F., & Hopson, J. A. (1992). Evolution of the auditory system in Synapsida ("mammal-like reptiles" and primitive mammals) as seen in the fossil record. In D. B. Webster, A. N. Popper, & R. R. Fay (Eds.), *The evolutionary biology of hearing*. Springer-Verlag.

Angielczyk, K. D., & Kammerer, C. F. (2018). Non-mammalian synapsids: The deep roots of the mammalian family tree. In F. Zachos & R. J. Asher (Eds.), *Mammalian evolution, diversity and systematics* (pp. 117–198). De Gruyter.

Angielczyk, K. D., Sidor, C. A., Nesbitt, S. J., Smith, R. M. H., & Tsuji, L. A. (2009). Taxonomic revision and new observations on the postcranial skeleton, biogeography, and biostratigraphy of the dicynodont genus *Dicynodontoides*, the senior subjective synonym of *Kingoria* (Therapsida, Anomodontia). *Journal of Vertebrate Paleontology*, *29*, 1174–1187.

Anzai, W., Omura, A., Diaz, A. C., Kawata, M., & Endo, H. (2014). Functional morphology and comparative anatomy of appendicular musculature in Cuban *Anolis* lizards with different locomotor habits. *Zoological Science*, *31*, 454–463.

Araújo, R., David, R., Benoit, J., Lungmus, J. K., Stoessel, A., Barrett, P. M., Maisano, J. A., Ekdale, E., Orliac, M., Luo, Z.-X., Martinelli, A. G., Hoffman, E. A., Sidor, C. A., Martins, R. M. S., Spoor, F., & Angielczyk, K. D. (2022). Inner ear biomechanics reveals a late Triassic origin for mammalian endothermy. *Nature*, *607*, 726–731.

Attridge, J. (1956). The morphology and relationships of a complete therocephalian skeleton from the Cistecephalus zone of South Africa. *Proceedings of the Royal Society of Edinburgh, Series B*, *66*, 59–93.

Barbour, R. A. (1963). The musculature and limb plexuses of *Trichosurus vulpecula*. *Australian Journal of Zoology*, *11*, 488–610.

Barnett, C. H., & Lewis, O. J. (1958). The evolution of some traction epiphyses in birds and mammals. *Journal of Anatomy*, *92*, 593–601.

Baumel, J. J., King, A. S., Breazile, J. E., Evans, H. E., & vanden Berge, J. C. (1993). *Handbook of Avian Anatomy: Nomina Anatomica Avium* (2nd ed.). Nuttal Ornithological Club.

Bendel, E.-M., Kammerer, C. F., Luo, Z.-X., Smith, R. M. H., & Fröbisch, J. (2022). The earliest segmental sternum in a Permian synapsid and its implications for the evolution of mammalian locomotion and breathing. *Scientific Reports*, *12*, 13472.

Benoit, J., Dollman, K. N., Smith, R. M. H., & Manger, P. R. (2022). At the root of the mammalian mind: The sensory organs, brain and behavior of pre-mammalian synapsids. *Progress in Brain Research*, *275*, 25–72.

Benoit, J., Nxumalo, M., Norton, L. A., Fernandez, V., Gaetano, L. C., Rubidge, B. S., & Abdala, F. (2022). Synchrotron scanning sheds new light on *Lumkuia fuzzi* (Therapsida, Cynodontia) from the middle Triassic of South Africa and its phylogenetic placement. *Journal of African Earth Sciences*, *196*, 104689.

Benton, M. J. (2020). The origin of endothermy in synapsids and archosaurs and arms races in the Triassic. *Gondwana Research*, *100*, 261–289.

Berman, D. S., Henrici, A. C., Kissel, R. A., Sumida, S. S., & Martens, T. (2004). A new diadectid (Diadectomorpha), *Orobates pabsti*, from the early Permian of Central Germany. *Bulletin of Carnegie Museum of National History*, *35*, 1–36.

Berman, D. S., Maddin, H. C., Henrici, A. C., Sumida, S. S., Scott, D., & Reisz, R. R. (2020). New primitive caseid (Synapsida, Caseasauria) from the Early Permian of Germany. *Annals of Carnegie Museum*, *86*, 43–75.

Berman, D. S., & Sumida, S. S. (1990). A new species of *Limnoscelis* (Amphibia, Diadectomorpha) from the late Pennsylvanian Sangre de Cristo formation of Central Colorado. *Annals of Carnegie Museum*, *59*, 303–341.

Bhullar, B.-A. S., Manafzadeh, A. R., Miyamae, J. A., Hoffman, E. A., Brainerd, E. L., Musinsky, C., & Crompton, A. W. (2019). Rolling of the jaw is essential for mammalian chewing and tribosphenic molar function. *Nature*, *566*, 528–532.

Bishop, P. J. (2014). The humerus of *Ossinodus pueri*, a stem tetrapod from the carboniferous of Gondwana, and the early evolution of the tetrapod forelimb. *Alcheringa*, *38*, 209–238.

Bishop, P. J., Cuff, A. R., & Hutchinson, J. R. (2021). How to build a dinosaur: Musculoskeletal modelling and simulation of locomotor biomechanics in extinct animals. *Paleobiology*, *47*, 1–38.

Bishop, P. J., Norton, L. A., Jirah, S., Day, M. O., Rubidge, B. S., & Pierce, S. E. (2023). Enigmatic humerus from the mid-Permian of South Africa bridges the anatomical gap between "pelycosaurs" and therapsids. *Journal of Vertebrate Paleontology*, *42*, e2170805.

Bishop, P. J., & Pierce, S. E. (2023). The fossil record of appendicular muscle evolution in Synapsida on the line to mammals: Part II—Hindlimb. *The Anatomical Record: Advances in Integrative Anatomy and Evolutionary Biology*. https://doi.org/10.1002/ar.25310

Bishop, P. J., Wright, M. A., & Pierce, S. E. (2021). Whole-limb scaling of muscle mass and force-generating capacity in amniotes. *PeerJ*, *9*, e12574.

Blob, R. W. (2001). Evolution of hindlimb posture in nonmammalian therapsids: Biomechanical tests of paleontological hypotheses. *Paleobiology*, *27*, 14–38.

Bonaparte, J. F. (1963). Descripción del esqueleto postcraneano de Exaeretodon (Cynodontia–Traversodontidae). *Acta Geológica Lilloana*, *4*, 5–52.

Boonstra, L. D. (1934). A contribution to the morphology of the Gorgonopsia. *Annals of the South African Museum*, *31*, 137–174.

Boonstra, L. D. (1955). The girdles and limbs of the south African Deinocephalia. *Annals of the South African Museum*, *42*, 185–326.

Boonstra, L. D. (1964). The girdles and limbs of the pristerognathid Therocephalia. *Annals of the South African Museum*, *48*, 121–165.

Boonstra, L. D. (1965). The girdles and limbs of the Gorgonopsia of the *Tapinocephalus* zone. *Annals of the South African Museum*, *48*, 237–249.

Boonstra, L. D. (1967). An early stage in the evolution of the mammalian quadrupedal walking gait. *Annals of the South African Museum*, *50*, 27–42.

Botha, J., Abdala, F., & Smith, R. M. H. (2007). The oldest cynodont: New clues on the origin and early diversification of the Cynodontia. *Zoological Journal of the Linnean Society*, *149*, 477–492.

Botha-Brink, J., Huttenlocker, A. K., & Modesto, S. P. (2014). Vertebrate paleontology of Nooitgedacht 68: A *Lystrosaurus maccaigi*-rich Permo-Triassic boundary locality in South Africa. In C. F. Kammerer, K. D. Angielczyk, & J. Fröbisch (Eds.), *Early Evolutionary History of the Synapsida* (pp. 289–304). Springer.

Botha-Brink, J., & Modesto, S. P. (2011). A new skeleton of the therocephalian synapsid *Olivierosuchus parringtoni* from the lower Triassic south African Karoo Basin. *Palaeontology*, *54*, 591–606.

Brent, A. E., Bucholtz, E. A., & Mansfield, J. H. (2023). Evolutionary assembly and disassembly of the mammalian sternum. *Current Biology*, *33*, 197–205.

Brink, A. S. (1955). A study of the skeleton of *Diademodon*. *Palaeontologia Africana*, *3*, 3–46.

Brink, A. S. (1965). A new ictidosuchid (Scaloposauria) from the *Lystrosaurus*-zone. *Palaeontologia Africana*, *9*, 129–138.

Brink, A. S., & Kitching, J. W. (1951). On Leavachia, a Procynosuchid Cynodont from the middle Cistecephalus zone. *South African Journal of Science*, *47*, 342–347.

Brink, A. S., & Kitching, J. W. (1953). On *Leavachia duvenhagei* and some other procynosuchids in the Rubidge collection. *South African Journal of Science*, *49*, 313–317.

Brinkman, D. (1981). The structure and relationships of the dromasaurs (Reptilia: Therapsida). *Breviora*, *465*, 1–34.

Brinkman, D., & Eberth, D. A. (1983). The interrelationships of pelycosaurs. *Breviora*, *473*, 1–35.

Brinkman, J. (2000). Die Muskulatur der Vorderextremität von *Alligator mississippiensis* (DAUDIN, 1802) (Crocodilia). Eberhard Karls Universität.

Brocklehurst, R. J., Fahn-Lai, P., Regnault, S., & Pierce, S. E. (2022). Musculoskeletal modeling of sprawling and parasagittal forelimbs provides insight into synapsid postural transition. *iScience*, *25*, 103578.

Broom, R. (1947). A contribution to our knowledge of the vertebrates of the Karroo beds of South Africa. *Transactions of the Royal Society of Edinburgh*, *61*, 577–629.

Bryant, H. N., & Russell, A. P. (1993). The occurrence of clavicles within the Dinosauria: Implications for the homology of the avian furcula and the utility of negative evidence. *Journal of Vertebrate Paleontology*, *13*, 171–184.

Burch, S. H. (2014). Complete forelimb myology of the basal theropod dinosaur *Tawa hallae* based on a novel robust muscle reconstruction method. *Journal of Anatomy*, *225*, 271–297.

Butler, E., Abdala, F., & Botha-Brink, J. (2019). Postcranial morphology of the early Triassic epicynodont *Galesaurus planiceps* (Owen) from the Karoo Basin, South Africa. *Papers in Palaeontology*, *5*, 1–32.

Byerly, T. C. (1925). The myology of Sphenodon punctatum. *University of Iowa Studies in Natural History*, *11*, 3–50.

Camp, C. L., & Welles, S. P. (1956). Triassic dicynodont reptiles. Part I. the north American genus *Placerias*. *Memoirs of the University of California*, *13*, 255–304.

Campione, N. E., & Reisz, R. R. (2010). *Varanops brevirostris* (Eupelycosauria: Varanopidae) from the lower Permian of Texas, with discussion of Varanopid morphology and interrelationships. *Journal of Vertebrate Paleontology*, *30*, 724–746.

Carrano, M. T., & Hutchinson, J. R. (2002). Pelvic and hindlimb musculature of *Tyrannosaurus rex* (Dinosauria: Theropoda). *Journal of Morphology*, *253*, 207–228.

Carrier, D. R. (1987). The evolution of locomotor stamina in tetrapods: Circumventing a mechanical constraint. *Paleobiology*, *13*, 326–341.

Carry, M. R., Horan, S. E., Reed, S. M., & Farrell, R. V. (1993). Structure, innervation, and age-associated changes of mouse forearm muscles. *The Anatomical Record*, *237*, 345–357.

Cheng, C.-C. (1955). The development of the shoulder region of the opossum, *Didelphys virginiana*, with special reference to the musculature. *Journal of Morphology*, *97*, 415–471.

Chinsamy-Turan, A. (Ed.). (2011). *Forerunners of Mammals: Radiation, Histology, Biology*. Indiana University Press.

Cisneros, J. C., Abdala, F., Jashashvili, T., Bueno, A. O., & Dentzien-Dias, P. (2015). *Tiarajudens eccentricus* and *Anomocephalus africanus*, two bizarre anomodonts (Synapsida, Therapsida) with dental occlusion from the Permian of Gondwana. *Royal Society Open Science*, *2*, 150090.

Cluver, M. A. (1978). The skeleton of the mammal-like reptile *Cistecephalus* with evidence for a fossorial model of life. *Annals of the South African Museum*, *76*, 213–246.

Coates, M. I. (1996). The Devonian tetrapod *Acanthostega gunnari* Jarvik: Postcranial anatomy, basal tetrapod interrelationships and patterns of skeletal evolution. *Transactions of the Royal Society of Edinburgh*, *87*, 363–421.

Colbert, E. H. (1948). The mammal-like reptile *Lycaenops*. *Bulletin of the American Museum of Natural History*, *89*, 353–404.

Cong, L., Hou, L.-H., & Wu, X.-C. (1998). *The gross anatomy of Alligator sinensis Fauvel*. Beijing Science Press.

Coues, E., & Wyman, J. (1872). The Osteology and Myology of Didelphys Virginiana. *Memoirs of the Boston Society of Natural History*, *11*, 11–154.

Cox, C. B. (1959). On the anatomy of a new dicynodont genus with evidence of the position of the tympanum. *Proceedings of the Zoological Society of London*, *132*, 321–367.

Cox, C. B. (1972). A new digging dicynodont from the upper Permian of Tanzania. In K. A. Joysey & T. S. Kemp (Eds.), *Studies in Vertebrate Evolution* (pp. 173–189). Oliver & Boyd.

Crompton, A. W., Musinsky, C., & Owerkowicz, T. (2015). Evolution of the mammalian nose. In K. P. Dial, N. H. Shubin, & E. L. Brainerd (Eds.), *Great Transformations in Vertebrate Evolution*. University of Chicago Press.

Cruickshank, A. R. I. (1967). A new dicynodont genus from the Manda formation of Tanzania (Tanganyika). *Journal of Zoology*, *153*, 163–208.

Cys, J. M. (1967). Osteology of the pristerognathid *Cynariognathus platyrhinus* (Reptilia: Theriodonta). *Journal of Paleontology*, *41*, 776–790.

Davison, A. (1895). A contribution to the anatomy and phylogeny of *Amphiuma means* (Gardner). *Journal of Morphology*, *11*, 375–410.

de Oliveira, T. V., & Schultz, C. L. (2016). Functional morphology and biomechanics of the cynodont *Trucidocynodon riograndensis* from the Triassic of Southern Brazil: Pectoral girdle and forelimb. *Acta Palaeontologica Polonica*, *61*, 377–386.

de Oliveira, T. V., Soares, M. B., & Schultz, C. L. (2010). *Trucidocynodon riograndensis* gen. nov. *et* sp. nov. (Eucynodontia), a new cynodont from the Brazilian upper Triassic (Santa Maria formation). *Zootaxa*, *2382*, 1–71.

de Pinna, M. C. C. (1991). Concepts and tests of homology in the cladistic paradigm. *Cladistics*, *7*, 367–394.

de Vis, C. W. (1884). Myology of Chalmydosaurus Kingii. *Proceedings of the Linnean Society of New South Wales*, *8*, 300–320.

DeFauw, S. L. (1986). *The appendicular skeleton of African dicynodonts*. Wayne State University.

Dilkes, D. W. (1999). Appendicular myology of the hadrosaurian dinosaur *Maiasaura peeblesorum* from the late cretaceous (Campanian) of Montana. *Transactions of the Royal Society of Edinburgh*, *90*, 87–125.

Diogo, R., Bello-Hellegouarch, G., Kohlsdorf, T., Esteve-Altava, B., & Molnar, J. (2016). Comparative myology and evolution of marsupials and other vertebrates, with notes on complexity, Bauplan and "Scala Naturae". *The Anatomical Record*, *299*, 1224–1255.

Diogo, R., & Tanaka, E. M. (2012). Anatomy of the pectoral and forelimb muscles of wildtype and green fluorescent protein-transgenic axolotls and comparison with other tetrapods including humans: A basis for regenerative, evolutionary and developmental studies. *Journal of Anatomy*, *221*, 622–635.

Fahn-Lai, P., Biewener, A. A., & Pierce, S. E. (2020). Broad similarities in shoulder muscle architecture and organization across two amniotes: Implications for reconstructing non-mammalian synapsids. *PeerJ*, *8*, 8556.

Fernández-Jalvo, Y., & Andrews, P. (2016). *Atlas of Taphonomic Identifications*. Springer.

Fourie, H. (2013). The postcranial description of *Ictidosuchoides* (Therapsida: Therocephalia: Baurioidea). *Annals of the Ditsong National Museum of Natural History*, *3*, 1–10.

Fourie, H., & Rubidge, B. S. (2007). The postcranial skeletal anatomy of the therocephalian *Regisaurus* (Therapsida: Regisauridae) and its utilization for biostratigraphic correlation. *Palaeontologia Africana*, *42*, 1–16.

Fourie, H., & Rubidge, B. S. (2009). The postcranial skeleton of the basal therocephalian *Glanosuchus macrops* (Scylacosauridae) and comparison of morphological and phylogenetic trends amongst the Theriodontia. *Palaeontologia Africana*, *44*, 27–39.

Fox, R. C., & Bowman, M. C. (1966). Osteology and relationships of *Captorhinus aguti* (cope) (Reptilia: Captorhinomorpha). *The University of Kansas Paleontological Contributions, Vertebrata*, *11*, 1–79.

Francis, E. T. B. (1934). *The Anatomy of the Salamander*. Oxford University Press.

Fröbisch, J., & Reisz, R. R. (2011). The postcranial anatomy of *Suminia getmanovi* (Synapsida: Anomodontia), the earliest known arboreal tetrapod. *Zoological Journal of the Linnean Society*, *162*, 661–698.

Fürbringer, M. (1900). Zur vergleichenden Anatomie des Brustschulterapparates und der Schultermuskeln. *Jenaische Zeitschrift für Naturwissenschaft*, *34*, 215–718.

Gaetano, L. C., Abdala, F., & Govender, R. (2017). The postcranial skeleton of the Lower Jurassic *Tritylodon longaevus* from southern Africa. *Ameghiniana*, *54*, 1–35.

Gambaryan, P. P., & Kielan-Jaworowska, Z. (1997). Sprawling *versus* parasagittal stance in multituberculate mammals. *Acta Palaeontologica Polonica*, *42*, 13–44.

Gambaryan, P. P., Kuznetsov, A. N., Panyutina, A. A., & Gerasimov, S. V. (2015). Shoulder girdle and forelimb myology of extant Monotremata. *Russian Journal of Theriology*, *14*, 1–56.

George, R. M. (1977). The limb musculature of the Tupaiidae. *Primates*, *18*, 1–34.

Gould, S. J., & Lewontin, R. C. (1979). The spandrels of San Marco and the Panglossian paradigm: A critique of the adaptationist programme. *Proceedings of the Royal Society of London. Series B*, *205*, 581–598.

Govender, R. (2008). Description of the postcranial anatomy of *Aulacephalodon baini* and its possible relationship with '*Aulacephalodon peavoti*'. *South African Journal of Science*, *104*, 479–486.

Govender, R., Hancox, P. J., & Yates, A. M. (2008). Re-evaluation of the postcranial skeleton of the Triassic dicynodont *Kannemeyeria simocephalus* from the *Cynognathus* assemblage zone (subzone B) of South Africa. *Palaeontologia Africana*, *43*, 19–37.

Gow, C. E. (2001). A partial skeleton of the tritheledontid *Pachygenelus* (Therapsida: Cynodontia). *Palaeontologia Africana*, *37*, 93–97.

Greene, E. C. (1935). Anatomy of the rat. *Transactions of the American Philosophical Society*, *27*, 1–370.

Gregory, W. K., & Camp, C. L. (1918). Studies in comparative myology and osteology. *Bulletin of the American Museum of Natural History*, *38*, 447–563.

Guignard, M. L., Martinelli, A. G., & Soares, M. B. (2018). Reassessment of the postcranial anatomy of *Prozostrodon brasiliensis* and implications for postural evolution of non-mamaliaform cynodonts. *Journal of Vertebrate Paleontology*, *38*, e1511570.

Guignard, M. L., Martinelli, A. G., & Soares, M. B. (2019a). The postcranial anatomy of *Brasilodon quadrangularis* and the acquisition of mammaliaform traits among non-mammaliaform cynodonts. *PLoS One*, *14*, e0216672.

Guignard, M. L., Martinelli, A. G., & Soares, M. B. (2019b). Postcranial anatomy of *Riograndia guaibensis* (Cynodontia: Ictidosauria). *Geobios*, *53*, 9–21.

Haines, R. W. (1939). A revision of the extensor muscles of the forearm in tetrapods. *Journal of Anatomy*, *73*, 211–233.

Haines, R. W. (1950). The flexor muscles of the forearm and hand in lizards and mammals. *Journal of Anatomy*, *84*, 13–29.

Haines, R. W. (1952). The shoulder joint of lizards and the primitive reptilian shoulder mechanism. *Journal of Anatomy*, *86*, 412–422.

Hammer, Ø., Harper, D. A. T., & Ryan, P. D. (2001). PAST: Paleontological statistics software package for education and data analysis. *Palaeontologia Electronica*, *4*, 4.

Hellert, S. M., Grossnickle, D. M., Lloyd, G. T., Kammerer, C. F., & Angielczyk, K. D. (in press). Derived faunivores are the forerunners of major synapsid radiations. *Nature Ecology & Evolution*. https://doi.org/10.21203/rs.3.rs-1582761/v1

Hoffman, E. A., & Rowe, T. (2018). Jurassic stem-mammal perinates and the origin of mammalian reproduction and growth. *Nature*, *561*, 104–108.

Holmes, R. (1977). The osteology and musculature of the pectoral limb of small Captorhinids. *Journal of Morphology*, *152*, 101–140.

Howell, A. B. (1936). The musculature of antebrachium and manus in the platypus. *American Journal of Anatomy*, *59*, 425–432.

Howell, A. B. (1937). Morphogenesis of the shoulder architecture. Part V. Monotremata. *Quarterly Review of Biology*, *12*, 191–205.

Hu, Y. (2006). *Postcranial morphology of Repenomamus (Eutriconodonta, Mammalia): Implications for the higher-level phylogeny of mammals*. The City University of New York.

Hurum, J. H., & Kielan-Jaworowska, Z. (2008). Postcranial skeleton of a Cretaceous multituberculate mammal *Catopsbaatar*. *Acta Palaeontologica Polonica*, *53*, 545–566.

Hutchinson, J. R. (2001a). The evolution of femoral osteology and soft tissues on the line to extant birds (Neornithes). *Zoological Journal of the Linnean Society*, *131*, 169–197.

Hutchinson, J. R. (2001b). The evolution of pelvic osteology and soft tissues on the line to extant birds (Neornithes). *Zoological Journal of the Linnean Society*, *131*, 123–168.

Hutchinson, J. R. (2002). The evolution of hindlimb tendons and muscles on the line to crown-group birds. *Comparative Biochemistry and Physiology, Part A*, *133*, 1051–1086.

Jenkins, F. A., Jr., & Goslow, G. E., Jr. (1983). The Functional Anatomy of the Shoulder of the Savannah Monitor Lizard (*Varanus exanthematicus*). *Journal of Morphology*, *175*, 195–216.

Jenkins, F. A., Jr., & Parrington, F. R. (1976). The postcranial skeletons of the Triassic mammals *Eozostrodon*, *Megazostrodon* and *Erythrotherium*. *Philosophical Transactions of the Royal Society of London, Series B*, *273*, 387–431.

Jenkins, F. A., Jr., & Weijs, W. A. (1979). The functional anatomy of the shoulder in the Virginia opossum (*Didelphis virginiana*). *Journal of Zoology*, *188*, 379–410.

Jenkins, F. A., Jr. (1970a). The Chañares (Argentina) Triassic reptile fauna VII. The postcranial skeleton of the traversodontid *Massetognathus pascuali* (Therapsida, Cynodontia). *Breviora*, *352*, 1–28.

Jenkins, F. A., Jr. (1970b). Cynodont postcranial anatomy and the "prototherian" level of mammalian organization. *Evolution*, *24*, 230–252.

Jenkins, F. A., Jr. (1971). The Postcranial Skeleton of African Cynodonts. *Bulletin of the Peabody Museum of Natural History*, *36*, 1–216.

Jenkins, F. A., Jr. (1973). The functional anatomy and evolution of the mammalian Humero-ulnar articulation. *American Journal of Anatomy*, *137*, 281–298.

Jones, K. E., Angielczyk, K. D., Polly, P. D., Head, J. J., Fernandez, V., Lungmus, J. K., Tulga, S., & Pierce, S. E. (2018). Fossils reveal the complex evolutionary history of the mammalian regionalized spine. *Science*, *361*, 1249–1252.

Jones, K. E., Dickson, B. V., Angielczyk, K. D., & Pierce, S. E. (2021). Adaptive landscapes challenge "lateral-to-sagittal" paradigm for mammalian vertebral evolution. *Current Biology*, *31*, 1883–1892.

Kammerer, C. F., Fröbisch, J., & Angielczyk, K. D. (2013). On the validity and phylogenetic position of *Eubrachiosaurus browni*, a kannemeyeriiform dicynodont (Anomodontia) from Triassic North America. *PLoS One*, *8*, e64203.

Kammerer, C. F., Viglietti, P. A., Butler, E., & Botha, J. (2023). Rapid turnover of top predators in African terrestrial faunas around the Permian-Triassic mass extinction. *Current Biology*, *33*, 2283–2290.

Kemp, T. S. (1978). Stance and gait in the hindlimb of a therocephalian mammal-like reptile. *Journal of Zoology*, *186*, 143–161.

Kemp, T. S. (1980a). Aspects of the structure and functional anatomy of the Middle Triassic cynodont *Luangwa*. *Journal of Zoology*, *191*, 193–239.

Kemp, T. S. (1980b). The primitive cynodont *Procynosuchus*: Structure, function and evolution of the postcranial skeleton. *Philosophical Transactions of the Royal Society of London, Series B*, *288*, 217–258.

Kemp, T. S. (1982). *Mammal-like Reptiles and the Origin of Mammals*. Academic Press.

Kemp, T. S. (1986). The skeleton of a baurioid therocephalian therapsid from the Lower Triassic (*Lystrosaurus* zone) of South Africa. *Journal of Vertebrate Paleontology*, *6*, 215–232.

Kemp, T. S. (2005). *The Origin and Evolution of Mammals*. Oxford University Press.

Kemp, T. S. (2016). *The Origin of Higher Taxa*. Oxford University Press.

Kerber, L., Martinelli, A. G., Müller, R. T., & Pretto, F. A. (2022). A new specimen provides insight into the anatomy of *Irajatherium hernandezi*, a poorly known probainognathian cynodont from the late Triassic of southern Brazil. *The Anatomical Record*, *305*, 3113–3132.

Kielan-Jaworowska, Z., & Gambaryan, P. P. (1994). Postcranial anatomy and habits of Asian multituberculate mammals. *Fossils and Strata*, *36*, 1–92.

Kielan-Jaworowska, Z., & Dashzeveg, D. (1978). New late cretaceous mammal locality in Mongolia and a description of a new multituberculate. *Acta Palaeontologica Polonica*, *23*, 117–130.

King, G. M. (1981a). The functional anatomy of a Permian dicynodont. *Philosophical Transactions of the Royal Society of London, Series B*, *291*, 243–322.

King, G. M. (1981b). The postcranial skeleton of *Robertia broomiana*, an early dicynodont (Reptilia, Therapsida) from the south African Karoo. *Annals of the South African Museum*, *84*, 203–231.

King, G. M. (1985). The postcranial skeleton of *Kingoria nowacki* (von Huene) (Therapsida: Dicynodontia). *Zoological Journal of the Linnean Society*, *84*, 263–289.

King, G. M. (1996). A description of the skeleton of a bauriid therocephalian from the early Triassic of South Africa. *Annals of the South African Museum*, *104*, 379–393.

Krause, D. W., & Jenkins, F. A., Jr. (1983). The postcranial skeleton of North American multituberculates. *Bulletin of the Museum of Comparative Zoology at Harvard College*, *150*, 199–246.

Kühne, W. G. (1956). *The Liassic Therapsid Oligokyphus*. British Museum (Natural History).

Kümmel, S. B., Abdala, F., Sassoon, J., & Abdala, V. (2020). Evolution and identity of synapsid carpal bones. *Acta Palaeontologica Polonica*, *65*, 649–678.

Lai, P. H., Biewener, A. A., & Pierce, S. E. (2018). Three-dimensional mobility and muscle attachments in the pectoral limb of the Triassic cynodont *Massetognathus pascuali* (Romer, 1967). *Journal of Anatomy*, *232*, 383–406.

Landsmeer, J. M. F. (1984). Morphology of the anterior limb in relation to sprawling gait in *Varanus*. *Symposium of the Zoological Society of London*, *52*, 27–45.

Lautenschlager, S., Gill, P. G., Luo, Z.-X., Fagan, M. J., & Rayfield, E. J. (2018). The role of miniaturization in the evolution of the mammalian jaw and middle ear. *Nature*, *561*, 533–537.

Le Gros Clark, W. E. (1924). The myology of the tree-shrew (*Tupaia minor*). *Proceedings of the Zoological Society of London*, *31*, 461–497.

Le Gros Clark, W. E. (1926). On the anatomy of the pen-tailed tree-shrew (*Ptilocercus lowii*). *Proceedings of the Zoological Society of London*, *96*, 1179–1309.

Lécuru, S. (1968). Myologie et innervation du membre antérieur des lacertiliens. *Mémoires du Muséum National d'histoire Naturelle*, *48*, 127–215.

Lewis, P. O. (2001). A likelihood approach to estimating phylogeny from discrete morphological character data. *Systematic Biology*, *50*, 913–925.

Liu, J., & Powell, J. (2009). Osteology of *Andescynodon* (Cynodontia:Traversodontidae) from the Middle Triassic of Argentina. *American Museum Novitates*, *3674*, 1–19.

Liu, J., Schneider, V. P., & Olsen, P. E. (2017). The postcranial skeleton of *Boreogomphodon* (Cynodontia: Traversodontidae) from the Upper Triassic of North Carolina, USA and the comparison with other traversodontids. *PeerJ*, *5*, e3521.

Lungmus, J. K., & Angielczyk, K. D. (2019). Antiquity of forelimb ecomorphological diversity in the mammalian stem lineage (Synapsida). *Proceedings of the National Academy of Sciences of the United States of America*, *116*, 6903–6907.

Lungmus, J. K., & Angielczyk, K. D. (2021). Phylogeny, function and ecology in the deep evolutionary history of the mammalian forelimb. *Proceedings of the Royal Society of London. Series B*, *288*, 20210494.

Luo, Z.-X. (2011). Developmental patterns in Mesozoic evolution of mammal ears. *Annual Review of Ecology, Evolution, and Systematics*, *42*, 355–380.

Luo, Z.-X. (2015). Origin of the mammalian shoulder. In K. P. Dial, N. H. Shubin, & E. L. Brainerd (Eds.), *Great Transformations in Vertebrate Evolution* (pp. 167–187). University of Chicago Press.

Luo, Z.-X., & Wible, J. R. (2005). A late Jurassic digging mammal and early mammalian diversification. *Science*, *308*, 103–107.

MacCormick, A. (1887). The myology of the limbs of *Dasyurus viverrinus*. A. Myology of the fore-limb. *Journal of Anatomy and Physiology*, *21*, 103–137.

Maddison, W. P., & Maddison, D. R. (2021). Mesquite: A modular system for evolutionary analysis. Version 3.61. http://www.mesquiteproject.org

Maidment, S. C. R., & Barrett, P. M. (2011). The locomotor musculature of basal ornithischian dinosaurs. *Journal of Vertebrate Paleontology*, *31*, 1265–1291.

Maisch, M. W., Matzke, A. T., & Sun, G. (2004). A new tritylodontid from the Upper Jurassic Shishuguo formation of the Junggar Basin (Xinjiang, China). *Journal of Vertebrate Paleontology*, *24*, 649–656.

Martin, T. (2005). Postcranial anatomy of *Haldanodon exspectatus* (Mammalia, Docodonta) from the Late Jurassic (Kimmeridgian) of Portugal and its bearing for mammalian evolution. *Zoological Journal of the Linnean Society*, *145*, 219–248.

Martinelli, A. G., Bonaparte, J. F., Schultz, C. L., & Rubert, R. (2005). A new tritheledontid (Therapsida, Eucynodontia) from the Late Triassic of Rio Grande do Sul (Brazil) and its phylogenetic relationships among carnivorous non-mammalian eucynodonts. *Ameghiniana*, *42*, 191–208.

McKay, W. J. S. (1894). The morphology of the muscles of the shoulder-girdle in monotremes. *Proceedings of the Linnean Society of New South Wales*, *9*, 263–360.

Meers, M. B. (2003). Crocodylian forelimb musculature and its relevance to Archosauria. *The Anatomical Record*, *274A*, 891–916.

Miner, R. W. (1925). The pectoral limb of *Eryops* and other primitive tetrapods. *Bulletin of the American Museum of Natural History*, *51*, 145–312.

Mivart, S. G. (1869). Notes on the myology of *Menopoma alleghaniense*. *Proceedings of the Zoological Society of London*, *37*, 254–271.

Mocke, H. B., Gaetano, L. C., & Abdala, F. (2020). A new species of the carnivorous cynodont *Chiniquodon* (Cynodontia, Chiniquodontidae) from the Namibian Triassic. *Journal of Vertebrate Paleontology*, *39*, e1754321.

Molnar, J. L., Diogo, R., Hutchinson, J. R., & Pierce, S. E. (2018). Reconstructing pectoral appendicular muscle anatomy in fossil fish and tetrapods over the fins-to-limbs transition. *Biological Reviews*, *93*, 1077–1107.

Molnar, J. L., Diogo, R., Hutchinson, J. R., & Pierce, S. E. (2020). Evolution of hindlimb muscle anatomy across the tetrapod water-to-land transition, including comparisons with forelimb anatomy. *The Anatomical Record*, *303*, 218–234.

Murie, J., & Mivart, S. G. (1865). On the Myology of Hyrax capensis. *Proceedings of the Zoological Society of London*, *33*, 329–352.

Olson, R. A., Womble, M. D., Thomas, D. R., Glenn, Z. D., & Butcher, M. T. (2016). Functional morphology of the forelimb of the nine-banded armadillo (*Dasypus novemcinctus*): Comparative perspectives on the myology of the Dasypodidae. *Journal of Mammalian Evolution*, *23*, 49–69.

Orlov, J. A. (1958). Predatory deinocephalians from the Isheevo Fauna (titanosuchians). *Trudy Paleontologicheskogo Instituta Akademiya Nauk SSSR*, *72*, 1–114.

Osawa, G. (1897). Beiträge zur Anatomie der Hatteria punctata. *Archive of Microscopic Anatomy*, *51*, 481–691.

Otero, A. (2018). Forelimb musculature and osteological correlates in Sauropodomorpha (Dinosauria, Saurischia). *PLoS One*, *13*, e0198988.

Otoo, B. K. A., Bolt, J. R., Lombard, R. E., Angielczyk, K. D., & Coates, M. I. (2021). The postcranial anatomy of *Whatcheeria deltae* and its implications for the family Whatcheeriidae. *Zoological Journal of the Linnean Society*, *193*, 700–745.

Paradis, E., Claude, J., & Strimmer, K. (2004). APE: Analysis of phylogenetics and evolution in R language. *Bioinformatics*, *20*, 289–290.

Parrington, F. R. (1961). The evolution of the mammalian femur. *Proceedings of the Zoological Society of London*, *137*, 285–298.

Patterson, C. (1982). Morphological Characters and Homoplasy. In K. A. Joysey & A. E. Friday (Eds.), *Problems of Phylogenetic Reconstruction*. Academic Press.

Pawley, K. (2007). The postcranial skeleton of *Trimerorhachis insignis* Cope, 1878 (Temnospondyli): A plesiomorphic temnospondyl from the lower Permian of North America. *Journal of Paleontology*, *81*, 873–894.

Pawley, K., & Warren, A. A. (2006). The appendicular skeleton of *Eryops megacephalus* Cope, 1877 (Temnospondyli: Eryopoidea). *Journal of Paleontology*, *80*, 561–580.

Phillips, M. J., Bennett, T. H., & Lee, M. S. Y. (2009). Molecules, morphology, and ecology indicate a recent, amphibious ancestry for echidnas. *Proceedings of the National Academy of Sciences*, *106*, 17089–17094.

Polly, P. D. (2007). Limbs in Mammalian Evolution. In B. K. Hall (Ed.), *Fins into Limbs: Evolution, Development, and Transformation*. University of Chicago Press.

Pravoslavev, P. A. (1927). *Gorgonopsidae from the north Dwina excavations of V.P. Amalitzki*. U.S.S.R. Academy of Sciences.

Prendini, L. (2001). Species or supraspecific taxa as terminals in cladistic analysis? Groundplans versus exemplars revisited. *Systematic Biology*, *50*, 290–300.

R Core Team. (2021). *R: A language and environment for statistical computing*. R Foundation for Statistical Computing.

Ray, S. (2006). Functional and evolutionary aspects of the postcranial anatomy of dicynodonts (Synapsida, Therapsida). *Palaeontology*, *49*, 1263–1286.

Ray, S., & Chinsamy, A. (2003). Functional aspects of the postcranial anatomy of the Permian dicynodont *Diictodon* and their ecological implications. *Palaeontology*, *46*, 151–183.

Regnault, S., Fahn-Lai, P., Norris, R. M., & Pierce, S. E. (2020). Shoulder muscle architecture in the echidna (Monotremata: *Tachyglossus aculeatus*) indicates conserved functional properties. *Journal of Mammalian Evolution, 27*, 591–603.

Regnault, S., & Pierce, S. E. (2018). Pectoral girdle and forelimb musculoskeletal function in the echidna (*Tachyglossus aculeatus*): Insights into mammalian locomotor evolution. *Royal Society Open Science*, *5*, 181400.

Revell, L. J. (2012). Phytools: An R package for phylogenetic comparative biology (and other things). *Methods in Ecology and Evolution*, *3*, 217–223.

Richards, H. L., Adams, J. W., & Evans, A. R. (2023). Hanging on and digging deep: Comparative forelimb myology of the koala (*Phascolarctos cinereus*) and common wombat (*Vombatus ursinus*). *Zoological Journal of the Linnean Society*. https://doi.org/10.1093/zoolinnean/zlad018

Rinker, G. C. (1954). The comparative myology of the mammalian genera *Sigmodon*, *Oryzomys*, *Neotoma*, and *Peromyscus* (Crecetinae), with remarks on their intergeneric relationships. *Miscellaneous Publications Museum of Zoology, University of Michigan*, *83*, 1–124.

Romer, A. S. (1922). The locomotor apparatus of certain primitive and mammal-like reptiles. *Bulletin of the American Museum of Natural History*, *46*, 517–606.

Romer, A. S. (1924). The lesser trochanter of the mammalian femur. *The Anatomical Record*, *28*, 95–102.

Romer, A. S. (1944). The development of tetrapod limb musculature—The shoulder region of *Lacerta*. *Journal of Morphology*, *74*, 1–41.

Romer, A. S. (1956). *Osteology of the Reptiles*. University of Chicago Press.

Romer, A. S. (1962). *The Vertebrate Body* (3rd ed.). W. B. Saunders Company.

Romer, A. S., & Price, L. I. (1940). Review of the Pelycosauria. *Special Papers of the Geological Society of America*, *28*, 1–538.

Ronquist, F., Teslenko, M., van der Mark, P., Ayres, D. L., Darling, A., Höhna, S., Larget, B., Liu, L., Suchard, M. A., & Huelsenbeck, J. P. (2012). MRBAYES 3.2: Efficient Bayesian phylogenetic inference and model selection across a large model space. *Systematic Biology*, *61*, 539–542.

Rougier, G. W. (1993). *Vincelestes neuquenianus Bonaparte (Mammalia, Theria) un primitivo mamifero del Cretacio Inferior de la Cuenca Neuquina*. Universidad Nacional de Buenos Aires.

Rubidge, B. S., King, G. M., & Hancock, J. A. (1994). The postcranial skeleton of the earliest dicynodont synapsid *Eodicynodon* from the Upper Permian of South Africa. *Palaeontology*, *37*, 397–408.

Russell, A. P., & Bauer, A. M. (2008). The appendicular locomotor apparatus of *Sphenodon* and normal-limbed squamates. In C. Gans, A. S. Gaunt, & K. Adler (Eds.), *Biology of the Reptilia 24, Morphology 1* (pp. 1–466). Society for the Study of Amphibians and Reptiles.

Sánchez-Villagra, M. R., & Maier, W. (2003). Ontogenesis of the scapula in marsupial mammals, with special emphasis on perinatal stages of Didelphids and remarks on the origin of the therian scapula. *Journal of Morphology*, *258*, 115–129.

Sereno, P. C. (2006). Shoulder girdle and forelimb in Multituberculates: Evolution of parasagittal forelimb posture in mammals. In M. T. Carrano, T. J. Gaudin, R. W. Blob, & J. R. Wible (Eds.), *Amniote Paleobiology: Perspectives on the Evolution of Mammals, Birds, and Reptiles* (pp. 315–366). University of Chicago Press.

Sereno, P. C., & McKenna, M. C. (1995). Cretaceous multituberculate skeleton and the early evolution of the mammalian shoulder girdle. *Nature*, *377*, 144–147.

Shubin, N. H., Tabin, C., & Carroll, S. (2009). Deep homology and the origins of evolutionary novelty. *Nature*, *457*, 818–823.

Sidor, C. A., & Hopson, J. A. (1998). Ghost lineages and "mammalness": Assessing the temporal pattern of character acquisition in the Synapsida. *Paleobiology*, *24*, 254–273.

Sidor, C. A., & Hopson, J. A. (2017). *Cricodon metabolus* (Cynodontia: Gomphodontia) from the Triassic Ntawere formation of northeastern Zambia: Patterns of tooth replacement and a systematic review of Trirachodontidae. *Journal of Vertebrate Paleontology*, *37*(suppl. 1), 39–64.

Sigogneau, D., & Tchudinov, P. K. (1972). Reflections on some Russian eotheriodonts (Reptilia, Synapsida, Therapsida). *Palaeovertebrata*, *5*, 79–109.

Sigogneau-Russell, D. (1989). Theriodontia I. *Handbuch der Paläoherpetologie*, *17B*, 1–123.

Simões, T. R., Kammerer, C. F., Caldwell, M. W., & Pierce, S. E. (2022). Successive climate crises in the deep past drove the early evolution and radiation of reptiles. *Science Advances*, *8*, eabq1898.

Smith-Paredes, D., Vergara-Cereghino, M. E., Lord, A., Moses, M. M., Behringer, R. R., & Bhullar, B.-A. S. (2022). Embryonic muscle splitting patterns reveal homologies of

amniote forelimb muscles. *Nature Ecology & Evolution*, *6*, 604–613.

Stein, B. R. (1981). Comparative limb myology of two opossums, *Didelphis* and *Chironectes*. *Journal of Morphology*, *169*, 113–140.

Stein, B. R. (1986). Comparative limb myology of four Arvicolid rodent genera (Mammalia, Rodentia). *Journal of Morphology*, *187*, 321–342.

Sues, H.-D., & Jenkins, F. A., Jr. (2006). The postcranial skeleton of *Kayentatherium wellesi* from the lower Jurassic Kayenta formation of Arizona and the phylogenetic significance of postcranial features in Tritylodontid Cynodonts. In M. T. Carrano, T. J. Gaudin, R. W. Blob, & J. R. Wible (Eds.), *Amniote Paleobiology: Perspectives on the Evolution of Mammals, Birds, and Reptiles* (pp. 114–152). Chicago University Press.

Sulej, T., & Niedźwiedzki, G. (2018). An elephant-sized late Triassic synapsid with erect limbs. *Science*, *363*, 78–80.

Sumida, S. S. (1997). Locomotor features of taxa spanning the origin of amniotes. In S. S. Sumida & K. L. M. Martin (Eds.), *Amniote Origins: Completing the Transition to Land* (pp. 353–398). Academic Press.

Sumida, S. S., Pelletier, V., & Berman, D. S. (2014). New information on the basal Pelycosaurian-grade synapsid *Oedaleops*. In C. F. Kammerer, K. D. Angielczyk, & J. Fröbisch (Eds.), *Early Evolutionary History of the Synapsida* (pp. 7–23). Springer.

Sun, A., & Li, Y. (1985). The postcranial skeleton of the late tritylodont *Bienotherioides*. *Vertebrata PalAsiatica*, *23*, 135–150.

Swofford, D. L., & Maddison, W. P. (1987). Reconstructing ancestral character states under Wagner parsimony. *Mathematical Biosciences*, *87*, 199–229.

Taylor, B. K. (1978). The anatomy of the forelimb in the anteater (*Tamandua*) and its functional implications. *Journal of Morphology*, *157*, 347–368.

Tchudinov, P. K. (1983). Early therapsids. *Trudy Paleontologicheskogo Instituta Akademiya Nauk SSSR*, *202*, 1–229.

Ungar, P. S. (2010). *Mammal Teeth: Origin, Evolution, and Diversity*. Johns Hopkins University Press.

Vickaryous, M. K., & Hall, B. K. (2006). Homology of the reptilian coracoid and a reappraisal of the evolution and development of the amniote pectoral apparatus. *Journal of Anatomy*, *208*, 263–285.

Walter, L. R. (1988a). Appendicular musculature in the echidna, *Tachyglossus aculeatus* (Monotremata: Tachyglossidae). *Australian Journal of Zoology*, *36*, 65–81.

Walter, L. R. (1988b). The limb posture of kannemeyeriid dicynodonts: Functional and ecological considerations. In K. Padian (Ed.), *The Beginning of the Age of Dinosaurs* (pp. 89–97). Cambridge University Press.

Walthall, J. C., & Ashley-Ross, M. A. (2006). Postcranial myology of the California newt, *Taricha torosa*. *The Anatomical Record*, *288A*, 46–57.

Warburton, N. M., Grégoire, L., Jacques, S., & Flandrin, C. (2013). Adaptations for digging in the forelimb muscle anatomy of the southern brown bandicoot (*Isoodon obesulus*) and bilby (*Macrotis lagotis*). *Australian Journal of Zoology*, *61*, 402–419.

Warburton, N. M., & Marchal, C.-R. (2017). Forelimb myology of carnivorous marsupials (Marsupialia: Dasyuridae): Implications for the ancestral body plan of the Australidelphia. *The Anatomical Record*, *300*, 1589–1608.

Watson, D. M. S. (1917). The evolution of the tetrapod shoulder girdle and fore-limb. *Journal of Anatomy*, *52*, 1–63.

Watson, D. M. S. (1931). On the skeleton of a bauriamorph reptile. *Proceedings of the Zoological Society of London*, *101*, 1163–1205.

Westling, C. (1889). Anatomische untersuchungen über Echidna. *Bihang till Kongl Svenska Vetenskaps-Akademiens Handlingar*, *15*, 1–69.

White, T. E. (1939). Osteology of *Seymouria baylorensis* Broili. *Bulletin of the Museum of Comparative Zoology at Harvard College*, *85*, 325–409.

Wilder, H. H. (1912). The appendicular muscles of *Necturus maculosus*. *Zoologischen Jarbüchern Supplement*, *15*, 383–424.

Williston, S. W. (1911). *American Permian Vertebrates*. University of Chicago Press.

Wilson, J. D., Koch, N. M., & Ramírez, M. J. (2022). Chronogram or phylogram for ancestral state estimation? Model-fit statistics indicate the branch lengths underlying a binary character's evolution. *Methods in Ecology and Evolution*, *13*, 1679–1689.

Witmer, L. M. (1995). The extant phylogenetic bracket and the importance of reconstructing soft tissues in fossils. In J. J. Thomason (Ed.), *Functional Morphology in Vertebrate Paleontology* (pp. 19–33). Cambridge University Press.

Wynd, B. M., Peecook, B. R., Whitney, M. R., & Sidor, C. A. (2017). The first occurrence of *Cynognathus crateronotus* (Cynodontia: Cynognathia) in Tanzania and Zambia, with implications for the age and biostratigraphic correlation of Triassic strata in southern Pangea. *Journal of Vertebrate Paleontology*, *37*(suppl. 1), 228–239.

Young, C.-C. (1947). Mammal-like reptiles from Lufeng, Yunnan, China. *Proceedings of the Zoological Society of London*, *117*, 537–597.

Zaaf, A., Herrel, A., Aerts, P., & De Vree, F. (1999). Morphology and morphometrics of the appendicular musculature in geckoes with different locomotor habits (Lepidosauria). *Zoomorphology*, *119*, 9–22.

SUPPORTING INFORMATION

Additional supporting information can be found online in the Supporting Information section at the end of this article.

How to cite this article: Bishop, P. J., & Pierce, S. E. (2024). The fossil record of appendicular muscle evolution in Synapsida on the line to mammals: Part I—Forelimb. *The Anatomical Record*, *307*(5), 1764–1825. https://doi.org/10.1002/ar.25312